HEAT TRANSFER DURING MELTING AND SOLIDIFICATION IN HETEROGENEOUS MATERIALS

By

Sepideh Sayar

Thesis submitted to the Faculty of the Virginia Polytechnic Institute and State University in partial fulfillment of the requirements for the degree of

Master of Science

In

Mechanical Engineering

Dr. Brian Vick, Chairman

Dr. Elaine P. Scott

Dr. Karen A. Thole

Dr. James R. Thomas

December, 2000

Blacksburg, Virginia

Keywords: Heterogeneous Material, Phase changing, Melting, Solidification, Numerical Method, Finite Difference Method (FDM)

HEAT TRANSFER DURING MELTING AND SOLIDIFICATION IN HETEROGENEOUS MATERIALS

By

Sepideh Sayar

Dr. Brian Vick, Chairman

Department of Mechanical Engineering

ABSTRACT

A one-dimensional model of a heterogeneous material consisting of a matrix with embedded separated particles is considered, and the melting or solidification of the particles is investigated. The matrix is in imperfect contact with the particles, and the lumped capacity approximation applies to each individual particle. Heat is generated inside the particles or is transferred from the matrix to the particles coupled through a contact conductance. The matrix is not allowed to change phase and energy is either generated inside the matrix or transferred from the boundaries, which is initially conducted through the matrix material. The physical model of this coupled, two-step heat transfer process is solved using the energy method.

The investigation is conducted in several phases using a building block approach. First, a lumped capacity system during phase transition is studied, then a one-dimensional homogeneous material during phase change is investigated, and finally the one-dimensional heterogeneous material is analyzed. A numerical solution based on the finite difference method is used to solve the model equations. This method allows for any kind of boundary conditions, any combination of material properties, particle sizes and contact conductance. In addition, computer programs, using Mathematica, are developed for the lumped capacity system, homogeneous material, and heterogeneous material. Results show the effects of control volume thickness, time step, contact conductance, material properties, internal sources, and external sources.

ACKNOWLEDGEMENTS

I would personally like to thank the following individuals who have made this thesis possible.

First I would like to thank my advisor and committee chair, Dr. Brian Vick, for all his patience and guidance throughout my research. I would like to thank Dr. Elaine Scott for serving on my committee and for her significant advice on my thesis. I thank Dr. Karen Thole and Dr. James Thomas for serving on my committee. Also I thank the thermal system program of the National Science Foundation for its support through NSF grant number CTS-9612044.

I also thank my family friend Dr. Mehdi Ahmadian for his guidance through my academic years as a graduate student.

I may not forget to thank my family for their unconditional love and great support, emotional as well as financial. Last, but never ever least, I would like to thank my fiancee, Siavash Enayati, for his emotional support and motivation.

TABLE OF CONTENTS

LIST OF FIGURES

LIST OF TABLES

NOMENCLATURE

A	area	$[m^2]$
C_m	matrix heat capacity per total volume $= (1 - NV_p)(\rho Cp)_m$	$[\frac{J}{m^3 \, ^\circ C}]$
Cp	heat capacity	$[\frac{J}{kg \, ^\circ C}]$
Cr	heat capacity ratio$= \frac{Cp}{Cp_{ref}}$	
E	designates the east side face of the control volume	
e	specific internal energy	$[\frac{kJ}{kg}]$
eo	solid saturated energy	$[\frac{kJ}{kg}]$
H_c	matrix-particle coupling coefficient $= h_c (NA_p)$	$[\frac{W}{m^3 \, ^\circ C}]$
h_c	matrix-particle contact conductance	$[\frac{W}{m^2 \, ^\circ C}]$
h	heat transfer coefficient	$[\frac{W}{m^2 \, ^\circ C}]$
$hx0$	heat transfer coefficient at $x=0$	$[\frac{W}{m^2 \, ^\circ C}]$
hxL	heat transfer coefficient at $x=L$	$[\frac{W}{m^2 \, ^\circ C}]$
K_m	conductance through the matrix $= (1 - NV_p)k_m$	$[\frac{W}{m \, ^\circ C}]$
Kr	conductivity ratio$= \frac{k}{k_{ref}}$	
k	conductivity	$[\frac{W}{m \, ^\circ C}]$
L	length	$[m]$

Mr	mass ratio= $\frac{\rho_p (NV_p)}{\rho_m (1-NV_p)}$	
mm	total number of control volumes	
N	number of particles per total volume (number density)	$[\frac{1}{m^3}]$
nn	total number of control volumes	
$q_0^{"}$	surface heat flux	$[\frac{W}{m^2}]$
qx0	surface heat flux at *x=0*	$[\frac{W}{m^2}]$
qxL	surface heat flux at *x=L*	$[\frac{W}{m^2}]$
S	*s* times the matrix or particle volume fraction	$[\frac{W}{m^3}]$
s	volumetric heat source	$[\frac{W}{m^3}]$
Sc	*sc* times the matrix or particle volume fraction	$[\frac{W}{m^3}]$
sc	temperature-independent portion of volumetric heat source	$[\frac{W}{m^3}]$
Sp	*sp* times the matrix or particle volume fraction	$[\frac{W}{m^3 \circ K}]$
sp	proportional-to-temperature portion of volumetric heat source	$[\frac{W}{m^3 \circ K}]$
Ste	Stefan number= $\frac{Cp_{ref} \Delta T_{ref}}{\lambda}$	
T	temperature	$[^\circ C]$
Tm	melting temperature	$[^\circ C]$
Tm_b	beginning melting temperature	$[^\circ C]$
Tm_f	finishing melting temperature	$[^\circ C]$
T_0	surface temperature	$[^\circ C]$
T_∞	environment temperature	$[^\circ C]$

$Tx0$	surface temperature at $x=0$	$[^{\circ}C]$
$Tx0_{\infty}$	environment temperature at $x=0$	$[^{\circ}C]$
TxL	surface temperature at $x=L$	$[^{\circ}C]$
TxL_{∞}	environment temperature at $x=L$	$[^{\circ}C]$
t	time	$[s]$
V	volume	$[m^3]$
W	designates the west side face of the control volume	
x, y, z	space co-ordinates	$[m]$
α	thermal diffusivity	$[\frac{m^2}{\sec}]$
β	explicit, implicit method indicator (explicit $\beta=0$, implicit $\beta=1$)	
Δe	energy change per mass	$[\frac{kJ}{kg}]$
ΔT	temperature rise	$[^{\circ}C]$
Δt	length of time step	$[s]$
Δx	length of a typical control volume	
Γ	contact conductance= $\frac{h_c L^2}{\rho_{ref} Cp_{ref} \alpha_{ref}}$	$[m]$
λ	latent heat	$[\frac{J}{kg}]$
ρ	density	$[\frac{kg}{m^3}]$
Ψ	coupling coefficient= $\frac{(NA_p)}{(1-NV_p)}\Gamma$	

Subscripts

i	initial
j	time level

l	liquid
m	matrix
n	at or associated with control volume *n*
p	particle
ref	reference
s	solid

Superscripts

+	dimensionless
j	time level

Function

H[a]	step function

CHAPTER 1
INTRODUCTION

1.1. Rationale

Transient heat-transfer problems involving melting or solidification are generally referred to as phase-change or moving boundary problems. Sometimes, they are referred to as Stefan problems, with reference to the pioneering work of Stefan around 1890. Phase change problems have numerous applications in such areas as the making of ice, the freezing of food, the solidification of metals in castings, the cooling of large masses of igneous rock and recently new protective clothing are being developed that provide significant enhancements in thermal storage and comfort using encapsulated phase change materials.

There are many important applications involving heat transfer in heterogeneous materials like advanced composites used in aerospace structures to thermal treatments of biological materials or freezing of biological materials, which is important in both medical applications and in the preservation of food materials.

The transient thermal response of a heterogeneous material depends on the microstructure of the material. Homogeneous approximations with averaged properties are often used to model heterogeneous materials with good results. However, these types of approximations could lead to significant errors if the thermal properties of material constituents are substantially different. Homogeneous approximations using averaged properties cannot account for this. Thus, there is a need for more accurate mathematical models that consider the details of the microstructure to better understand the heat transfer phenomenon occurring within these materials. A better understanding of the mechanisms governing heat transfer within these materials could not only lead to more accurate modeling efforts, but could also possibly lead to new designs and/or treatments in which the non-homogeneous responses could be exploited.

1.2. Literature Review

Phase change boundary are nonlinear and their analytic solution is very difficult. A limited number of exact analytic solutions for idealized situations can be found in the textbooks. Purely numerical methods of solving phase change problems have been reported by a number of investigators, including Crank and Gupta [1972], Gupta [1974], Patanker [1980], Gupta and Kumar [1980], Crank [1981], Pham [1985], Tacke [1985], Poirier [1988], Ozisik [1994], Ketkar [1999]. Many books have been written on numerical heat transfer analysis, They address finite difference, finite element, control volume, and boundary element approaches to solving the governing thermal equations.

The finite difference method for solving homogeneous materials with phase-change problems has been proposed by many investigators. Shamsundar and Sparrow [1975] propose the analysis of multidimensional conduction phase change via the energy model. Hsiao [1985] presents an effective algorithm incorporating the equivalent heat capacity model. In Hsiao's formulation the method falls in the class of explicit temperature methods, applicable only to sharp phase change fronts. Pham [1987] aims to simplify the formulation of Hsiao's method, extending its application to materials that exhibit a gradual phase change. Kim and Kaviany [1990] present a method, which can be applied to specific problems that involve volumetric effects, heat generation and multiple moving boundaries. Date [1991] presents an enthalpy formulation for solving a one-dimensional Stefan problem; and many other literatures.

On the other hand, in heterogeneous materials the literature becomes very limited. Furmanski [1992] proposes an effective macroscopic description for heat conduction in heterogeneous materials. Also Furmanski [1994] presents the wall effects in heat conduction through a heterogeneous material. Colvin and Bryant [1996] present the results of a study of liquid-coupled heat exchange incorporating a microencapsulated phase-change material suspension as the working fluid. Vick and Scott [1998] propose the transient heat transfer characteristics of heterogeneous materials consisting of a

microstructure of relatively small particles embedded in a matrix which is the base of this thesis. Colvin and Bryant [1998] present the experimental results of protective clothing containing encapsulated phase-change materials such as foams with embedded microencapsulated phase-change materials and macroencapsulated phase-change material particle garments. Fomin and Saitoh [1999] investigated numerically and analytically on melting of unfixed material in a spherical capsule with a non-isothermal wall.

1.3. Problem Statement and Objectives

A one-dimensional model of a heterogeneous material consisting of a matrix with embedded separated particles is considered. The matrix is in imperfect contact with the particles, which means the contact conductance is finite. The lumped capacity approximation applies to each individual particle, which means the particles have a small Biot number (Biot number<0.1). The melting or solidification of the particles is investigated. Heat is generated inside the particles or is transferred from the matrix to the particles coupled through a contact conductance. The matrix is not allowed to change phase and energy is either generated inside the matrix or transferred from the boundaries, which is initially conducted through the matrix material. The physical model of this coupled, two-step process is solved using the energy method.

The investigation is conducted in several phases using a building block approach. First, a lumped capacity system during phase transition is studied. Then, a one-dimensional homogeneous material during phase change is investigated. Finally, the one-dimensional heterogeneous material is analyzed. A numerical solution based on the finite difference method is used to solve the model equations. This method readily allows for any kind of boundary conditions, any combination of material properties, particle sizes and contact conductance. In addition, computer programs, using Mathematica, are developed for the lumped capacity systems, homogeneous materials, and heterogeneous materials. Also this thesis investigates the effects of the control volume thickness, time step, contact conductance, material properties, internal source, and external source by using the provided computer programs.

1.4. Thesis Organization

Chapter 2 describes the physical model of energy-temperature relationship and dimensional and non-dimensional problem formulation of lumped capacity systems, homogeneous materials and heterogeneous materials.

Chapter 3 analyses a numerical solution, the finite difference method, for lumped capacity systems, homogeneous materials and heterogeneous materials.

Chapter 4 presents an investigation of the effectives of important parameters such as material properties, internal sources and external sources for lumped capacity systems, homogeneous materials and heterogeneous materials. It also discusses these results.

Chapter 5 concludes the thesis, and highlights areas of future research and development.

Appendices provide a complete listing of main software written for this thesis.

CHAPTER 2
PHYSICAL MODEL

2.1. Energy Method

The energy method is applicable for the solution of phase change problems involving both a distinct phase change at a discrete temperature as well as phase change taking place over an extended range of temperatures.

In the energy method formulation, the energy function *e(T*), which is the total internal energy content of the substance, enters the problem as a dependent variable along with the temperature.

The energy formulation of the phase change problem is given by,

$$\rho \frac{\partial e}{\partial t} = \nabla.(k\nabla T) + s(x, y, z, t, T)$$

which is considered valid over the entire solution domain, including both the solid and the liquid phases as well as the solid-liquid interface. The energy generation term *s(x,y,z,t,T)* is omitted if the problem involves no internal energy generation.

Therefore, the method is attractive in that the solution of the phase change problem is reduced to the solution of a single equation in terms of energy. There are no boundary conditions to be satisfied at the solid-liquid interface, there is no need to accurately track the phase-change boundary, there is no need to consider liquid and solid regions separately, and any numerical scheme such as the finite-difference or finite-element method can be used for its solution.

2.2. Energy-Temperature Relationship

In pure materials the phase-change takes place at a discrete temperature, and is associated with the latent heat λ as shown in Fig 2.2.1.(a). While in other cases, there is no discrete melting point temperature, because the phase change takes place over an extended range of temperatures as indicated in Fig 2.2.1.(b).

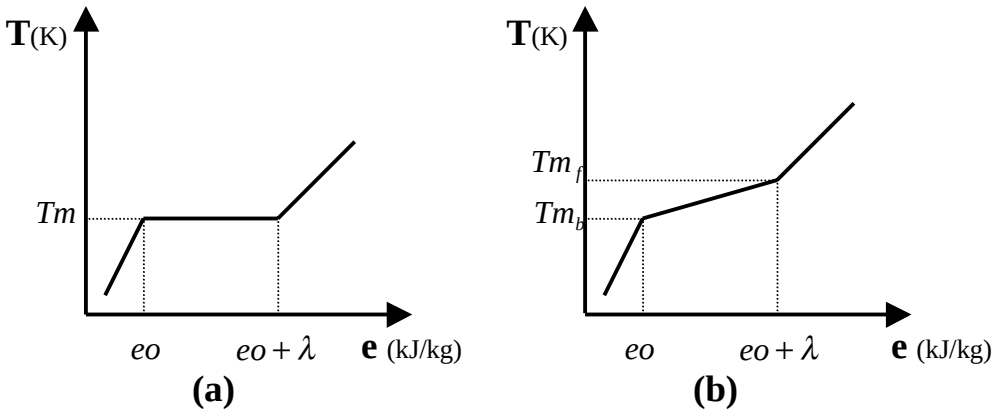

Fig 2.2.1. Energy-Temperature Relationship for:
(a) Pure Materials
(b) Hypothetical Materials

Consider a pure material that changes phase at temperature Tm, by assuming constant thermal properties (solid and liquid specific heat), and sharp phase transition at melting temperature Tm, the energy-temperature relationship takes the form,

$$T(e)=\begin{cases} Tm+\dfrac{1}{Cp_l}(e-eo-\lambda), & e>eo+\lambda \\ Tm, & eo\le e\le eo+\lambda \\ Tm+\dfrac{1}{Cp_s}(e-eo), & e<eo \end{cases} \qquad (2.1)$$

This can be reformulated in terms of the step function as,

$$T(e)=Tm+\frac{1}{Cp_s}(e-eo)H[e-eo]+\frac{1}{Cp_l}(e-eo-\lambda)H[e-eo-\lambda] \qquad (2.2)$$

Where e is specific internal energy, eo is the energy of the saturated solid, Tm is the temperature of phase change, $H[a]$ is the step function, and T, λ, Cp_s, Cp_l are as defined in the nomenclature.

In a hypothetical case, by assuming a linear function of the energy-temperature relationship during phase change as shown in Fig 2.2.1. (b) the equations take the form,

$$T(e) = \begin{cases} Tm_f + \dfrac{1}{Cp_l}(e - eo - \lambda), & e > eo + \lambda \\ Tm_b + \dfrac{Tm_f - Tm_b}{\lambda}(e - eo), & eo \le e \le eo + \lambda \\ Tm_b + \dfrac{1}{Cp_s}(e - eo), & e < eo \end{cases} \qquad (2.3)$$

This relationship can be reformulated in terms of the step function as,

$$\begin{aligned} T(e) = & \left\{ Tm_b + (e - eo)\left(\frac{Tm_f - Tm_b}{\lambda}\right) \right\} H[e - eo]\, H[eo + \lambda - e] + \\ & \left\{ Tm_b + \frac{1}{Cp_s}(e - eo) \right\} H[eo - e] + \left\{ Tm_f + \frac{1}{Cp_l}(e - eo - \lambda) \right\} H[e - eo - \lambda] \end{aligned} \qquad (2.4)$$

Tm_b and Tm_f are the beginning and finishing temperature of phase change.

In other cases, when the relationship between energy and temperature is not linear during phase change, this relationship must be defined by a nonlinear function or obtained from experimental data.

2.3. Problem Formulation for Lumped Capacity Systems

In a lumped system the variation of temperature within the medium can be neglected and temperature is considered to be a function of time only and spatially uniform. The lumped system analysis is valid only for Biot Number less than 0.1, where the Biot Number is the ratio of the internal thermal resistance to external thermal resistance. The lumped capacity system is indicated in Fig 2.3.1.

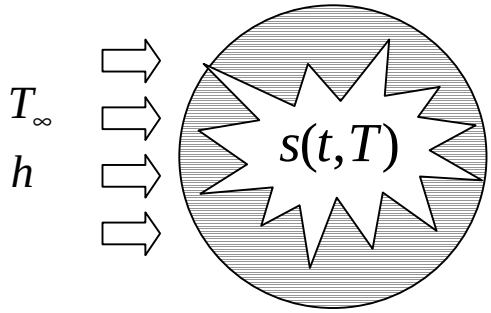

Fig 2.3.1. Lumped Capacity System

The energy balance equation for the lumped system takes the form,

$$\rho V \frac{de}{dt} = hA(T_\infty - T) + V s(t,T) \qquad (2.5)$$

The volumetric heat source term $s(t,T)$ (W/m^3) can be taken as a portion independent of temperature T and a portion proportional to T.

$$s(t,T) = sc(t) - sp(t)T \qquad (2.6)$$

Therefore the energy balance equation can be reformulated as,

$$\boxed{\rho V \frac{de}{dt} = hA(T_\infty - T) + V(sc(t) - sp(t)T)} \qquad (2.7)$$

This equation (2.7) must be solved simultaneously with the energy-temperature relationship equation (2.2) or (2.4) to compute energy and temperature. Once the initial condition is specified, the formulation is complete.

$$T(t) = T_i \qquad t = t_{initial} \qquad (2.8)$$

2.4. Problem Formulation for Homogeneous Materials

Consider melting or solidification of a one-dimensional homogeneous material as shown in Fig 2.4.1 with prescribed volumetric heat sources and boundary conditions, where the heat transfer is by conduction. A typical control volume for the one-dimensional homogenous material is shown in Fig 2.4.2.

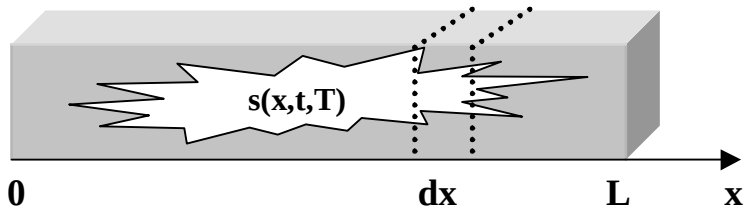

Fig 2.4.1. One-dimensional homogeneous material.

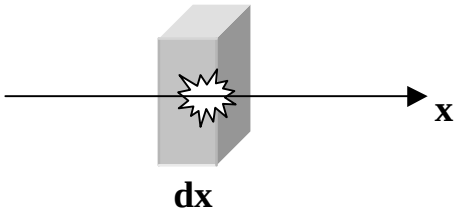

Fig 2.4.2. Typical control volume for a one dimensional homogeneous material.

In terms of the total energy, the governing equation takes the form,

$$\frac{\partial}{\partial x}(k\frac{\partial T}{\partial x}) + s(x,t,T) = \rho\frac{\partial e}{\partial t} \qquad (2.9)$$

The volumetric source term $s(x,t,T)$ (W/m^3) is taken as a portion independent of Temperature T and a portion proportional to T.

$$s(x,t,T) = sc(x,t) - sp(x,t)T \qquad (2.10)$$

Thermal conductivity k may vary with position x in order to model layered or composite structures and could vary with temperature T to model temperature dependent properties. The equation can be reformulated as,

$$\boxed{\frac{\partial}{\partial x}(k\frac{\partial T}{\partial x}) + sc(x,t) - sp(x,t)T = \rho\frac{\partial e}{\partial t}} \qquad (2.11)$$

Once again, equation (2.11) must be solved simultaneously with equation (2.2) or (2.4) to compute energy and temperature. Once boundary conditions and initial condition are specified, the formulation is complete.

The initial condition can be written as,

$$T(x,t) = T_i(x) \qquad t = t_{initial} \tag{2.12}$$

The type of boundary condition at *x=0* can be considered as,

1. Specified temperature, *Tx0*
   $$T(0,t) = Tx0 \tag{2.13}$$

2. Specified heat flux *qx0* with convection *hx0* and $Tx0_\infty$
   $$-k\frac{\partial T}{\partial x} = qx0 + hx0[Tx0_\infty - T(0,t)] \tag{2.14}$$

And also the type of boundary condition at *x=L* can be considered as,

1. Specified temperature, *TxL*
   $$T(L,t) = TxL \tag{2.15}$$

2. Specified heat flux *qxL* with convection *hxL* and TxL_∞
   $$-k\frac{\partial T}{\partial x} = qxL + hxL[TxL_\infty - T(L,t)] \tag{2.16}$$

2.5. Problem Formulation for Heterogeneous Materials

Consider a one-dimensional heterogeneous material composed of a matrix containing uniformly distributed particles as shown in Fig 2.5.1. with possible melting or solidification of the particles. The particles are separated and the lumped capacity approximation is valid within each particle. Heat is transferred from the boundaries or is generated inside the particles or matrix. The heat exchange between the matrix and particles is characterized by a contact conductance. A typical control volume for the one-dimensional heterogeneous material is shown in Fig 2.5.2.

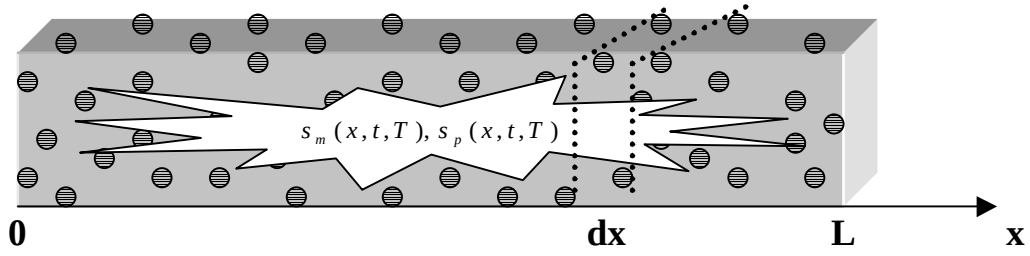

Fig 2.5.1. One-dimensional heterogeneous materials.

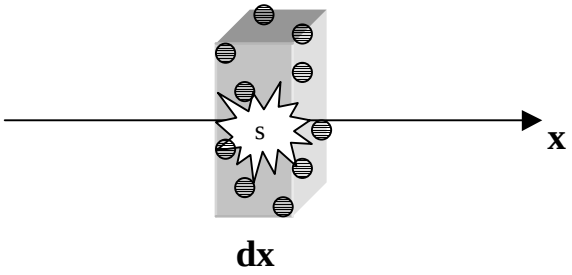

Fig 2.5.2. Typical control volume for a one-dimensional heterogeneous material.

The microstructure is characterized by the number density of the particles (number of particles per total volume) N and an average particle diameter d.

In addition a contact conductance, h_c, characterizes the contact between the particles and the matrix, and s_m and s_p are volumetric heat sources in the matrix and particles respectively.

The volume fractions of the particles and matrix are NV_p and $(1-NV_p)$ respectively, where $A_p = \pi d^2$ is the average surface area of a single particle and $V_p = \pi d^3/6$ is the average volume of a single particle. The area fractions at a given cross section are equal to the volume fractions.

With this physical model, the energy equations for the matrix and particles for one-dimensional heat flow can be expressed as,

Matrix:

$$(1-NV_p)(\rho Cp)_m \frac{\partial T_m}{\partial t} = \frac{\partial}{\partial x}((1-NV_p)k_m \frac{\partial T_m}{\partial x}) - h_c(NA_p)(T_m - T_p) + (1-NV_p)s_m(x,t,T) \quad (2.17)$$

Particles:

$$(NV_p)\rho_p \frac{\partial e}{\partial t} = h_c(NA_p)(T_m - T_p) + (NV_p)s_p(x,t,T) \quad (2.18)$$

These energy equations for the matrix and particles can be reformed as,

Matrix:

$$C_m \frac{\partial T_m}{\partial t} = \frac{\partial}{\partial x}(K_m \frac{\partial T_m}{\partial x}) - H_c(T_m - T_p) + Sc_m(x,t) - Sp_m(x,t)T_m \quad (2.19)$$

Particles:

$$(NV_p)\rho_p \frac{\partial e}{\partial t} = H_c(T_m - T_p) + Sc_p(x,t) - Sp_p(x,t)T_p \quad (2.20)$$

where $C_m = (1-NV_p)(\rho Cp)_m$ is the heat capacity of the matrix per total volume, $K_m = (1-NV_p)k_m$ is the conductance through the matrix, and $H_c = h_c(NA_p)$ is the coefficient coupling the matrix and particle temperatures. Also the matrix and particle heat sources are as,

$$(1-NV_p)s_m(x,t,T) = Sc_m(x,t) - Sp_m(x,t)T_m \quad (2.21)$$

$$(NV_p)s_p(x,t,T) = Sc_p(x,t) - Sp_p(x,t)T_p \quad (2.22)$$

Once again, the particles energy equation (2.20) must be solved simultaneously with the energy-temperature relationship equation (2.2) or (2.4) to evaluate the energy and temperature of the particles.

Once boundary conditions and initial conditions are specified, the formulation is complete. The initial conditions can be written as,

$$T_m(x,t) = T_i(x) \qquad t = t_{initial} \qquad (2.23)$$

$$T_p(x,t) = T_i(x) \qquad t = t_{initial} \qquad (2.24)$$

Since there is no particle on the boundaries, as for the homogeneous case two types of boundary considered. At $x=0$:

1. Specified temperature, $Tx0$

$$T_m(0,t) = Tx0 \qquad (2.25)$$

2. Specified heat flux $qx0$ with convection $hx0$ *and* $Tx0_\infty$

$$-k_m \frac{\partial T_m}{\partial x} = qx0 + hx0[Tx0_\infty - T_m(0,t)] \qquad (2.26)$$

At $x=L$:

1. Specified temperature, TxL

$$T_m(L,t) = TxL \qquad (2.27)$$

2. Specified heat flux qxL with convection hxL *and* TxL_∞

$$-k_m \frac{\partial T_m}{\partial x} = qxL + hxL[TxL_\infty - T_m(L,t)] \qquad (2.28)$$

2.6. Dimensionless Formulation

The result of a dimensional analysis of a problem is a reduction of the number of variables in the problem. A function of one variable may be plotted as a single curve. A function of two variables is represented by a family of curves (chart), one curve for each value of the second variable. A function of three variables is represented by a set of charts, one chart for each value of the third variable, and so on. Therefore, a reduction of the number of variables in a problem, dimensional analysis, is an important mathematical tool. The dimensionless formulation for the lumped capacity systems, homogeneous materials, and heterogeneous materials are developed in this section.

2.6.1. Lumped Capacity Systems

The energy balance equation for a lumped system and the energy-temperature relationship for a hypothetical material with a linear function relationship during phase transition are given by equations (2.7) and (2.4).

In order to scale the physical problem, five reference quantities are chosen: solid thermal properties, ρ_s, Cp_s, characteristic length $L = \frac{V}{A}$, temperature rise $\Delta T_{ref} = T_i - T_\infty$ and the heat convection coefficient h. This choice produces dimensional reference quantities, and also these references provide the following dimensionless variables and parameters, as indicated in Tables 2.6.1.-2.6.3.

Table 2.6.1. Dependent variables of a lumped capacity system.

Real Quantity	***Units***	***Reference Quantity***	***Dimensionless Quantity***
Temperature rise $T - T_\infty$	$^\circ C$	$\Delta T_{ref} = T_i - T_\infty$	$T^+ = \frac{T - T_\infty}{\Delta T_{ref}}$
Energy Change Per mass *e-eo*	$\frac{kJ}{kg}$	$\Delta e_{ref} = Cp_s \Delta T_{ref}$	$e^+ = \frac{e - eo}{\Delta e_{ref}} = \frac{e - eo}{Cp_s \Delta T_{ref}}$

Table 2.6.2. Independent variables of a lumped capacity system.

Real Quantity	***Units***	***Reference Quantity***	***Dimensionless Quantity***
Time t	sec	$t_{ref} = \dfrac{\rho_s Cp_s L}{h}$	$t^+ = \dfrac{t}{t_{ref}} = \dfrac{t}{\rho_s Cp_s L / h}$

Table 2.6.3. Parameters of a lumped capacity system.

Real Quantity	***Units***	***Reference Quantity***	***Dimensionless Quantity***
Characteristic Length $L = \dfrac{V}{A}$	m	$L_{ref} = L = \dfrac{V}{A}$	$L^+ = \dfrac{L}{L_{ref}} = \dfrac{(V/A)}{(V/A)} = 1$
Density ρ	$\dfrac{kg}{m^3}$	$\rho_{ref} = \rho_s$	$\rho^+ = \dfrac{\rho_s}{\rho_{ref}} = 1$
Heat Capacity Cp	$\dfrac{kJ}{kg^\circ C}$	$Cp_{ref} = Cp_s$	$Cp_s^+ = \dfrac{Cp_s}{Cp_{ref}} = \dfrac{Cp_s}{Cp_s} = 1$ $Cp_l^+ = \dfrac{Cp_l}{Cp_{ref}} = \dfrac{Cp_l}{Cp_s} = Cr$
Melting Temperature Tm	$^\circ C$	ΔT_{ref}	$Tm_b{}^+ = \dfrac{Tm_b - T_\infty}{\Delta T_{ref}}$ $Tm_f{}^+ = \dfrac{Tm_f - T_\infty}{\Delta T_{ref}}$
Latent Heat λ	$\dfrac{kJ}{kg}$	$\lambda_{ref} = Cp_s \Delta T_{ref}$	$\lambda^+ = \dfrac{\lambda}{\lambda_{ref}} = \dfrac{\lambda}{Cp_s \Delta T_{ref}} = \dfrac{1}{Ste}$

Convective Environment h, T_∞	$\frac{W}{m^2 {}^\circ C}$ $^\circ C$	$h_{ref} = h$ ΔT_{ref}	$h^+ = \frac{h}{h_{ref}} = 1$ $T_\infty{}^+ = \frac{T_\infty - T_\infty}{\Delta T_{ref}} = 0$
Heat Source	$\frac{W}{m^3}$ $\frac{W}{m^3 {}^\circ C}$	$sc_{ref} = \frac{h\Delta T_{ref}}{L}$ $sp_{ref} = \frac{h}{L}$	$sc^+ = \frac{sc - spT_\infty}{sc_{ref}} = \frac{sc - spT_\infty}{h\Delta T_{ref}/L}$ $sp^+ = \frac{sp}{sp_{ref}} = \frac{sp}{h/L}$
Initial Temperature	$^\circ C$	ΔT_{ref}	$T_i{}^+ = \frac{T_i - T_\infty}{\Delta T_{ref}} = 1$

Substituting these dimensionless variables into equations (2.4) and (2.7) produces,

$$\frac{de^+}{dt^+} = -T^+ + sc^+(t^+) - sp^+(t^+)T^+ \qquad (2.29)$$

$$T^+(e^+) = \left\{Tm_b^+ + e^+(Tm_f^+ - Tm_b^+)Ste\right\} H[e^+]\, H[\frac{1}{Ste} - e^+] + \left\{Tm_b^+ + e^+\right\} H[-e^+] + \left\{Tm_f^+ + \frac{1}{Cr}(e^+ - \frac{1}{Ste})\right\} H[e^+ - \frac{1}{Ste}] \qquad (2.30)$$

These two equations (2.29) and (2.30) must be solved simultaneously to compute energy and temperature. The initial condition is defined below and the formulation is complete.

$$T^+(t^+) = T_i^+ = 1 \quad , \; t^+ = 0 \qquad (2.31)$$

Six important dimensionless groups result from this dimensionless scaling,

Stefan Number $= Ste = \dfrac{Cp_s \Delta T_{ref}}{\lambda}$

Heat Capacity Ratio $= Cr = \dfrac{Cp_l}{Cp_s}$

$$sc^+ = \frac{sc - spT_\infty}{h\Delta T_{ref} / L}$$

$$sp^+ = \frac{sp}{h / L}$$

$$Tm_b{}^+ = \frac{Tm_b - T_\infty}{\Delta T_{ref}}$$

$$Tm_f{}^+ = \frac{Tm_f - T_\infty}{\Delta T_{ref}}$$

2.6.2. Homogeneous Materials

The energy equation for one-dimensional homogeneous materials and the energy-temperature relationship for a hypothetical material with a linear function relationship during phase transition are given by equations (2.11) and (2.4).

In order to scale the physical problem, five reference quantities are chosen: Solid thermal properties, ρ_s, Cp_s, k_s, the region length L and temperature difference ΔT_{ref}. This choice produces dimensional reference quantities, and also these references provide the following dimensionless variables and parameters, as indicated in Tables 2.6.4.-2.6.6.

Table 2.6.4. Dependent variables of a homogeneous material system.

Real Quantity	***Units***	***Reference Quantity***	***Dimensionless Quantity***
Temperature rise $T - T_{ground}$	$^{\circ}C$	**Specified Temp.** $\Delta T_{ref} = T_i - T_0$ **Specified Heat Flux** $\Delta T_{ref} = \frac{q_0'' L}{k_s}$ **Convection** $\Delta T_{ref} = T_i - T_\infty$ **Specified Heat Source** $\Delta T_{ref} = \frac{scL^2}{k_s}$	$T^+ = \frac{T - T_{ground}}{\Delta T_{ref}}$ $T_{ground} = T_0$ **Specified Temp.** $T_{ground} = T_i$ **Specified Heat Flux** $T_{ground} = T_\infty$ **Convection** $T_{ground} = T_i$ **Specified Heat Source**
Energy Change Per mass *e-eo*	$\frac{kJ}{kg}$	$\Delta e_{ref} = Cp_s \Delta T_{ref}$	$e^+ = \frac{e - eo}{\Delta e_{ref}} = \frac{e - eo}{Cp_s \Delta T_{ref}}$

Table 2.6.5. Independent variables of a homogeneous material system.

Real Quantity	***Units***	***Reference Quantity***	***Dimensionless Quantity***
Distance x	m	$x_{ref} = L$	$x^+ = \frac{x}{x_{ref}} = \frac{x}{L}$

Time t	sec	$t_{ref} = \frac{\rho Cp_s L^2}{k_s}$	$t^+ = \frac{t}{t_{ref}} = \frac{t}{\rho Cp_s L^2 / k_s}$

Table 2.6.6. Parameters of a homogeneous material system.

Real Quantity	***Units***	***Reference Quantity***	***Dimensionless Quantity***
Length L	m	$L_{ref} = L$	$L^+ = \frac{L}{L_{ref}} = 1$
Conductivity k	$\frac{W}{m^\circ C}$	$k_{ref} = k_s$	$k_s^+ = \frac{k_s}{k_{ref}} = \frac{k_s}{k_s} = 1$ $k_l^+ = \frac{k_l}{k_{ref}} = \frac{k_l}{k_s} = Kr$
Density ρ	$\frac{kg}{m^3}$	$\rho_{ref} = \rho_s$	$\rho^+ = \frac{\rho_s}{\rho_{ref}} = 1$
Heat Capacity Cp	$\frac{kJ}{kg^\circ C}$	$Cp_{ref} = Cp_s$	$Cp_s^+ = \frac{Cp_s}{Cp_{ref}} = \frac{Cp_s}{Cp_s} = 1$ $Cp_l^+ = \frac{Cp_l}{Cp_{ref}} = \frac{Cp_l}{Cp_s} = Cr$
Melting Temperature Tm	$^\circ C$	ΔT_{ref}	$Tm_b{}^+ = \frac{Tm_b - T_{ground}}{\Delta T_{ref}}$ $Tm_f{}^+ = \frac{Tm_f - T_{ground}}{\Delta T_{ref}}$
Latent Heat λ	$\frac{kJ}{kg}$	$\lambda_{ref} = Cp_s \Delta T_{ref}$	$\lambda^+ = \frac{\lambda}{\lambda_{ref}} = \frac{\lambda}{Cp_s \Delta T_{ref}} = \frac{1}{Ste}$

Boundary Condition:			
Specified Temperature T_0	$^\circ C$	$\Delta T_{ref} = T_i - T_0$	$T_0^+ = \dfrac{T_0 - T_{ground}}{\Delta T_{ref}} = 0$
Heat Flux $q_0^{"}$	$\dfrac{W}{m^2}$	$q_{ref}^{"} = \dfrac{k_s \Delta T_{ref}}{L}$	$q_0^{"+} = \dfrac{q_0^{"}}{q_{ref}} = \dfrac{q_0^{"}}{k_s \Delta T_{ref} / L}$
Convection h_∞, T_∞	$\dfrac{W}{m^2\,^\circ C}$	$h_{ref} = \dfrac{k_s}{L}$	$h_\infty^+ = \dfrac{h_\infty}{h_{ref}} = \dfrac{h_\infty}{k_s / L}$
	$^\circ C$	$\Delta T_{ref} = T_i - T_\infty$	$T_\infty^+ = \dfrac{T_\infty - T_{ground}}{\Delta T_{ref}} = 0$
Heat Source	$\dfrac{W}{m^3}$	$sc_{ref} = \dfrac{k_s \Delta T_{ref}}{L^2}$	$sc^+ = \dfrac{sc - spT_{ground}}{sc_{ref}} = \dfrac{sc - spT_{ground}}{k_s \Delta T_{ref} / L^2}$
	$\dfrac{W}{m^3\,^\circ C}$	$sp_{ref} = \dfrac{k_s}{L^2}$	$sp^+ = \dfrac{sp}{sp_{ref}} = \dfrac{sp}{k_s / L^2}$
Initial Temperature	$^\circ C$	ΔT_{ref}	$T_i^+ = \dfrac{T_i - T_{ground}}{\Delta T_{ref}}$ $T_i^+ = 1$ Specified Temp. or Convection $T_i^+ = 0$ Specified Heat Flux or Heat Source

Substituting these dimensionless variables into equations (2.11) and (2.4) produces,

$$\frac{\partial}{\partial x^+}(k^+ \frac{\partial T^+}{\partial x^+}) + sc^+(x^+, t^+) - sp^+(x^+, t^+)T^+ = \frac{\partial e^+}{\partial t^+} \qquad (2.32)$$

$$T^+(e^+) = \left\{Tm_b^+ + e^+(Tm_f^+ - Tm_b^+)Ste\right\} H[e^+]\, H[\frac{1}{Ste} - e^+] + \left\{Tm_b^+ + e^+\right\} H[-e^+] + \left\{Tm_f^+ + \frac{1}{Cr}(e^+ - \frac{1}{Ste})\right\} H[e^+ - \frac{1}{Ste}] \qquad (2.33)$$

Equations (2.32) and (2.33) must be solved simultaneously to compute energy and temperature. The initial condition and boundary conditions are defined as below and the formulation is complete.

The initial condition can be written as,

$$T^+(x^+,t^+)=\begin{cases}1 & \textit{Specified Temperature or Convection}\\ 0 & \textit{Specified Heat Flux or Heat Source}\end{cases}, \quad t^+=0 \qquad (2.34)$$

The type of boundary condition at $x^+=0$ can be considered as,

1. Specified temperature, $Tx0^+$

$$T^+(0,t^+)=Tx0^+ \qquad (2.35)$$

2. Specified heat flux $qx0^+$ with convection $hx0^+$ and $Tx0^+_\infty$

$$-\frac{\partial T^+}{\partial x^+}=qx0^+ + hx0^+[Tx0^+_\infty - T^+(0,t^+)] \qquad (2.36)$$

Also the type of boundary condition at $x^+=L^+=1$ can be considered as,

1.Specified temperature, TxL^+

$$T^+(1,t^+)=TxL^+ \qquad (2.37)$$

2. Specified heat flux qxL^+ with convection hxL^+ and TxL^+_∞

$$-\frac{\partial T^+}{\partial x^+}=qxL^+ + hxL^+[TxL^+_\infty - T^+(1,t^+)] \qquad (2.38)$$

Nine important dimensionless groups result from this dimensionless scaling,

Stefan Number $= Ste = \dfrac{Cp_{ref}\Delta T_{ref}}{\lambda}$

Heat Capacity Ratio $= Cr = \dfrac{Cp_l}{Cp_s}$

Conductivity Ratio $= Kr = \dfrac{k_l}{k_s}$

$$sc^{+} = \frac{sc - spT_{ground}}{k_s \Delta T_{ref} / L^2}$$

$$sp^{+} = \frac{sp}{k_s / L^2}$$

$$Tm_b{}^{+} = \frac{Tm_b - T_{ground}}{\Delta T_{ref}}$$

$$Tm_f{}^{+} = \frac{Tm_f - T_{ground}}{\Delta T_{ref}}$$

$$q_0^{"+} = \frac{q_0^{"}}{k_s \Delta T_{ref} / L}$$

$$h_\infty^{+} = \frac{h_\infty}{k_s / L}$$

2.6.3. Heterogeneous Materials

The energy equation for one-dimensional heterogeneous materials and the energy-temperature relationship for a hypothetical material with a linear function relationship during phase transition are given by equations (2.19), (2.20) and (2.4).

In order to scale the physical problem, five reference quantities are chosen: the matrix solid thermal properties, $\rho_{m,s}, Cp_{m,s}, k_{m,s}$, the region length L and temperature rise ΔT_{ref}.

This choice produces dimensional reference quantities, and also these references provide the following dimensionless variables and parameters, as indicated in Tables 2.6.7.-2.6.9.

Table 2.6.7. Dependent variables of a heterogeneous material system.

Real Quantity	***Units***	***Reference Quantity***	***Dimensionless Quantity***
Temperature rise $T - T_{ground}$	$^{\circ}C$	**Specified Temp.** $\Delta T_{ref} = T_i - T_0$ **Specified Heat Flux** $\Delta T_{ref} = \frac{q_0^{"} L}{k_{m,s}}$ **Convection** $\Delta T_{ref} = T_i - T_\infty$ **Specified Heat Source** $\Delta T_{ref} = \frac{scL^2}{k_{m,s}}$	$T^+ = \frac{T - T_{ground}}{\Delta T_{ref}}$ $T_{ground} = T_0$ **Specified Temp.** $T_{ground} = T_i$ **Specified Heat Flux** $T_{ground} = T_\infty$ **Convection** $T_{ground} = T_i$ **Specified Heat Source**
Energy Change Per mass *e-eo*	$\frac{kJ}{kg}$	$\Delta e_{ref} = Cp_{m,s} \Delta T_{ref}$	$e^+ = \frac{e - eo}{\Delta e_{ref}} = \frac{e - eo}{Cp_{m,s} \Delta T_{ref}}$

Table 2.6.8. Independent variables of a heterogeneous material system.

Real Quantity	***Units***	***Reference Quantity***	***Dimensionless Quantity***
Distance x	m	$x_{ref} = L$	$x^+ = \frac{x}{x_{ref}} = \frac{x}{L}$
Time t	sec	$t_{ref} = \frac{\rho_{m,s} Cp_{m,s} L^2}{k_{m,s}}$	$t^+ = \frac{t}{t_{ref}} = \frac{t}{\rho_{m,s} Cp_{m,s} L^2 / k_{m,s}}$

Table 2.6.9. Parameters of a heterogeneous material system.

Real Quantity	***Units***	***Reference Quantity***	***Dimensionless Quantity***
Length L	m	$L_{ref} = L$	$L^+ = \frac{L}{L_{ref}} = 1$
Conductivity k	$\frac{W}{m^\circ C}$	$k_{ref} = k_{m,s}$	$k_{m,s}^+ = \frac{k_{m,s}}{k_{ref}} = 1$
Density ρ	$\frac{kg}{m^3}$	$\rho_{ref} = \rho_{m,s}$	$\rho_{m,s}^+ = \frac{\rho_{m,s}}{\rho_{ref}} = 1$
Heat Capacity Cp	$\frac{kJ}{kg^\circ C}$	$Cp_{ref} = Cp_{m,s}$	$Cp_{m,s}^+ = \frac{Cp_{m,s}}{Cp_{ref}} = 1$ $Cp_{p,s}^+ = \frac{Cp_{p,s}}{Cp_{ref}} = Cr_s$ $Cp_{p,l}^+ = \frac{Cp_{p,l}}{Cp_{ref}} = Cr_l$
Melting Temperature Tm	$^\circ C$	ΔT_{ref}	$Tm_b{}^+ = \frac{Tm_b - T_{ground}}{\Delta T_{ref}}$ $Tm_f{}^+ = \frac{Tm_f - T_{ground}}{\Delta T_{ref}}$

Latent Heat λ	$\frac{kJ}{kg}$	$\lambda_{ref} = Cp_{m,s}\Delta T_{ref}$	$\lambda^{+} = \frac{\lambda}{\lambda_{ref}} = \frac{\lambda}{Cp_{m,s}\Delta T_{ref}}$
Boundary Condition:			
Specified Temperature T_0	$^{\circ}C$	$\Delta T_{ref} = T_i - T_0$	$T_0^{+} = \frac{T_0 - T_{ground}}{\Delta T_{ref}} = 0$
Heat Flux $q_0^{"}$	$\frac{W}{m^2}$	$q_{ref}^{"} = \frac{k_{m,s}\Delta T_{ref}}{L}$	$q_0^{"+} = \frac{q_0^{"}}{q_{ref}} = \frac{q_0^{"}}{k_{m,s}\Delta T_{ref} / L}$
Convection h_∞, T_∞	$\frac{W}{m^2\,^{\circ}C}$	$h_{ref} = \frac{k_{m,s}}{L}$	$h_\infty^{+} = \frac{h_\infty}{h_{ref}} = \frac{h_\infty}{k_{m,s} / L}$
	$^{\circ}C$	$\Delta T_{ref} = T_i - T_\infty$	$T_\infty^{+} = \frac{T_\infty - T_{ground}}{\Delta T_{ref}} = 0$
Heat Source	$\frac{W}{m^3}$	$Sc_{ref} = \frac{(1 - NV_p)k_{m,s}\Delta T_{ref}}{L^2}$	$Sc^{+} = \frac{Sc - SpT_{ground}}{Sc_{ref}}$
	$\frac{W}{m^3\,^{\circ}C}$	$Sp_{ref} = \frac{(1 - NV_p)k_{m,s}}{L^2}$	$Sp^{+} = \frac{Sp}{Sp_{ref}}$
Initial Temperature	$^{\circ}C$	ΔT_{ref}	$T_i^{+} = \frac{T_i - T_{ground}}{\Delta T_{ref}}$ $T_i^{+} = 1$ Specified Temp. or Convection $T_i^{+} = 0$ Specified Heat Flux Heat Source

Substituting these dimensionless variables into energy equations (2.19), (2.20) and (2.4), produces,

Matrix:

$$\frac{\partial T_m^+}{\partial t^+} = \frac{\partial}{\partial x^+}(k_m^+ \frac{\partial T_m^+}{\partial x^+}) - \Psi(T_m^+ - T_p^+) + Sc_m^+(x^+, t^+) - Sp_m^+(x^+, t^+)T_m^+ \quad (2.39)$$

Particles:

$$Mr\frac{\partial e^+}{\partial t^+} = \Psi(T_m^+ - T_p^+) + Sc_p^+(x^+, t^+) - Sp_p^+(x^+, t^+)T_p^+ \quad (2.40)$$

$$T_p^+(e^+) = \{Tm_s^+ + e^+(Tm_f^+ - Tm_s^+)Ste\}H[e^+]\,H[\frac{1}{Ste} - e^+] + \left\{Tm_s^+ + \frac{1}{Cr_s}e^+\right\}H[-e^+] + \left\{Tm_f^+ + \frac{1}{Cr_l}(e^+ - \frac{1}{Ste})\right\}H[e^+ - \frac{1}{Ste}] \quad (2.41)$$

The equations (2.40) and (2.41) must be solved simultaneously to compute energy and temperature of particles.

The initial conditions and boundary conditions are defined as below and the formulation is complete.

The initial conditions can be written as,

$$T_m^+(x^+, t^+) = T_p^+(x^+, t^+) = \begin{cases} 1 & Specified\ Temp.\ or\ Convection \\ 0 & Specified\ Heat\ Flux\ Heat\ Source \end{cases}, \quad t^+ = 0 \quad (2.42)$$

The type of boundary condition at $x^+ = 0$ can be considered as,

1. Specified temperature, $Tx0^+$

$$T_m^+(0, t^+) = Tx0^+ \quad (2.43)$$

2. Specified heat flux $qx0^+$ with convection $hx0^+$ and $Tx0_\infty^+$

$$-\frac{\partial T_m^+}{\partial x^+} = qx0^+ + hx0^+[Tx0_\infty^+ - T_m^+(0, t^+)] \quad (2.44)$$

Also the type of boundary condition at $x^+ = L^+ = 1$ can be considered as,

1.Specified temperature, TxL^+

$$T_m^+(1,t^+) = TxL^+ \qquad (2.45)$$

2. Specified heat flux qxL^+ with convection hxL^+ and TxL_∞^+

$$-\frac{\partial T_m^+}{\partial x^+} = qxL^+ + hxL^+[TxL_\infty^+ - T_m^+(1,t^+)] \qquad (2.46)$$

Ten important dimensionless groups result from this dimensionless scaling,

Stefan Number $= Ste = \dfrac{Cp_{m,s}\Delta T_{ref}}{\lambda}$

Heat Capacity Ratio $= Cr = \dfrac{Cp}{Cp_{m,s}}$

Mass Ratio $= Mr = \dfrac{\rho_p(NV_p)}{\rho_{m,s}(1-NV_p)}$

Coupling Coefficient $= \Psi = \dfrac{H_c L^2}{(1-NV_p)k_{m,s}} = \dfrac{(NA_p)h_c L^2}{(1-NV_p)k_{m,s}} = \dfrac{(NA_p)}{(1-NV_p)}\Gamma$

$$Sc^+ = \frac{Sc - SpT_{ground}}{(1-NV_p)k_{m,s}\Delta T_{ref}/L^2}$$

$$Sp^+ = \frac{Sp}{(1-NV_p)k_{m,s}/L^2}$$

$$Tm_b{}^+ = \frac{Tm_b - T_{ground}}{\Delta T_{ref}}$$

$$Tm_f{}^+ = \frac{Tm_f - T_{ground}}{\Delta T_{ref}}$$

$$q_0^{"+} = \frac{q_0^{"}}{k_{m,s}\Delta T_{ref}/L}$$

$$h_\infty^+ = \frac{h_\infty}{k_{m,s}/L}$$

CHAPTER 3
NUMERICAL ANALYSIS

3.1. Lumped Capacity Systems

The energy balance equation for the lumped system and the energy-temperature relationship equation for a hypothetical material with a linear function relationship during phase change are given by equations (2.7) and (2.4),

$$\rho V \frac{de}{dt} = hA(T_\infty - T) + V[sc(t) - sp(t)T] \qquad (2.7)$$

$$T(e) = \left\{ Tm_b + (e - eo)\frac{Tm_f - Tm_b}{\lambda} \right\} H[e - eo]\, H[eo + \lambda - e] + \left\{ Tm_b + \frac{1}{Cp_s}(e - eo) \right\} H[eo - e] + \left\{ Tm_f + \frac{1}{Cp_l}(e - eo - \lambda) \right\} H[e - eo - \lambda] \qquad (2.4)$$

This differential equation can be approximated with finite differences by using the explicit or implicit method.

3.1.1. Finite Difference Discretization

The time variable is discretized into a sequence of steps.

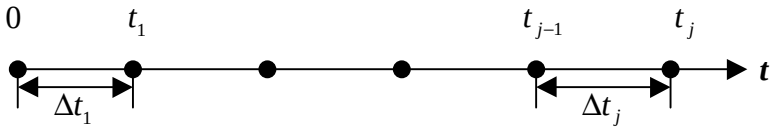

By integrating the equation (2.7) over the time interval t_{j-1} to t_j, this equation takes the form,

$$\int_{t=t_{j-1}}^{t=t_j} [\rho V \frac{de}{dt}] dt = \int_{t=t_{j-1}}^{t=t_j} \{hA(T_\infty - T) + V[sc(t) - sp(t)T]\} dt \qquad (3.1)$$

Integrating over time in an implicit method means that the temperature over each time interval is evaluated at the end of the interval. That is, the temperature T^j at time level t_j represents the average over the time interval Δt_j preceding time t_j. And in the explicit method, the temperature over each time interval is evaluated at the beginning of the interval.

By using the explicit and implicit method, each term of the equation (3.1) takes the form,

$$\int_{t=t_{j-1}}^{t=t_j} [\rho V \frac{de}{dt}]dt = \rho V(e^j - e^{j-1})$$

$$\int_{t=t_{j-1}}^{t=t_j} [hA(T_\infty - T)]dt = hA\{(1-\beta)[T_\infty - T^{j-1}] + \beta[T_\infty - T^j]\}\Delta t_j$$

$$\int_{t=t_{j-1}}^{t=t_j} V[sc(t) - sp(t)T]dt = V\{(1-\beta)[sc^{j-1} - sp^{j-1}T^{j-1}] + \beta[sc^j - sp^jT^j]\}\Delta t_j$$

where $\beta = 0$ for the explicit method, and $\beta = 1$ for the implicit method.

Now by substituting these terms into the equation (3.1), the finite difference form of the equation will be arranged as,

$$\rho V(e^j - e^{j-1}) = (1-\beta)[hA(T_\infty - T^{j-1}) + V(sc^{j-1} - sp^{j-1}T^{j-1})]\Delta t_j + \beta[hA(T_\infty - T^j) + V(sc^j - sp^jT^j)]\Delta t_j \quad (3.2)$$

The initial condition is defined as,

$$T^0 = T_{initial} \quad (3.3.a)$$

$$e^0 = e_{initial} \quad (3.3.b)$$

3.1.2. Explicit Method

According to the equation (3.2) for the explicit scheme with $\beta = 0$, at each time step e^j will be computed as,

$$e^j = e^{j-1} + \frac{hA}{\rho V}(T_\infty - T^{j-1})\Delta t_j + \frac{1}{\rho}(sc^{j-1} - sp^{j-1}T^{j-1})\Delta t_j \qquad (3.4)$$

By knowing e^j and using the equation (2.4) the temperature can be computed at each time step,

$$T^j(e^j) = \left\{Tm_b + (e^j - eo)\frac{Tm_f - Tm_b}{\lambda}\right\} H[e^j - eo]\, H[eo + \lambda - e^j] + \left\{Tm_b + \frac{1}{Cp_s}(e^j - eo)\right\} H[eo - e^j] + \left\{Tm_f + \frac{1}{Cp_l}(e^j - eo - \lambda)\right\} H[e^j - eo - \lambda] \qquad (3.5)$$

The explicit scheme has stability problems if the time step is too large, causing uncontrolled, nonphysical oscillations in the solutions. Therefore, to achieve a stable, physically meaningful solution, the coefficient of e^{j-1} in equation (3.4) has to be positive. After substituting T^{j-1} in terms of e^{j-1} by equation (3.5) or (2.3),

$$T^{j-1}(e) = \begin{cases} Tm_f + \frac{1}{Cp_l}(e^{j-1} - eo - \lambda), & e^{j-1} > eo + \lambda \\ Tm_b + \frac{Tm_f - Tm_b}{\lambda}(e^{j-1} - eo), & eo \le e^{j-1} \le eo + \lambda \\ Tm_b + \frac{1}{Cp_s}(e^{j-1} - eo), & e^{j-1} < eo \end{cases} \qquad (3.6)$$

As a result, the following condition has to be satisfied for stability,

$$\Delta t_j \le \begin{cases} [Cp_l]\frac{\rho V}{hA + Vsp^{j-1}}, & e^{j-1} > eo + \lambda \\ \left[\frac{\lambda}{Tm_f - Tm_b}\right]\frac{\rho V}{hA + Vsp^{j-1}}, & eo \le e^{j-1} \le eo + \lambda \\ [Cp_s]\frac{\rho V}{hA + Vsp^{j-1}}, & e^{j-1} < eo \end{cases} \qquad (3.7)$$

According to equation (3.7) for pure materials, when $Tm_f = Tm_b$, during phase change Δt_j has to be less than infinity, which means there is no restriction for the time step. As a result, the explicit method for pure materials is unconditionally stable during phase change but has a time step restriction during sensible heating.

3.1.3. Implicit Method

According to the equation (3.2) for the implicit scheme with $\beta = 1$, at each time step e^j will be computed as,

$$e^j = e^{j-1} + \frac{hA}{\rho V}(T_\infty - T^j)\Delta t_j + \frac{1}{\rho}(sc^j - sp^j T^j)\Delta t_j \qquad (3.8)$$

Therefore e^j and T^j will be computed by solving simultaneously equations (3.8) and (3.5) at each time step.

Since the equation (3.5) is nonlinear, solving equations (3.5) and (3.8) simultaneously requires iteration. Fig. 3.1.1 shows the flow chart of this iteration.

The implicit method requires iteration, and in general this method is more complicated than the explicit one. On the other hand, the implicit method is attractive in that it is unconditionally stable. Results will be presented to show that the implicit method is superior to the explicit method.

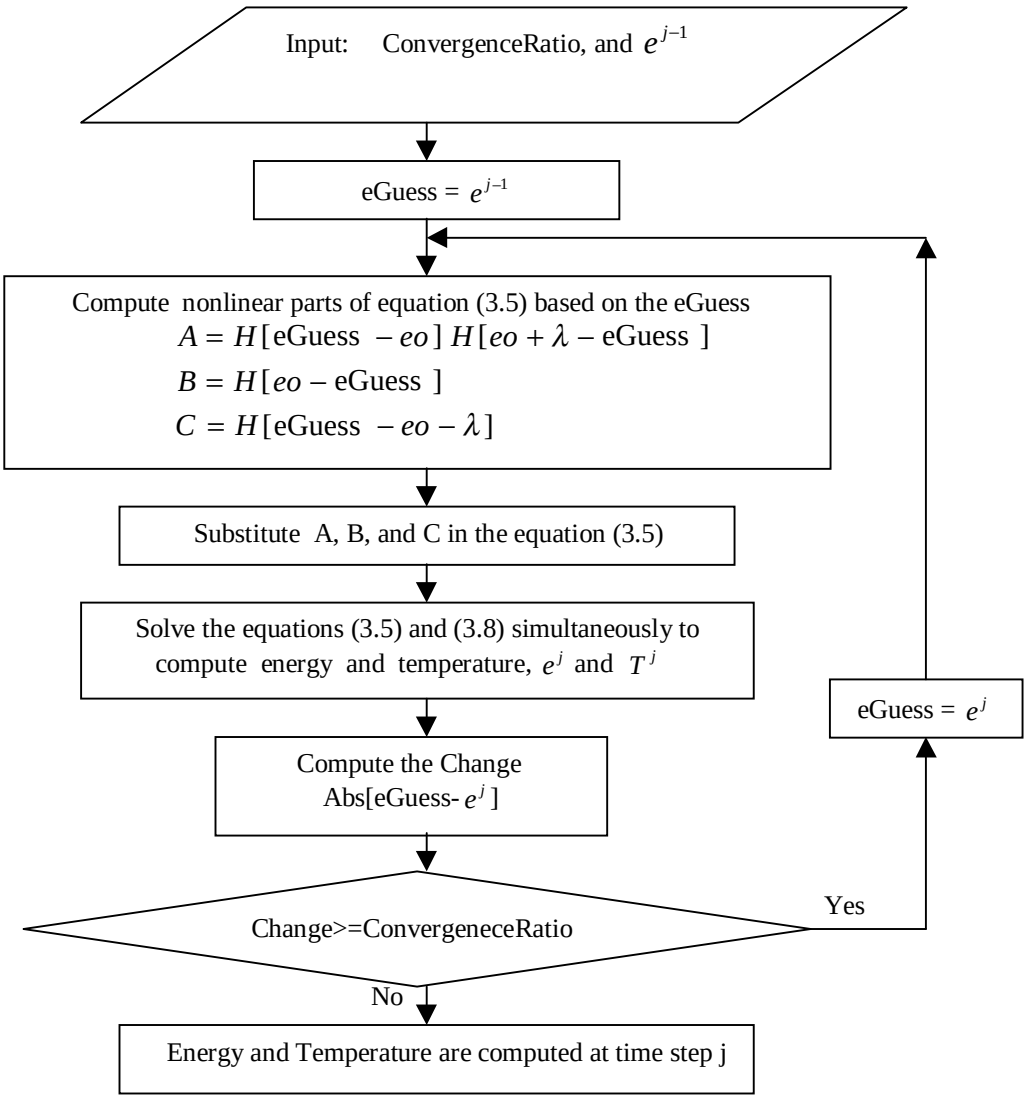

Fig. 3.1.1. Flow chart of the implicit method iteration for e^j and T^j at time step *j*.

3.2. Homogeneous Materials

The energy balance equation for a one-dimensional homogenous material and the energy-temperature relationship equation for hypothetical material with a linear function relationship during phase change, are given by equations (2.11) and (2.4),

$$\frac{\partial}{\partial x}(k\frac{\partial T}{\partial x}) + sc(x,t) - sp(x,t)T = \rho\frac{\partial e}{\partial t} \qquad (2.11)$$

$$T(e) = \left\{Tm_b + (e-eo)\frac{Tm_f - Tm_b}{\lambda}\right\} H[e-eo]\, H[eo+\lambda-e] + \left\{Tm_b + \frac{1}{Cp_s}(e-eo)\right\} H[eo-e] + \left\{Tm_f + \frac{1}{Cp_l}(e-eo-\lambda)\right\} H[e-eo-\lambda] \qquad (2.4)$$

Differential equation (2.11) can be approximated with finite differences by using the explicit or implicit method.

The physical domain is broken into discrete control volumes (CV) for numerical analysis. The control volumes are specified first and then grid points are placed in the center of each control volume. An additional grid point is placed on each boundary that is surrounded by a zero thickness control volume as shown in Fig 3.2.1.

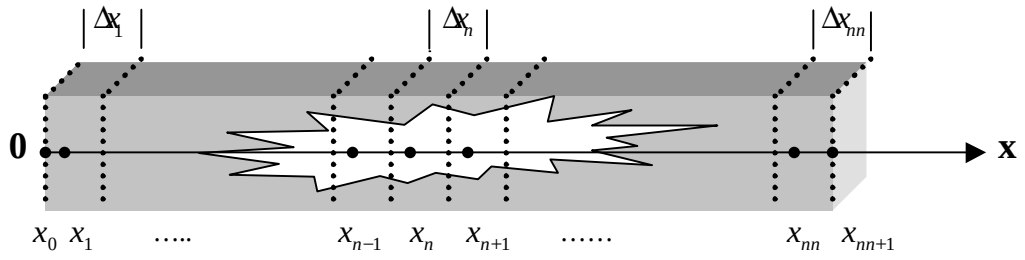

Fig. 3.2.1. Control volume discretization of a one-dimensional homogeneous material.

A typical control volume is shown in Fig 3.2.2.

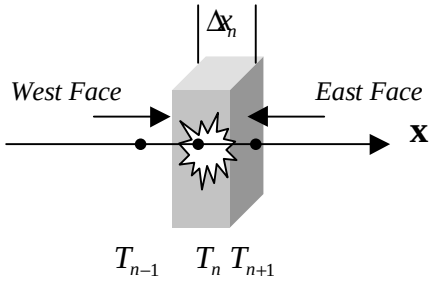

Fig. 3.2.2. Typical control volume for a one-dimensional homogeneous material

3.2.1. Finite Difference Discretization

The time variable is discretized into a sequence of steps.

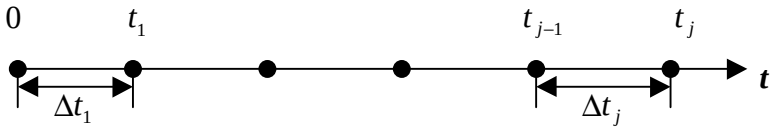

By integrating the equation (2.11) over CV "n" and over the time interval t_{j-1} to t_j, this equation takes the form,

$$\int_{t=t_{j-1}}^{t=t_j}\int_{W}^{E}\left\{\frac{\partial}{\partial x}(k\frac{\partial T}{\partial x})+sc(x,t)-sp(x,t)T\right\}dxdt=\int_{t=t_{j-1}}^{t=t_j}\int_{W}^{E}\rho\frac{\partial e}{\partial t}dxdt \qquad (3.9)$$

By using the explicit and implicit method, individual terms of the equation (3.9) take the form,

$$\int_{t=t_{j-1}}^{t=t_j}\int_{W}^{E}\rho\frac{\partial e}{\partial t}dxdt=\int_{W}^{E}\rho(e^{j}-e^{j-1})dx=\rho_n(e_n^j-e_n^{j-1})\Delta x_n$$

$$\int_{t=t_{j-1}}^{t=t_j}\int_{W}^{E}\frac{\partial}{\partial x}(k\frac{\partial T}{\partial x})dxdt=(1-\beta)\left[k_E(\frac{T_{n+1}^{j-1}-T_n^{j-1}}{\Delta x_E})-k_W(\frac{T_n^{j-1}-T_{n-1}^{j-1}}{\Delta x_W})\right]\Delta t_j+$$
$$\beta\left[k_E(\frac{T_{n+1}^{j}-T_n^{j}}{\Delta x_E})-k_W(\frac{T_n^{j}-T_{n-1}^{j}}{\Delta x_W})\right]\Delta t_j$$

$$\int_{t=t_{j-1}}^{t=t_j}\int_{W}^{E}[sc(x,t)-sp(x,t)T]dxdt=\left\{(1-\beta)\left[sc_n^{\,j-1}-sp_n^{\,j-1}T_n^{\,j-1}\right]+\beta\left[sc_n^{\,j}-sp_n^{\,j}T_n^{\,j}\right]\right\}\Delta x_n\Delta t_j$$

where $\beta=0$ for the explicit method, and $\beta=1$ for the implicit method.

Since the conductivity could vary from one CV to the next, it is important to be careful with the interface conductivities. An interface is shared by the CV's and does not belong to either. The heat flux across an interface must be represented by the same expression for both CV's. By using the thermal resistance concept, the heat flux at the east face is,

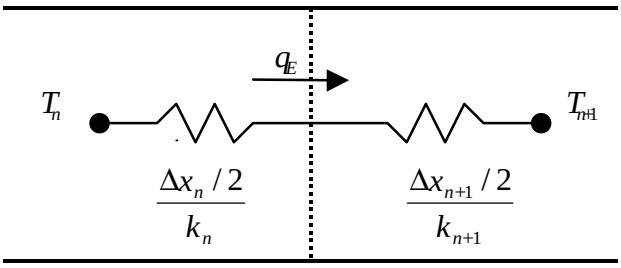

$$q_E=\frac{T_n-T_{n+1}}{\frac{\Delta x_n/2}{k_n}+\frac{\Delta x_{n+1}/2}{k_{n+1}}} \qquad (3.10)$$

The finite difference representation at the east face is,

$$q_E=k_E\frac{T_n-T_{n+1}}{\Delta x_E} \qquad (3.11)$$

Combining equations (3.10) and (3.11) gives,

$$\frac{k_E}{\Delta x_E}=\frac{2k_nk_{n+1}}{\Delta x_nk_{n+1}+\Delta x_{n+1}k_n} \qquad (3.12)$$

In a similar way,

$$\frac{k_W}{\Delta x_W}=\frac{2k_nk_{n-1}}{\Delta x_nk_{n-1}+\Delta x_{n-1}k_n} \qquad (3.13)$$

Now by substituting these terms into the equation (3.9), the finite difference form of the equation will be arranged as,

$$\rho_n(e_n^j - e_n^{j-1})\Delta x_n = \beta\left[\left[k_E(\frac{T_{n+1}^j - T_n^j}{\Delta x_E}) - k_W(\frac{T_n^j - T_{n-1}^j}{\Delta x_W})\right]\Delta t_j + [sc_n^j - sp_n^j T_n^j]\Delta x_n \Delta t_j\right] +$$
$$(1-\beta)\left[\left[k_E(\frac{T_{n+1}^{j-1} - T_n^{j-1}}{\Delta x_E}) - k_W(\frac{T_n^{j-1} - T_{n-1}^{j-1}}{\Delta x_W})\right]\Delta t_j + [sc_n^{j-1} - sp_n^{j-1} T_n^{j-1}]\Delta x_n \Delta t_j\right] \quad (3.14)$$

The type of boundary condition at $x=0$ can be written at each time step as,

1. Specified temperature, $Tx0$:

$$T(0,t) = Tx0$$
$$T_0^j = Tx0 \quad (3.15)$$

2. Specified heat flux $qx0$ with convection $hx0$ *and* $Tx0_\infty$:

$$-k\frac{\partial T}{\partial x} = qx0 + hx0[Tx0_\infty - T(0,t)]$$
$$k_1\frac{T_0^j - T_1^j}{\Delta x_1/2} = qx0 + hx0[Tx0_\infty - T_0^j]$$
$$T_0^j = \left\{[qx0 + hx0 * Tx0_\infty] + \frac{2k_1}{\Delta x_1}T_1^j\right\} / \left\{hx0 + \frac{2k_1}{\Delta x_1}\right\} \quad (3.16)$$

Also, the boundary condition at $x=L$ can be considered as,

1. Specified temperature, TxL :

$$T(L,t) = TxL$$
$$T_{nn+1}^j = TxL \quad (3.17)$$

2. Specified heat flux qxL with convection hxL *and* TxL_∞ :

$$-k\frac{\partial T}{\partial x} = qxL + hxL[TxL_\infty - T(L,t)]$$

$$k_{nn}\frac{T_{nn+1}^{j}-T_{nn}^{j}}{\Delta x_{nn}/2}=qxL+hxL[TxL_{\infty}-T_{nn+1}^{j}]$$

$$T_{nn+1}^{j}=\left\{[qxL+hxL*TxL_{\infty}]+\frac{2k_{nn}}{\Delta x_{nn}}T_{nn}^{j}\right\}/\left\{hxL+\frac{2k_{nn}}{\Delta x_{nn}}\right\} \qquad (3.18)$$

The initial condition is defined as,

$$T_{n}^{0}=T_{initial} \qquad (3.19.a)$$

$$e_{n}^{0}=e_{initial} \qquad (3.19.b)$$

3.2.2. Explicit Method

According to equation (3.14) for the explicit scheme with $\beta=0$, at each time step e_n^j will be computed for all control volumes from *n=1* to *n=nn*,

$$e_{n}^{j}=e_{n}^{j-1}+\frac{1}{\rho_n\Delta x_n}\left\{\left\{k_E\left(\frac{T_{n+1}^{j-1}-T_{n}^{j-1}}{\Delta x_E}\right)-k_W\left(\frac{T_{n}^{j-1}-T_{n-1}^{j-1}}{\Delta x_W}\right)\right\}\Delta t_j+[sc_n^{j-1}-sp_n^{j-1}T_n^{j-1}]\Delta x_n\Delta t_j\right\} \qquad (3.20)$$

By knowing e_n^j , and using equation (2.4), the temperature of all control volumes from *1* to *nn* can be computed at each time step,

$$T_n^j(e_n^j)=\left\{Tm_b+(e_n^j-eo)\frac{Tm_f-Tm_b}{\lambda}\right\}H[e_n^j-eo]\,H[eo+\lambda-e_n^j]+$$
$$\left\{Tm_b+\frac{1}{Cp_s}(e_n^j-eo)\right\}H[eo-e_n^j]+\left\{Tm_f+\frac{1}{Cp_l}(e_n^j-eo-\lambda)\right\}H[e_n^j-eo-\lambda] \qquad (3.21)$$

The boundaries temperature can be computed at each time step based on the equations (3.15)-(3.18).

Since the explicit scheme has stability problems, in order to achieve a stable, physically meaningful solution, the coefficient of e_n^{j-1} in equation (3.20) has to be positive after substituting T_n^{j-1} in terms of e_n^{j-1} from equation (3.21) or (2.3). Therefore, the time step one can use has to be restricted below a certain limit. In other words, the following condition has to be satisfied for stability,

$$\Delta t_j \le \begin{cases} [Cp_l]\dfrac{\rho_n \Delta x_n}{k_E/\Delta x_E + k_W/\Delta x_W + \Delta x_n sp_n^{j-1}}, & e_n^{j-1} > eo + \lambda \\ \left[\dfrac{\lambda}{Tm_f - Tm_b}\right]\dfrac{\rho_n \Delta x_n}{k_E/\Delta x_E + k_W/\Delta x_W + \Delta x_n sp_n^{j-1}}, & eo \le e_n^{j-1} \le eo + \lambda \\ [Cp_s]\dfrac{\rho_n \Delta x_n}{k_E/\Delta x_E + k_W/\Delta x_W + \Delta x_n sp_n^{j-1}}, & e_n^{j-1} < eo \end{cases} \quad (3.22)$$

Based on equation (3.22) for pure materials, when $Tm_f = Tm_b$, during phase change Δt_j has to be less than infinity, which means there is no restriction for the time step.

3.2.3. Implicit Method

According to equation (3.14) for the implicit scheme with $\beta = 1$, e_n^j will be arranged for all control volumes from *n=1 to n=nn* at each time step as,

$$e_n^j = e_n^{j-1} + \frac{1}{\rho_n \Delta x_n}\left\{\left\{k_E\left(\frac{T_{n+1}^j - T_n^j}{\Delta x_E}\right) - k_W\left(\frac{T_n^j - T_{n-1}^j}{\Delta x_W}\right)\right\}\Delta t_j + [sc_n^j - sp_n^j T_n^j]\Delta x_n \Delta t_j\right\} \quad (3.23)$$

Based on the equation (3.21), temperature is in terms of energy, therefore, by substituting temperature in terms of energy in equation (3.23) for all control volumes from *n=1 to n=nn* and also in equations (3.15) to (3.18) for boundaries, *nn+2* equations with *nn+2* unknown will be provided.

Since the equation (3.21) is nonlinear, solving simultaneously these *nn+2* equations requires iteration. Fig. 3.2.3 shows this iteration in flow chart form. According to the Fig. 3.2.3. *nn+2* simultaneous equations are formed as,

$$(cW)_n e_{n-1}^j + c_n e_n^j + (cE)_n e_{n+1}^j = d_n \qquad (3.24)$$

Where $(cW)_n$, c_n, $(cE)_n$, d_n are defined in appendix A.

These equations can be assembled in a tridiagonal matrix where every element is zero except the diagonal and the elements to the immediate west and east of the diagonal. As a result, e_n^j for all CV's will be determined by solving the tridiagonal matrix (TDM).

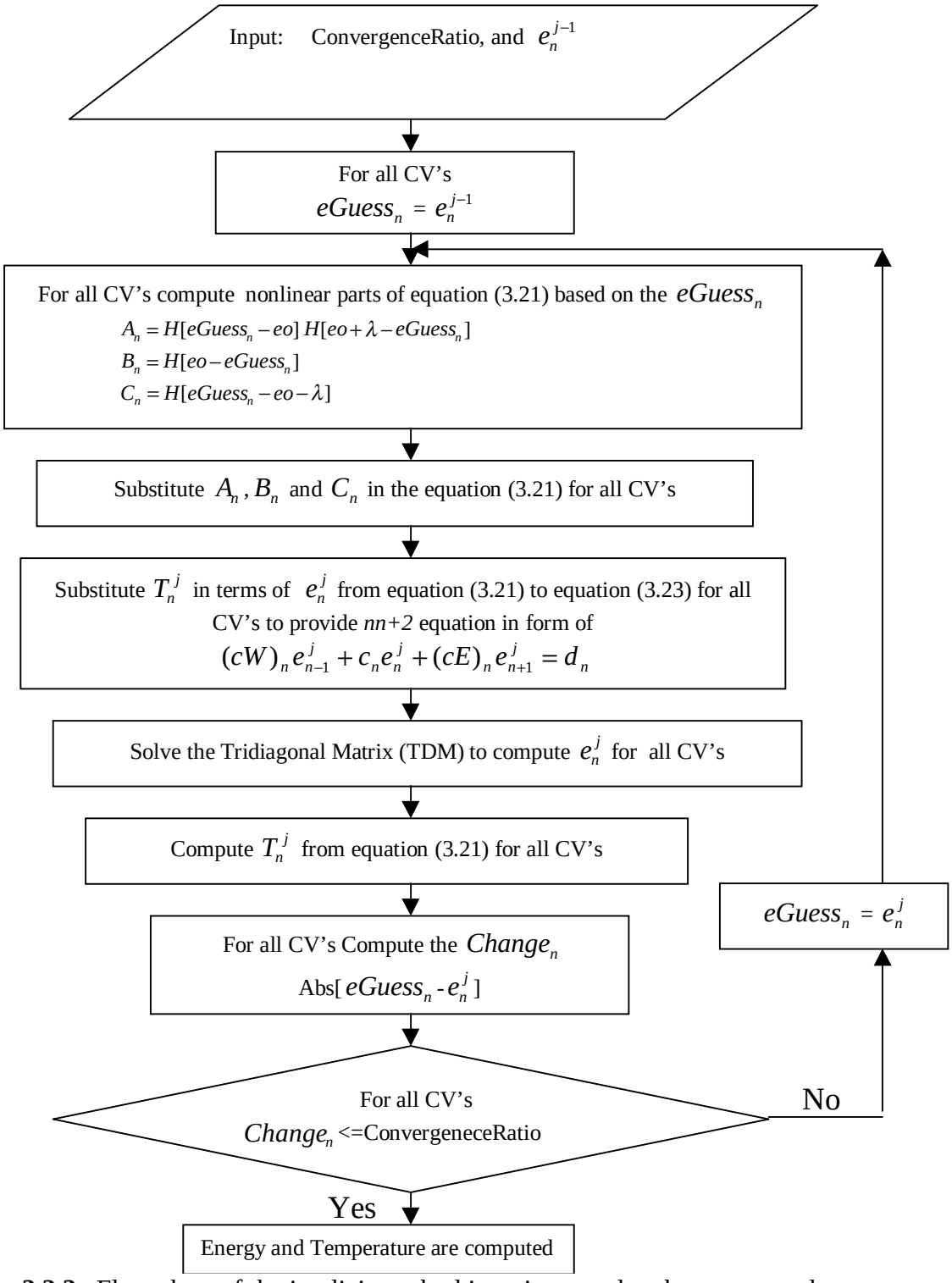

Fig. 3.2.3. Flow chart of the implicit method iteration to solve the energy and temperature of all control volumes at time step *j*.

3.3. Heterogeneous Materials

The energy balance equation for a one-dimensional heterogeneous material and the energy-temperature relationship equation for a hypothetical material with a linear function relationship during phase change, are given by equations (2.19), (2.20) and (2.4).

Matrix:

$$C_m \frac{\partial T_m}{\partial t} = \frac{\partial}{\partial x}(K_m \frac{\partial T_m}{\partial x}) - H_c(T_m - T_p) + Sc_m(x,t) - Sp_m(x,t)T_m \qquad (2.19)$$

Particles:

$$(NV_p)\rho_p \frac{\partial e_p}{\partial t} = H_c(T_m - T_p) + Sc_p(x,t) - Sp_p(x,t)T_p \qquad (2.20)$$

$$T(e) = \left\{Tm_b + (e-eo)\frac{Tm_f - Tm_b}{\lambda}\right\} H[e-eo]\, H[eo+\lambda-e] + \left\{Tm_b + \frac{1}{Cp_s}(e-eo)\right\} H[eo-e] + \left\{Tm_f + \frac{1}{Cp_l}(e-eo-\lambda)\right\} H[e-eo-\lambda] \qquad (2.4)$$

Differential equations (2.19) and (2.20) can be approximated with finite differences by using the explicit or implicit method.

The physical domain is broken into discrete control volumes (CV) for numerical analysis. The CV's are specified first and then grid points are placed in the center of each CV. An additional grid point is placed on each boundary that is surrounded by a zero thickness control volume as shown in Fig 3.3.1.

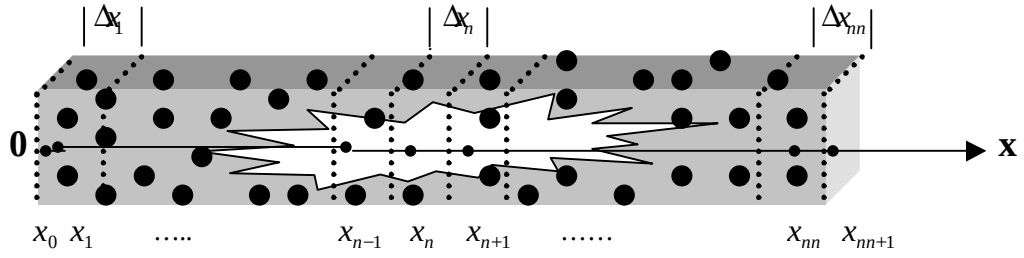

Fig 3.3.1. Control volume discretization of a one-dimensional heterogeneous material

A typical control volume is shown in Fig 2.3.2.

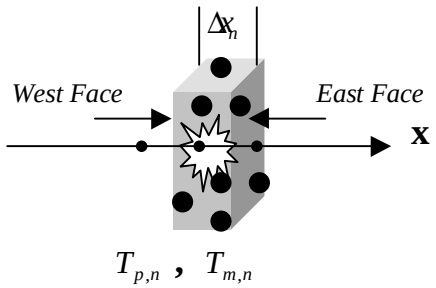

Fig 3.3.2. Typical control volume for a one-dimensional heterogeneous material

3.3.1. Finite Difference Discretization

The time variable is discretized into a sequence of steps.

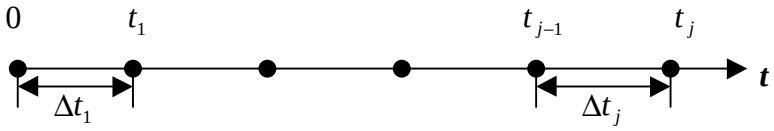

By integrating the equations (2.19) and (2.20) over CV "n" and over the time interval t_{j-1} to t_j ,these equations take the form,

Matrix:

$$\int_{t=t_{j-1}}^{t=t_j}\int_{W}^{E}\left[\frac{\partial}{\partial x}(K_m\frac{\partial T_m}{\partial x})-H_c(T_m-T_p)+Sc_m(x,t)-Sp_m(x,t)T_m\right]dxdt=\int_{t=t_{j-1}}^{t=t_j}\int_{W}^{E}C_m\frac{\partial T_m}{\partial t}dxdt \qquad (3.25)$$

Particle:

$$\int_{t=t_{j-1}}^{t=t_j}\int_{W}^{E}\left[H_c(T_m-T_p)+Sc_p(x,t)-Sp_p(x,t)T_p\right]dxdt=\int_{t=t_{j-1}}^{t=t_j}\int_{W}^{E}(NV_p)\rho_p\frac{\partial e_p}{\partial t}dxdt \qquad (3.26)$$

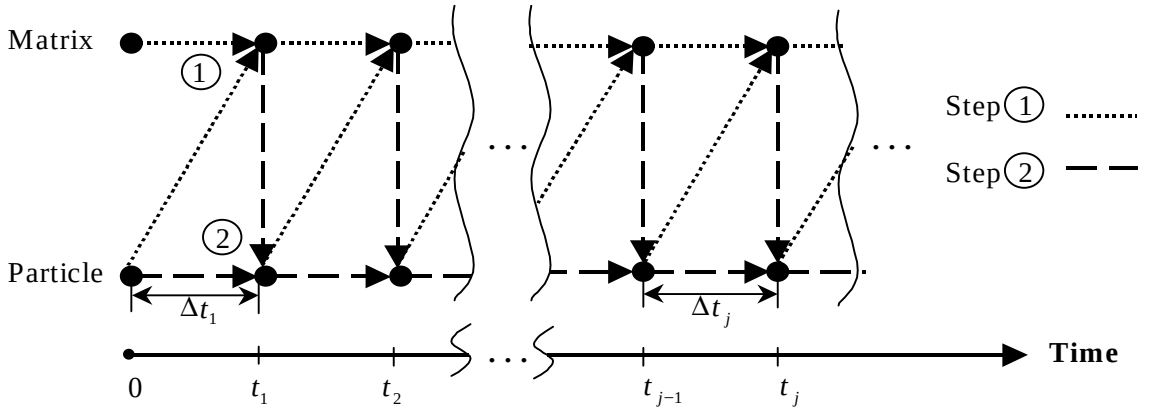

Fig. 3.3.3. Two-step numerical solution scheme for a heterogeneous material.

According to the Fig 3.3.3, each term of the equation (3.25) is evaluated in the step 1 fashion, where the matrix temperature over each time interval is evaluated at the end of the interval, while the particle temperature is evaluated at the beginning of the interval. As the results, individual terms of the equation (3.25) take the form,

$$\int_{t=t_{j-1}}^{t=t_j}\int_{W}^{E} C_m \frac{\partial T_m}{\partial t} dxdt = \int_{W}^{E} C_m (T_m^j - T_m^{j-1}) dx = C_m (T_{m,n}^j - T_{m,n}^{j-1}) \Delta x_n \qquad (3.25.a)$$

$$\int_{t=t_{j-1}}^{t=t_j}\int_{W}^{E} \frac{\partial}{\partial x}(K_m \frac{\partial T_m}{\partial x}) dxdt = \left[K_{m,E} (\frac{T_{m,n+1}^j - T_{m,n}^j}{\Delta x_E}) - K_{m,W} (\frac{T_{m,n}^j - T_{m,n-1}^j}{\Delta x_W}) \right] \Delta t_j \qquad (3.25.b)$$

$$\int_{t=t_{j-1}}^{t=t_j}\int_{W}^{E} \left[- H_c (T_m - T_p) \right] dxdt = \left[- H_c (T_{m,n}^j - T_{p,n}^{j-1}) \right] \Delta x_n \Delta t_j \qquad (3.25.c)$$

$$\int_{t=t_{j-1}}^{t=t_j}\int_{W}^{E} \left[Sc_m(x,t) - Sp_m(x,t) T_m \right] dxdt = \left[Sc_{m,n}^j - Sp_{m,n}^j T_{m,n}^j \right] \Delta x_n \Delta t_j \qquad (3.25.d)$$

Each term of the equation (3.26) is integrated over time in both the implicit and explicit methods for the particles in the step 2 fashion as shown on Fig 3.3.3. But since the

equations (3.25) and (3.26) have one term in common, this term must be evaluated the same way. Therefore for both the implicit and explicit methods this term is evaluated based on the equation (3.25.c). As the result, integration of each term of equation (3.26) produces,

$$\int_{t=t_{j-1}}^{t=t_j}\int_{W}^{E}(NV_p)\rho_p\frac{\partial e_p}{\partial t}dxdt=\int_{W}^{E}(NV_p)\rho_p(e_p^j-e_p^{j-1})dx=(NV_p)\rho_{p,n}(e_{p,n}^j-e_{p,n}^{j-1})\Delta x_n \quad (3.26.a)$$

$$\int_{t=t_{j-1}}^{t=t_j}\int_{W}^{E}\left[H_c(T_m-T_p)\right]dxdt=H_c\left[T_{m,n}^j-T_{p,n}^{j-1}\right]\Delta x_n\Delta t_j \quad (3.25.c)$$

$$\int_{t=t_{j-1}}^{t=t_j}\int_{W}^{E}\left[Sc_p(x,t)-Sp_p(x,t)T_p\right]dxdt=\left[(1-\beta)[Sc_{p,n}^{j-1}-Sp_{p,n}^{j-1}T_{p,n}^{j-1}]+\beta[Sc_{p,n}^{j}-Sp_{p,n}^{j}T_{p,n}^{j}]\right]\Delta x_n\Delta t_j \quad (3.26.b)$$

where $\beta=0$ for the explicit method, and $\beta=1$ for the implicit method.

The interface conductivity is evaluated using the thermal resistance concept as described with equations (3.10) and (3.11),

$$\frac{K_{m,E}}{\Delta x_E}=\frac{2K_{m,n}K_{m,n+1}}{\Delta x_n K_{m,n+1}+\Delta x_{n+1}K_{m,n}} \quad (3.27)$$

$$\frac{K_{m,W}}{\Delta x_W}=\frac{2K_{m,n}K_{m,n-1}}{\Delta x_n K_{m,n-1}+\Delta x_{n-1}K_{m,n}} \quad (3.28)$$

Now by substituting the equations (3.25.a)-(3.25.d) into the equation (3.25), the finite difference form of the integrated equation will be arranged for all control volumes from *n=1* to *n=nn* at each time step as,

$$\left\{\frac{K_{m,W}}{\Delta x_W}\Delta t_j\right\}T_{m,n-1}^j+\left\{-C_m\Delta x_n-\frac{K_{m,W}}{\Delta x_W}\Delta t_j-\frac{K_{m,E}}{\Delta x_E}\Delta t_j-H_c\,\Delta x_n\Delta t_j-Sp_{m,n}^j\,\Delta x_n\Delta t_j\right\}T_{m,n}^j+\left\{\frac{K_{m,E}}{\Delta x_E}\Delta t_j\right\}T_{m,n+1}^j=$$
$$\left\{-C_m T_{m,n}^{j-1}\Delta x_n-H_c\,T_{p,n}^{j-1}\Delta x_n\Delta t_j-Sc_{m,n}^j\Delta x_n\Delta t_j\right\} \quad (3.29)$$

Equation (3.29) can be reformed as,

$$(mcW)_n T^j_{m,n-1} + (mc)_n T^j_{m,n} + (mcE)_n T^j_{m,n+1} = (md)_n \qquad (3.30)$$

where,

$$(mcW)_n = \left\{ \frac{K_{m,W}}{\Delta x_W} \Delta t_j \right\}$$

$$(mcE)_n = \left\{ \frac{K_{m,E}}{\Delta x_E} \Delta t_j \right\}$$

$$(mc)_n = \left\{ -C_m \Delta x_n - \frac{K_{m,W}}{\Delta x_W} \Delta t_j - \frac{K_{m,E}}{\Delta x_E} \Delta t_j - H_c \Delta x_n \Delta t_j - Sp^j_{m,n} \Delta x_n \Delta t_j \right\}$$

$$(md)_n = \left\{ -C_m T^{j-1}_{m,n} \Delta x_n - H_c T^{j-1}_{p,n} \Delta x_n \Delta t_j - Sc^j_{m,n} \Delta x_n \Delta t_j \right\}$$

In addition, the boundary conditions at *x=0* and *x=L* can be written in the form of equation (3.30) as,

1. Specified temperature, *Tx0*

$$T_m(0,t) = Tx0$$

$$T^j_{m,0} = Tx0 \qquad (3.31)$$

$$(mcE)_0 = 0$$

$$(mc)_0 = 1$$

$$(md)_0 = Tx0$$

2. Specified heat flux *qx0* with convection *hx0 and* $Tx0_\infty$

$$-K_m \frac{\partial T_m}{\partial x} = qx0 + hx0[Tx0_\infty - T_m(0,t)]$$

$$K_{m,1} \frac{T^j_{m,0} - T^j_{m,1}}{\Delta x_1 / 2} = qx0 + hx0[Tx0_\infty - T^j_{m,0}] \qquad (3.32)$$

$$(mcE)_0 = \frac{2K_{m,1}}{\Delta x_1}$$

$$(mc)_0 = -\frac{2K_{m,1}}{\Delta x_1} - hx0$$

$$(md)_0 = -qx0 - hx0 * Tx0_\infty$$

Also the boundary condition at $x=L$ can be written as,

1. Specified temperature, *TxL*

$$T_m(L,t) = TxL$$

$$T^j_{m,nn+1} = TxL \qquad (3.33)$$

$$(mcW)_{nn+1} = 0$$
$$(mc)_{nn+1} = 1$$
$$(md)_{nn+1} = TxL$$

2. Specified heat flux qxL with convection hxL *and* TxL_∞

$$-K_m \frac{\partial T_m}{\partial x} = qxL + hxL[TxL_\infty - T_m(L,t)]$$

$$K_{m,nn} \frac{T^j_{m,nn+1} - T^j_{m,nn}}{\Delta x_{nn}/2} = qxL + hxL[TxL_\infty - T^j_{m,nn+1}] \qquad (3.34)$$

$$(mcW)_{nn+1} = \frac{2K_{m,nn}}{\Delta x_{nn}}$$
$$(mc)_{nn+1} = -\frac{2K_{m,nn}}{\Delta x_{nn}} - hxL$$
$$(md)_{nn+1} = -qxL - hxL * TxL_\infty$$

The initial condition is defined as,

$$T^0_{m,n} = T_{initial} \qquad (3.35)$$

$$T^0_{p,n} = T_{initial} \qquad (3.36)$$

Therefore, according to equation (3.30) for all control volumes from *n=1* to *n=nn* and also by equations (3.31) to (3.34) for the boundaries, *nn+2* equations with *nn+2* unknown will be formed. These equations can be assembled in a tridiagonal matrix where every element is zero except the diagonal and the elements to the immediate west and east of the diagonal. As a result, $T^j_{m,n}$ for all CV's will be determined by solving the tridiagonal matrix (TDM).

On the other hand, by substituting the equations (3.26.a), (3.26.b), and (3.25.c) into the integrated equation (3.26), the finite difference form of this equation can be arranged as,

$$e_{p,n}^{j} = e_{p,n}^{j-1} + \frac{1}{(NV_p)\rho_{p,n}\Delta x_n}\left[[H_c(T_{m,n}^{j} - T_{p,n}^{j-1})] + (1-\beta)[Sc_{p,n}^{j-1} - Sp_{p,n}^{j-1}T_{p,n}^{j-1}] + \beta[Sc_{p,n}^{j} - Sp_{p,n}^{j}T_{p,n}^{j}]\right]\Delta x_n \Delta t_j \qquad (3.37)$$

where $\beta = 0$ for the explicit method, and $\beta = 1$ for the implicit method.

3.3.2. Explicit Method for Particles

According to equation (3.37) for the explicit scheme with $\beta = 0$, at each time step $e_{p,n}^{j}$ will be computed for all control volumes from *n=1* to *n=nn*,

$$e_{p,n}^{j} = e_{p,n}^{j-1} + \frac{1}{(NV_p)\rho_{p,n}\Delta x_n}\left[[H_c(T_{m,n}^{j} - T_{p,n}^{j-1})] + [Sc_{p,n}^{j-1} - Sp_{p,n}^{j-1}\ T_{p,n}^{j-1}]\right]\Delta x_n \Delta t_j \qquad (3.38)$$

By knowing $e_{p,n}^{j}$, and using equation (2.4), the temperature of all control volumes from *1* to *nn* can be computed at each time step,

$$T_{p,n}^{j}(e_{p,n}^{j}) = \left\{Tm_b + (e_{p,n}^{j} - eo)\frac{Tm_f - Tm_b}{\lambda}\right\} H[e_{p,n}^{j} - eo]\, H[eo + \lambda - e_{p,n}^{j}] +$$

$$\left\{Tm_b + \frac{1}{Cp_{p,s}}(e_{p,n}^{j} - eo)\right\} H[eo - e_{p,n}^{j}] + \left\{Tm_f + \frac{1}{Cp_{p,l}}(e_{p,n}^{j} - eo - \lambda)\right\} H[e_{p,n}^{j} - eo - \lambda] \qquad (3.39)$$

Since the explicit scheme has stability problems, in order to achieve a stable, physically meaningful solution, the coefficient of $e_{p,n}^{j-1}$ in equation (3.38) has to be positive after substituting $T_{p,n}^{j-1}$ in terms of $e_{p,n}^{j-1}$ by equation (3.39) or (2.3).

As a result, the time step one can use has to be restricted below a certain limit. In other words, the following condition has to be satisfied for stability,

$$\Delta t_j \le \begin{cases} \left[Cp_{p,l}\right] \dfrac{\rho_{p,n}(NV_p)}{H_c + Sp_{p,n}^{j-1}}, & e_{p,n}^{j-1} > eo + \lambda \\ \left[\dfrac{\lambda}{Tm_f - Tm_b}\right] \dfrac{\rho_{p,n}(NV_p)}{H_c + Sp_{p,n}^{j-1}}, & eo \le e_{p,n}^{j-1} \le eo + \lambda \\ \left[Cp_{p,s}\right] \dfrac{\rho_{p,n}(NV_p)}{H_c + Sp_{p,n}^{j-1}}, & e_{p,n}^{j-1} < eo \end{cases} \qquad (3.40)$$

Based on equation (3.40) for pure materials, when $Tm_f = Tm_b$, during phase change Δt_j has to be less than infinite, which means there is no restriction for the time step.

3.3.3. Partly Implicit Method for Particles

According to equation (3.37) for the implicit scheme with $\beta = 1$, $e_{p,n}^{j}$ will be arranged for all control volumes from *n=1 to n=nn* at each time step as,

$$e_{p,n}^{j} = e_{p,n}^{j-1} + \frac{1}{(NV_p)\rho_{p,n}\Delta x_n}\left[[H_c\,(T_{m,n}^{j} - T_{p,n}^{j-1})] + [Sc_{p,n}^{j} - Sp_{p,n}^{j}\,T_{p,n}^{j}]\right]\Delta x_n \Delta t_j \qquad (3.41)$$

Therefore, $e_{p,n}^{j}$ and $T_{p,n}^{j}$ will be computed by solving simultaneously equations (3.41) and (3.39) at each time step.

Since the equation (3.39) is nonlinear, solving equations (3.39) and (3.41) simultaneously requires iteration. Fig. 3.3.4 shows the flow chart of this iteration.

The coefficient of $e_{p,n}^{j-1}$ in equation (3.41) has to be positive after substituting $T_{p,n}^{j-1}$ in terms of $e_{p,n}^{j-1}$ by equation (3.39) or (2.3), to achieve a stable, physically meaningful solution. As a result, the following condition has to be satisfied for stability,

$$\Delta t_j \le \begin{cases} \left[Cp_{p,l}\right] \dfrac{\rho_{p,n}(NV_p)}{H_c}, & e_{p,n}^{j-1} > eo + \lambda \\ \left[\dfrac{\lambda}{Tm_f - Tm_b}\right] \dfrac{\rho_{p,n}(NV_p)}{H_c}, & eo \le e_{p,n}^{j-1} \le eo + \lambda \\ \left[Cp_{p,s}\right] \dfrac{\rho_{p,n}(NV_p)}{H_c}, & e_{p,n}^{j-1} < eo \end{cases} \qquad (3.42)$$

Equation (3.42) states that this method is unconditionally stable during phase change for pure materials when $Tm_f = Tm_b$.

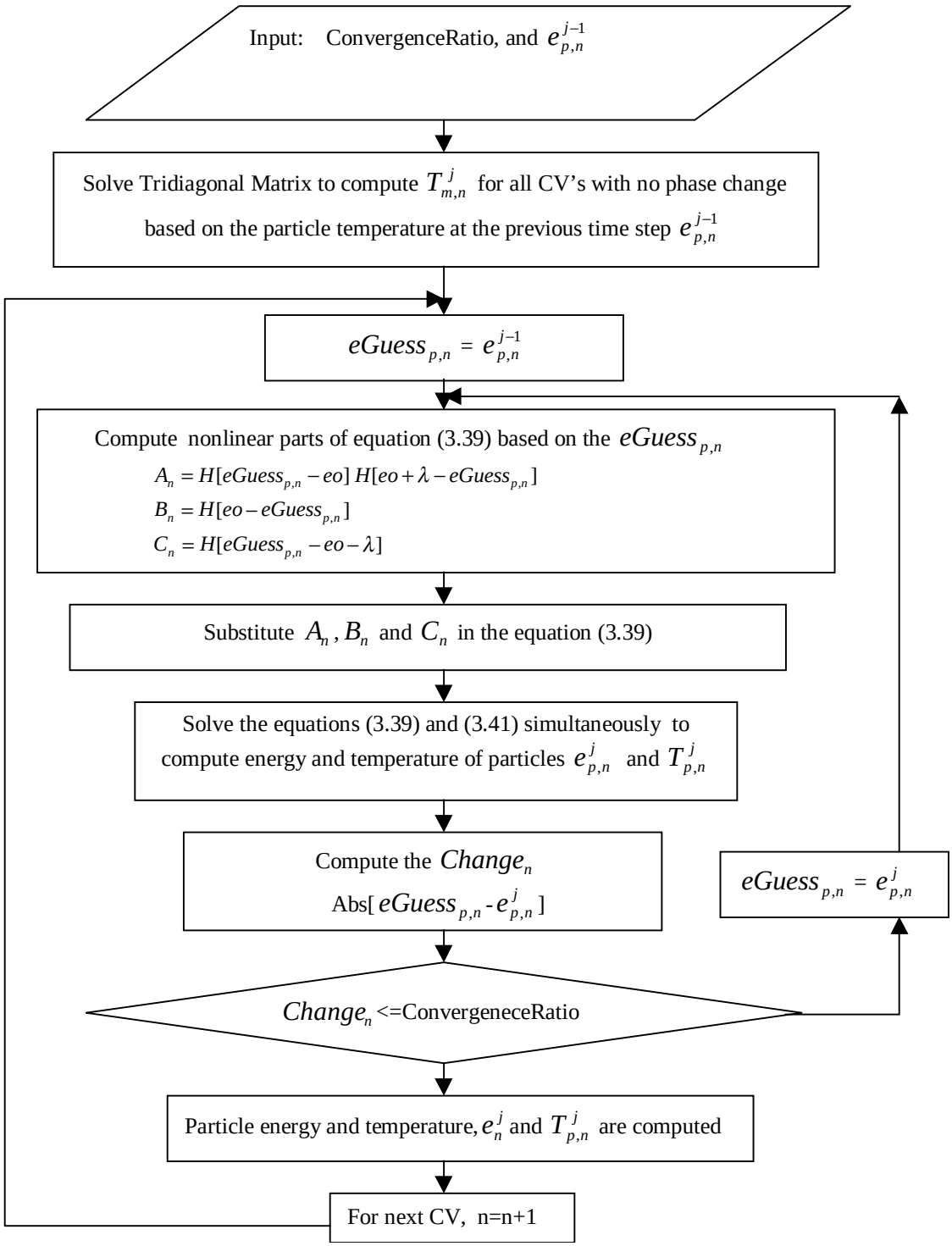

Fig. 3.3.4 Flow chart of the implicit method iteration for particle energy and temperature of control volume "n" at time step *j*.

CHAPTER 4
RESULTS AND DISCUSSION

4.1. Lumped Capacity Systems

The lumped capacity system study is intended to provide a bridge to the main part of this work which is the heterogeneous material, consisting of a matrix with relatively small particles embedded during melting or solidification, which are considered as a lumped capacity.

In this part of the study, first, the comparison between the explicit and implicit method is studied in order to analyze the stability problem. Next, the effect of the time steps Δt is examined. Then, the effects of the material properties such as heat capacity ratio, Stefan number, and melting temperature are investigated. Also, the effect of internal sources is studied. Last, the effect of the heat transfer coefficient is analyzed. Numerical results are presented in terms of the dimensionless variables.

4.1.1. Comparison between Explicit and Implicit Method

The stability problem is analyzed by comparing the explicit and implicit method for a lumped system, which is initially at temperature $\theta = 1$ with heat convection $\theta_\infty = 0$ and $h^+ = 0.01$(for lumped capacity system Bio<0.1). Phase change occurs at a single melting temperature $\theta mb = \theta mf = 0.5$ like a pure material. The Stefan number and heat capacity ratio are *Ste =1* and *Cr =1*.

4.1.1.1. Stability

Figure 4.1.1 displays the temperature and energy histories of the lumped capacity system for various values of Δt^+. According to the equation (3.7), the explicit critical Δt^+ in this case is $Ex\Delta t^+_{cri} = 100$. Figure 4.1.1 shows the explicit method is unstable when the Δt^+ is greater than $Ex\Delta t^+_{cri}$, while the implicit method is unconditionally stable. On the

other hand, Fig 4.1.2 shows when Δt^+ is small enough there is no noticeable difference between the implicit and explicit methods. Since the implicit method is unconditionally stable, this method will be used for further investigations.

4.1.2. Δt *Effects*

The effect of Δt^+ on the implicit method is analyzed for a lumped system, which is initially at temperature $\theta = 1$ with heat convection $\theta_\infty = 0$ and $h^+ = 0.01$ (for lumped capacity system Bi<0.1). Phase change occurs at a single melting temperature $\theta mb = \theta mf = 0.5$. The Stefan number and heat capacity ratio are *Ste =1* and *Cr =1*.

Table 4.1.1 displays the lumped system temperature at $t^+ = 400, 800, 2000$ for different Δt^+. It shows that the smaller Δt^+ provides more accurate results. On the other hand, when Δt^+ is small enough a negligible difference can be observed by decreasing the Δt^+.

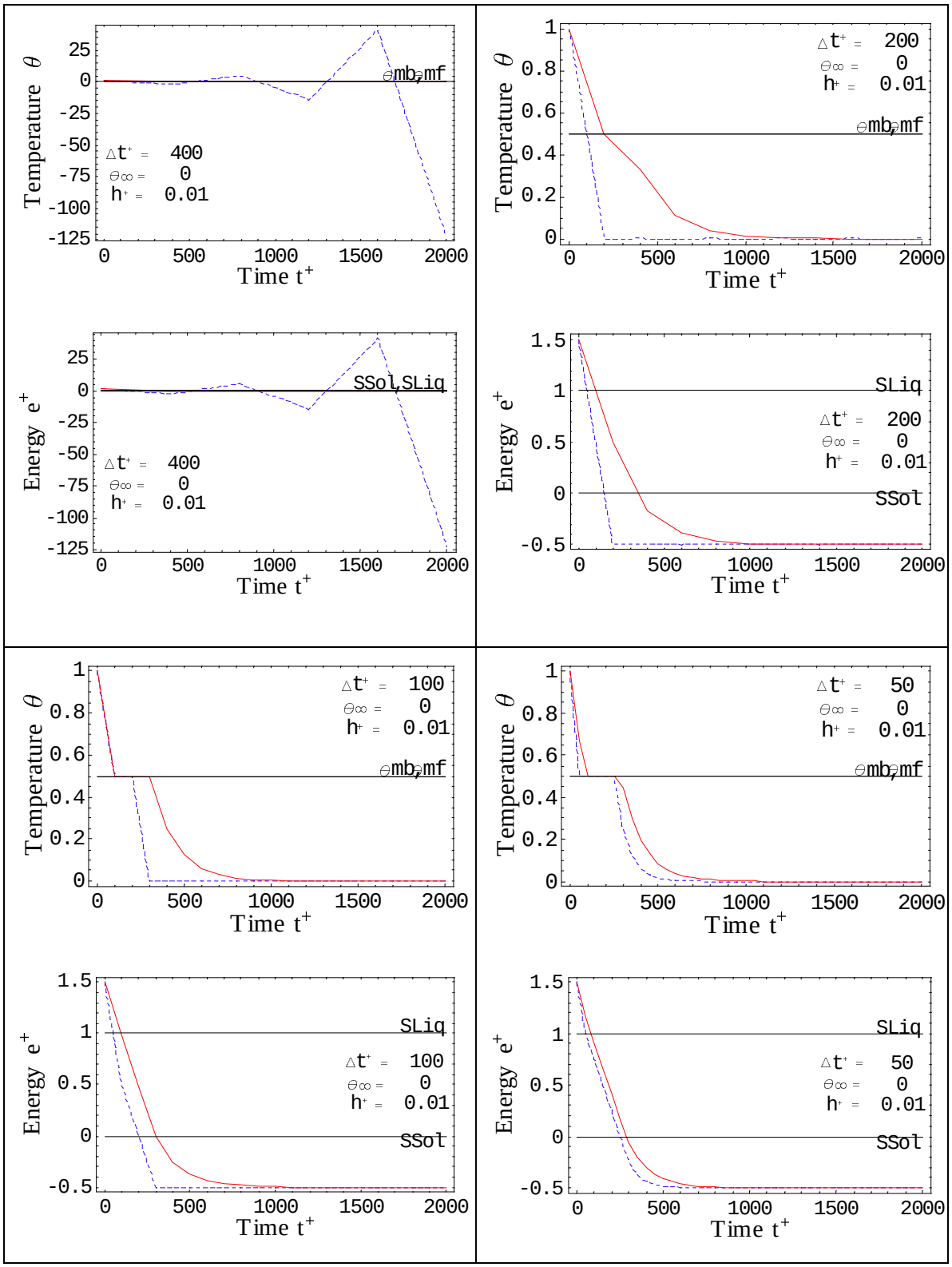

Fig. 4.1.1. Effect of Δt^+ on stability of implicit and explicit method for a lumped system With *Cr=1* and *Ste=1* ($Ex\Delta t^+_{cri} = 100$), (····· *Explicit,* —— *Implicit*).

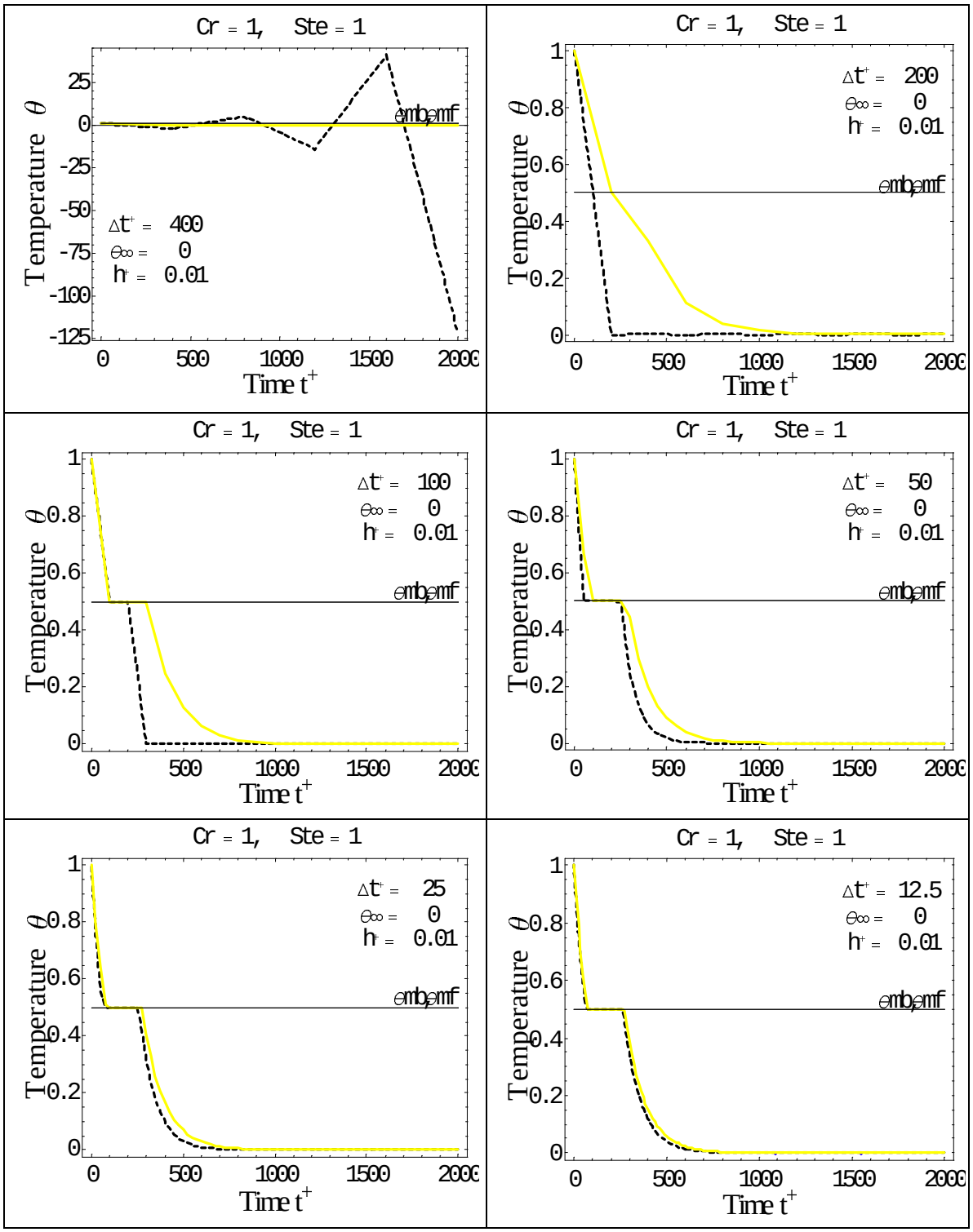

Fig. 4.1.2. Effect of Δt^{+} on implicit and explicit method for a lumped system ($Ex\Delta t^{+}_{cri} = 100$), (····· *Explicit*, —— *Implicit*).

Table 4.1.1. Effect of Δt^+ on temperature for lumped system, initially at $\theta = 1$ with convection $\theta_\infty = 0$ and $h^+ = 0.01$, with melting temp. $\theta m = 0.5$

Δt^+	$t^+ = 400$		$t^+ = 800$		$t^+ = 2000$	
	Temperature	***%Difference (next Δt^+)***	***Temperature***	***%Difference (next Δt^+)***	***Temperature***	***%Difference (next Δt^+)***
400.	0.3998	20.1799	0.07996	116.324	0.00063968	1161.6
200.	0.332668	33.4001	0.0369631	137.156	0.0000507039	1232.5
100.	0.249376	26.6417	0.015586	102.856	3.80518×10^{-6}	733.714
50.	0.196915	17.8065	0.0076833	63.3049	4.56413×10^{-7}	335.
25.	0.167151	10.4465	0.00470488	34.7325	1.04922×10^{-7}	144.587
12.5	0.151341	5.72356	0.00349202	18.1254	4.28977×10^{-8}	64.7621
6.25	0.143148	2.98862	0.0029562	9.22555	2.60362×10^{-8}	30.2954
3.125	0.138994	1.52911	0.00270651	4.65246	1.99824×10^{-8}	14.6109
1.5625	0.136901	0.773482	0.00258618	2.33578	1.7435×10^{-8}	7.16952
0.78125	0.13585	0.389428	0.00252716	1.17066	1.62686×10^{-8}	3.55102
0.390625	0.135323	0.195116	0.00249791	0.585739	1.57107×10^{-8}	1.76677
0.195313	0.135059	-----	0.00248337	-----	1.5438×10^{-8}	------

4.1.3. Material Properties

The effects of material properties such as heat capacity ratio, Stefan number and melting temperature are investigated for a lumped system. In this investigation the system is initially all liquid at temperature $\theta = 1$ with heat convection $\theta_\infty = 0$ and $h^+ = 0.01$(for lumped capacity system Bi<0.1). The time step is $\Delta t^+ = 0.5$.

4.1.3.1. Stefan Number Effects

The Stefan number is a dimensionless group, which is the sensible energy divided by the latent energy. In this investigation the heat capacity ratio is *Cr=1* and phase change occurs at a single melting temperature $\theta mb = \theta mf = 0.5$.

Figure 4.1.3 displays the temperature histories of the lumped system for relatively low, medium and high Stefan number *Ste= 0.1, 1, 10*. Phase transition happens very quickly for *Ste=10*, but it needs more time to complete phase change for *Ste=1*, and it takes much longer for *Ste=0.1*, because the latent heat increases as the Stefan number decreases.

4.1.3.2. Heat Capacity Ratio Effects

The heat capacity ratio is a dimensionless group, which is the ratio of liquid heat capacity to the solid heat capacity. The solid thermal properties are chosen as reference quantities. In this investigation the Stefan number is *Ste=1* and phase change occurs at a single melting temperature $\theta mb = \theta mf = 0.5$.

Figure 4.1.4 displays the temperature histories of the lumped system for relatively low, medium and high heat capacity ratio *Cr= 0.1, 1, 10*. Since the system is initially liquid the effect of the heat capacity ratio can be observed before phase change. Temperature drops very quickly for *Cr=0.1* but it takes more time to get to phase change for *Cr=1*, and it takes much longer for *Cr=10*. This is because it must release more energy to drop the temperature as the heat capacity ratio increases.

4.1.3.3. Melting Temperature Effects

In pure materials the phase-change takes place at a discrete temperature, while in the other cases there is no discrete melting point temperature. Here a hypothetical material is considered which changes phase in a linear way over an extended range of temperatures. In this investigation the heat capacity ratio and Stefan number are *Cr=1* and *Ste=1*.

Figure 4.1.5 displays the temperature histories of the lumped system for a pure material and two hypothetical materials. For the pure material phase change occurs at temperature *0.5*, while for the hypothetical materials, one occurs over temperature *0.5-0.6* and the other one occurs over temperature *0.5-0.7*. Since the lumped systems are initially liquid, each system reaches the phase transition at different times. The *Ste=1* for all the lumped systems, which means the total energy is the same for all systems to finish phase change. As a result, the lumped systems complete phase transition at different times, although the finishing phase change temperature is the same for all systems.

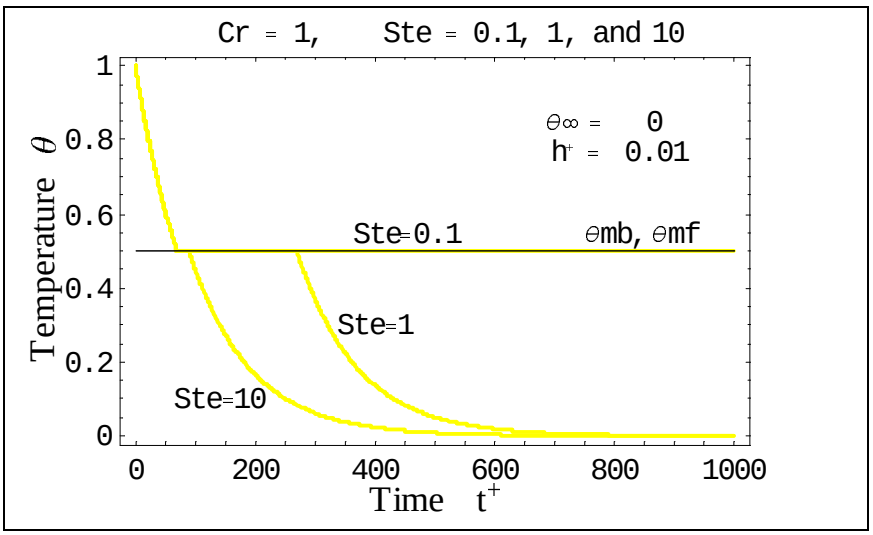

Fig. 4.1.3. Effect of Stefan number on temperature vs. time for a lumped system, ($\Delta t^+ = 0.5$).

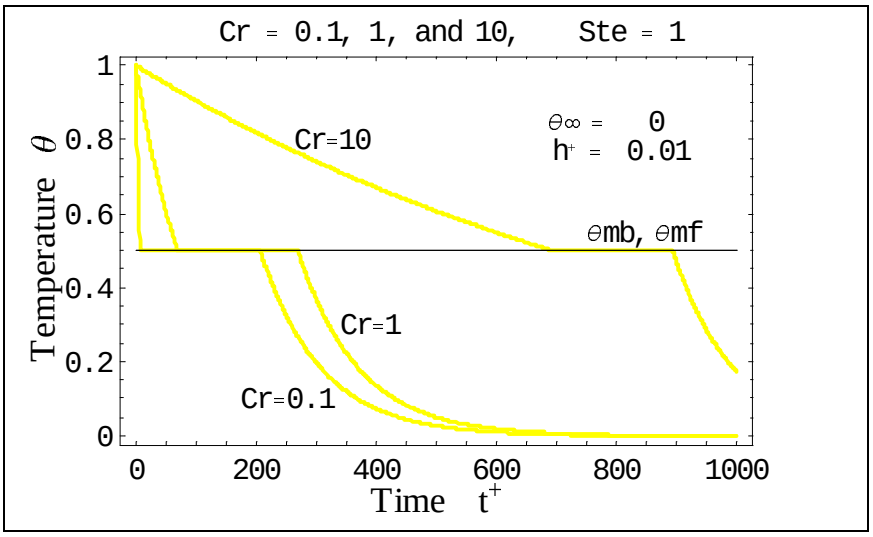

Fig. 4.1.4. Effect of heat capacity ratio on temperature vs. time for a lumped system, ($\Delta t^+ = 0.5$).

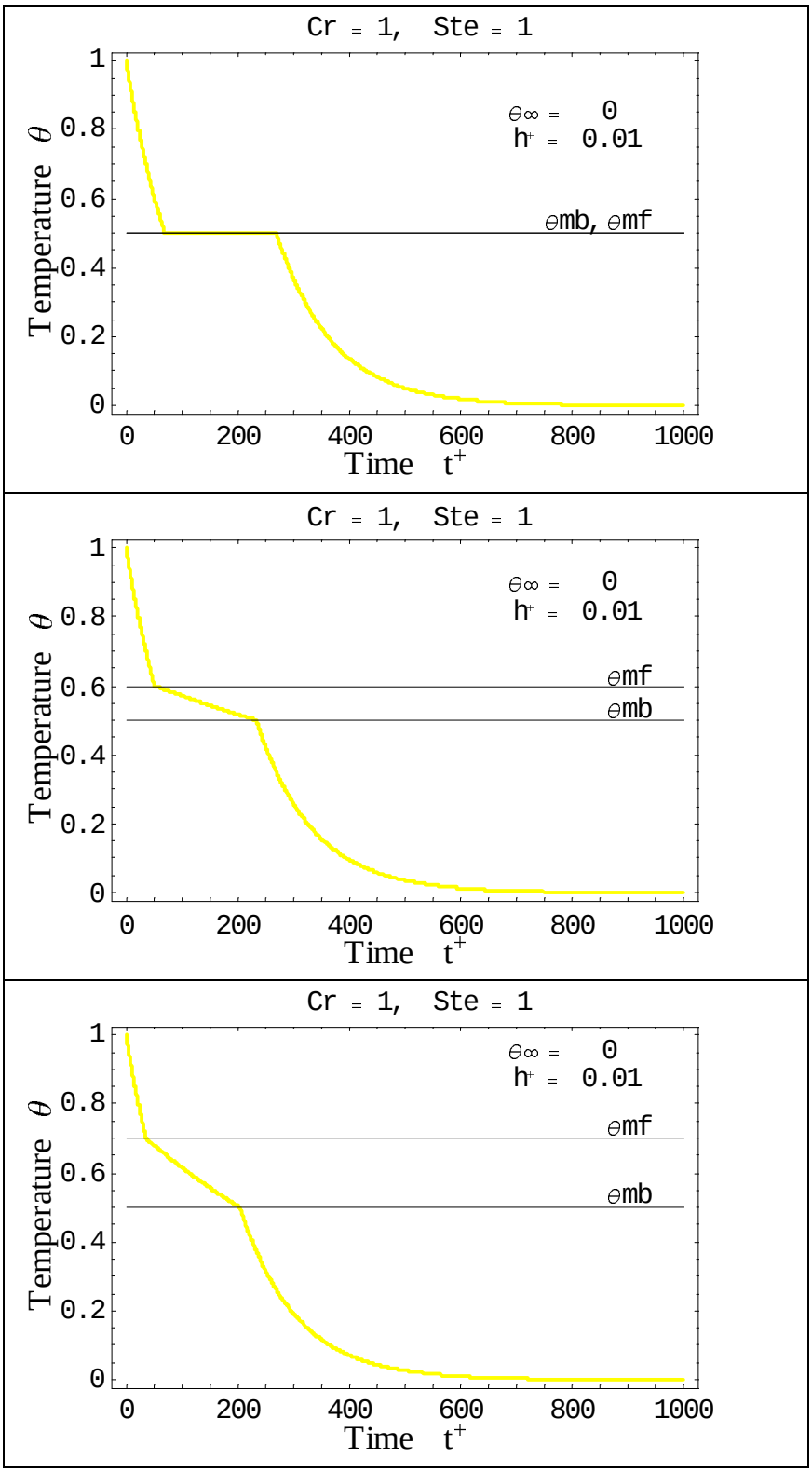

Fig. 4.1.5. Effect of melting temperature on temperature vs. time for a lumped system, ($\Delta t^+ = 0.5$).

4.1.4. Internal Source

The effect of an internal source is investigated for a lumped system, which is initially all solid at temperature $\theta = 0$ with heat convection $\theta_\infty = 0$ and $h^+ = 0.01$(for lumped capacity system Bi<0.1), with the heat capacity ratio and Stefan number *Cr=1* and *Ste=1*. Phase change occurs at a single melting temperature $\theta mb = \theta mf = 0.5$ and $\Delta t^+ = 0.5$ is taken as the time step.

Figure 4.1.6 displays the temperature histories of the lumped system for relatively low, medium and high values of the internal heat source $Sc^+ = 0.001,\ 0.01,\ and\ 0.1$. The effect of the internal source can be observed before, during and after phase change. When $Sc^+ = 0.001$ the generated energy is not enough to let the lumped system get to phase change, and temperature increases very slowly. In the other case with $Sc^+ = 0.01$ the energy is enough to let the system get to the phase change, but phase change happens very slowly and it takes a long time to finish the whole process. On the other hand when $Sc^+ = 0.1$ the generated energy is so high that the system gets to the saturation temperature very quickly and it completes the phase transition process in a very short time and the temperature increases rapidly.

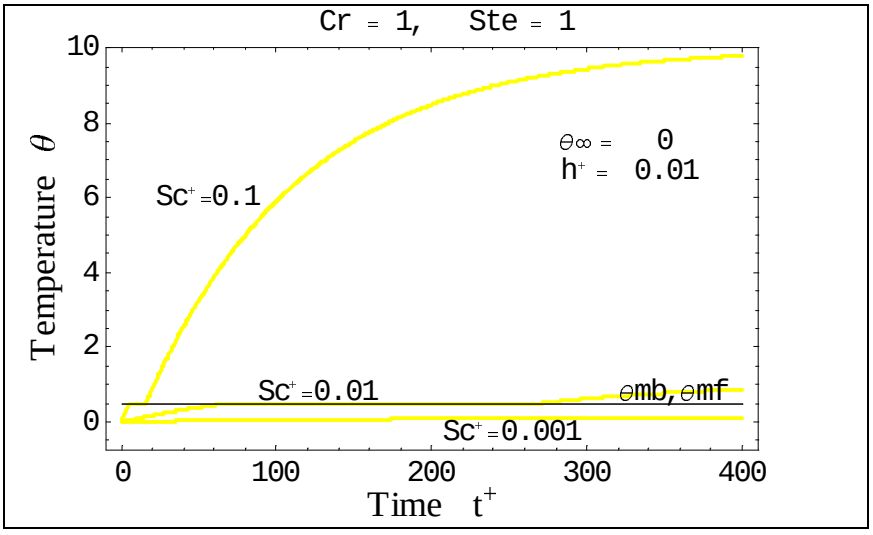

Fig. 4.1.6. Effect of heat source on temperature vs. time for a lumped system, ($\Delta t^+ = 0.5$).

4.1.5. Heat Transfer Coefficient

The effect of the heat transfer coefficient is investigated for a lumped system. The system is initially all liquid at temperature $\theta = 1$ with the heat capacity ratio and Stefan number *Cr=1* and *Ste=1*. Phase transition occurs at a single melting temperature $\theta mb = \theta mf = 0.5$. The environment temperature is $\theta_{\infty} = 0$, and $\Delta t^{+} = 0.5$ is taken as the time step.

Figure 4.1.7 displays the temperature histories of the lumped system for relatively low, medium and high heat transfer coefficient $h^{+} = 0.001$, 0.01, *and* 0.1(for lumped capacity system Bi<0.1). The effect of the heat transfer coefficient can be observed before, during and after phase change. When $h^{+} = 0.001$ energy is transferred to the environment relatively slowly. In the other case, when $h^{+} = 0.01$ temperature drops to the melting temperature very quickly, and takes less time to complete phase transition process. On the other hand when $h^{+} = 0.1$, the heat transfer coefficient is so high that the system energy is transferred to the environment very quickly and in a very short time the lumped system gets to the environment temperature.

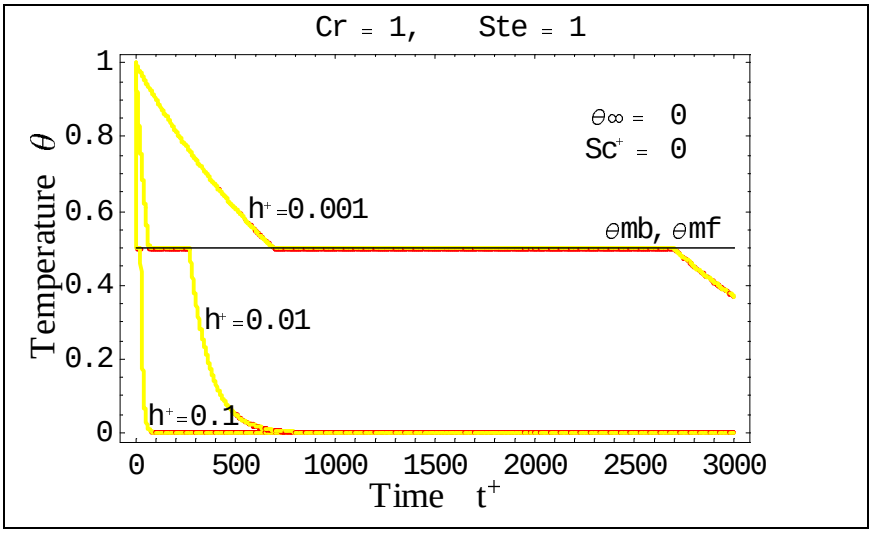

Fig. 4.1.7. Effect of heat transfer coefficient on temperature vs. time for a lumped system, ($\Delta t^{+} = 0.5$).

4.2. Homogeneous Materials

The homogeneous material during phase transition is investigated in this part. First, the comparison between the explicit and implicit method is studied in order to analyze the stability problem. Next, the effects of the time steps Δt and control volumes Δx are examined by comparing with an analytical solution. Then, the effects of the material properties such as Stefan number, heat capacity ratio, conductivity ratio, and melting temperature are investigated. Also, the effect of the internal source is studied. Last, the effect of the external source is analyzed. Numerical results are presented in terms of the dimensionless variables.

4.2.1. Comparison between Explicit and Implicit Methods

The stability problem is analyzed by comparing the explicit and implicit methods for a homogeneous material, which is initially all liquid at temperature $\theta = 1$ with a constant surface temperature $\theta_{sur} = 0$ at $x^+ = 0$ and insulated at $x^+ = 1$. Phase transition occurs at a single melting temperature $\theta mb = \theta mf = 0.5$. The Stefan number, heat capacity ratio, and conductivity ratio are, *Ste =1* , *Cr =1* and *Kr =1*. The number of control volumes is *8* in this investigation.

4.2.1.1. Stability

Figures 4.2.1-4.2.3 display the temperature distributions, temperature histories, and phase fronts of a homogeneous material for various values of Δt^+ to show the stability of the implicit and explicit method. According to the equation (3.25) the explicit critical Δt^+ is $Ex\Delta t^+_{cri} = 0.00781$ in this case. Figure 4.2.1 shows that when the Δt^+ is less than the explicit critical Δt^+ both the explicit and implicit methods are stable, and the results are very close. On the other hand, Fig 4.2.2 demonstrates that the explicit method becomes unstable as Δt^+ becomes greater than the explicit critical Δt^+, but based on the equation (3.25) it is stable during phase transition. Figure 4.2.3 illustrates when Δt^+ is much bigger than the critical Δt^+, the explicit method is extremely unstable. The temperature distribution graphs show when the explicit method is unstable, there are many phase

fronts at each time. As a result, since the implicit method is unconditionally stable, this method will be used for farther investigations.

4.2.2. Analytical Solution for Solidification in a Semi-infinite Region

A liquid at a uniform initial temperature T_i that is higher than the melting temperature *Tm* of the solid phase is confined to a semi- infinite region *x>0*. At time *t=0* the boundary surface at *x=0* is lowered to a temperature T_0 below *Tm* and maintained at that temperature for times *t>0*. As a result, the solidification starts at the surface *x=0* and the solid-liquid interface, or phase front, moves in the positive *x* direction. The problem formulation for the solid phase is given as,

$$\begin{aligned} &\frac{\partial^2 T_s}{\partial x^2} = \frac{1}{\alpha_s}\frac{\partial T_s(x,t)}{\partial t} && in \quad 0 < x < PhF(t), \qquad t > 0 \\ &T_s(x,t) = T_0 && at \qquad x = 0, \qquad t > 0 \end{aligned} \tag{4.1}$$

for the liquid phase as,

$$\begin{aligned} &\frac{\partial^2 T_l}{\partial x^2} = \frac{1}{\alpha_l}\frac{\partial T_l(x,t)}{\partial t} && in \quad PhF(t) < x < \infty, \qquad t > 0 \\ &T_l(x,t) \to T_i && as \qquad x \to \infty, \qquad t > 0 \\ &T_l(x,t) = T_i && for \qquad t = 0, \qquad in \qquad x > 0 \end{aligned} \tag{4.2}$$

and the coupling conditions at the phase front *x=PhF(t)* as,

$$\begin{aligned} &T_s(x,t) = T_l(x,t) = Tm && at \qquad x = PhF(t), \qquad t > 0 \\ &k_s\frac{\partial T_s}{\partial x} - k_l\frac{\partial T_l}{\partial x} = \rho\lambda\frac{dPhF(t)}{dt} && at \qquad x = PhF(t), \qquad t > 0 \end{aligned} \tag{4.3}$$

According to the solution in [Ozisik,1993], the temperatures for the solid and liquid phases are,

$$\frac{T_s(x,t) - T_0}{Tm - T_0} = \frac{erf[x/2(\alpha_s t)^{1/2}]}{erf[\eta]} \tag{4.4}$$

$$\frac{T_l(x,t) - T_i}{Tm - T_i} = \frac{erfc[x/2(\alpha_l t)^{1/2}]}{erfc[\eta(\alpha_s/\alpha_l)^{1/2}]} \tag{4.5}$$

where η is known from the solution of following equation,

$$\frac{e^{-\eta^2}}{erf[\eta]}+\frac{k_l}{k_s}\left(\frac{\alpha_s}{\alpha_l}\right)^{1/2}\frac{Tm-T_i}{Tm-T_0}\frac{e^{-\eta^2(\alpha_s/\alpha_l)}}{erfc[\eta(\alpha_s/\alpha_l)^{1/2}]}=\frac{\eta\lambda\sqrt{\pi}}{Cp_s(Tm-T_0)} \qquad (4.6)$$

and the location of phase front *PhF(t)* is determined from,

$$PhF(t)=2\eta(\alpha_s t)^{1/2} \qquad (4.7)$$

4.2.3. Comparison with Analytical Solution

The semi-infinite analytical solution with a constant surface temperature $\theta_{sur}=0$ at $x^+=0$ is compared to the implicit method with a constant surface temperature $\theta_{sur}=0$ at $x^+=0$ and insulated at $x^+=1$. Figure 4.2.4 illustrates the temperature distributions, temperature histories, and phase fronts of a homogeneous material, which is initially at temperature $\theta=1$ with melting temperature $\theta mb=\theta mf=0.5$, and the Stefan number, heat capacity ratio, and conductivity ratio *Ste =1* , *Cr =1* and *Kr =1*. This figure demonstrates that the results of these two solutions are very close when the back wall temperature stays at the initial temperature, which means the slab is behaving like a semi-infinite region. On the other hand, when the back wall temperature starts dropping, the validation of this assumption starts failing and a difference can be observed between the results of these two solutions. The comparison with the analytical solution verifies the accuracy of the finite difference solution.

4.2.3.1. Δt and Δx Effects

The effects of Δt^+ and Δx^+ on the implicit method are analyzed by comparing with the analytical solution in a time range where these two solutions give approximately very close results. Figure 4.2.5 displays the phase fronts of the homogeneous material with 64 control volumes at various Δt^+ for the same conditions used in Fig 4.2.4. It shows, by decreasing the Δt^+, the curves become more step-like, and the results are more accurate. On the other hand, when the Δt^+ is small enough negligible differences can be observed by decreasing Δt^+.

Figure 4.2.6 illustrates the phase fronts of the homogeneous material with $\Delta t^{+} = 0.01$ for various control volumes. The figure shows that the system with more control volumes provides more accurate results.

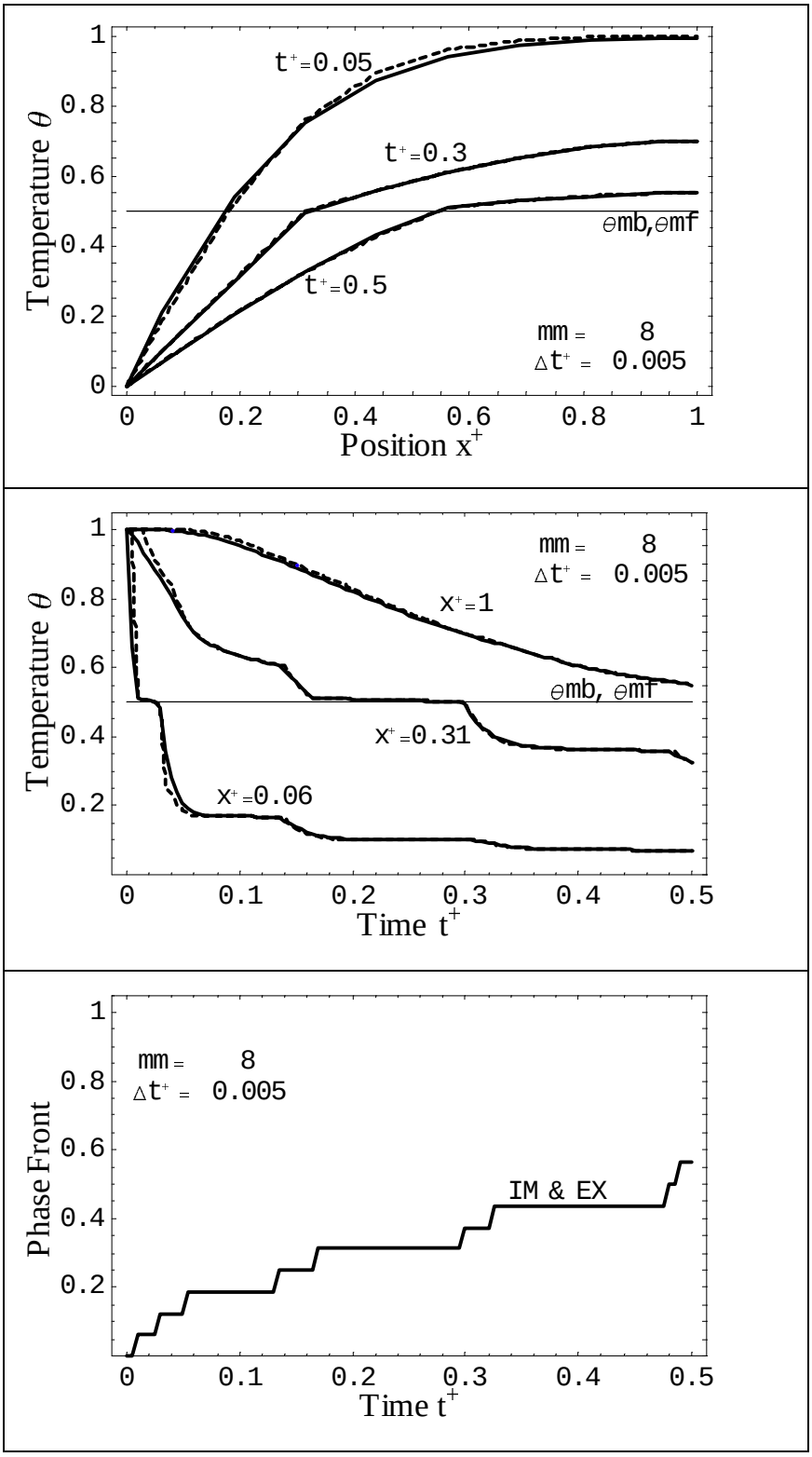

Fig. 4.2.1. Stability of implicit and explicit method for a homogeneous material, with a constant surface temperature $\theta_{sur}=0$ at $x^+=0$ and insulated at $x^+=1$, with $Cr=1,\quad Kr=1,\quad Ste=1$, ($Ex\Delta t^+_{crit}=0.00781$), (..... *Explicit,* —— *Implicit*).

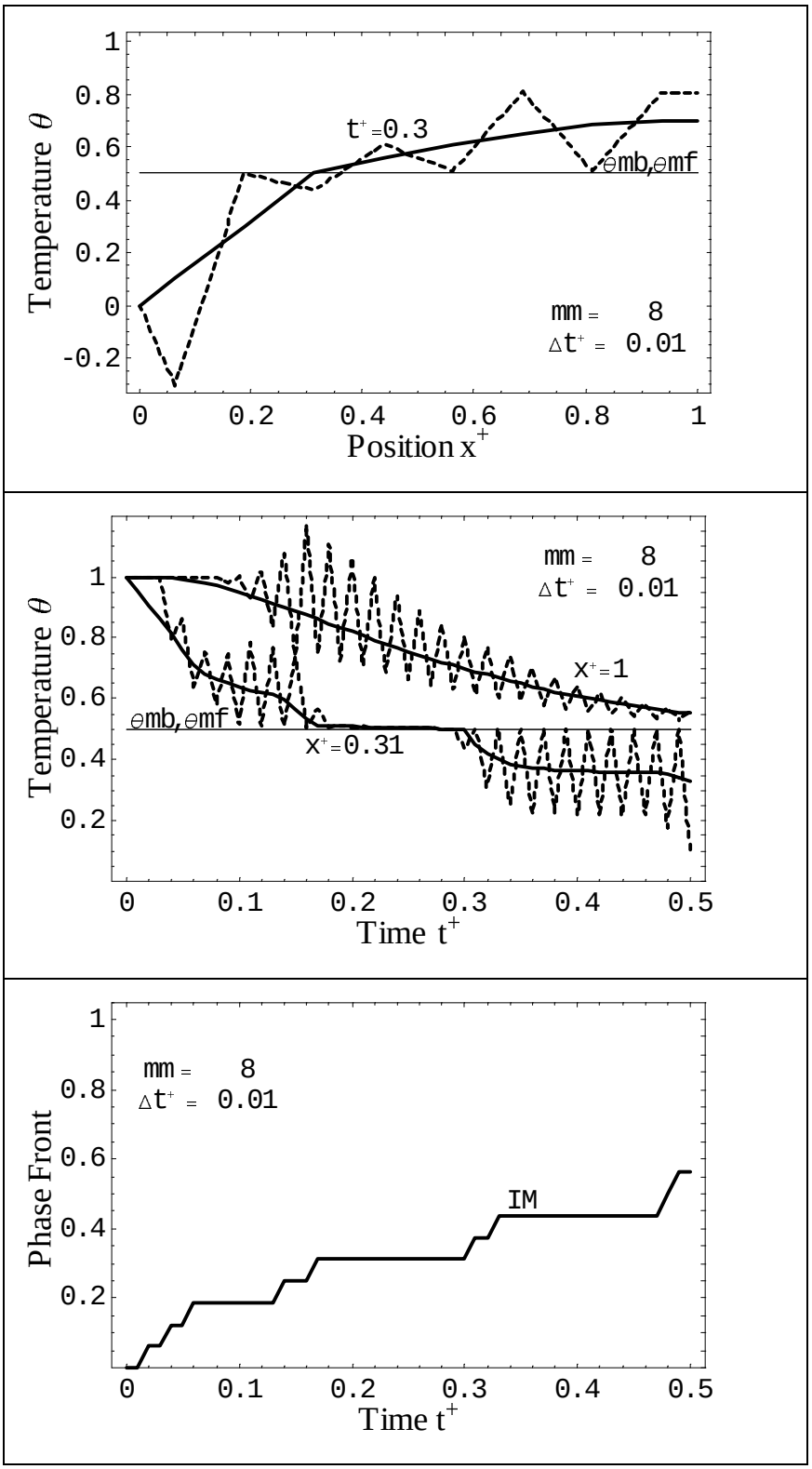

Fig. 4.2.2. Stability of implicit and explicit method for a homogeneous material, with a constant surface temperature $\theta_{sur}=0$ at $x^+=0$ and insulated at $x^+=1$, with $Cr=1$, $Kr=1$, $Ste=1$, ($Ex\Delta t^+_{crit}=0.00781$), (..... *Explicit,* —— *Implicit*).

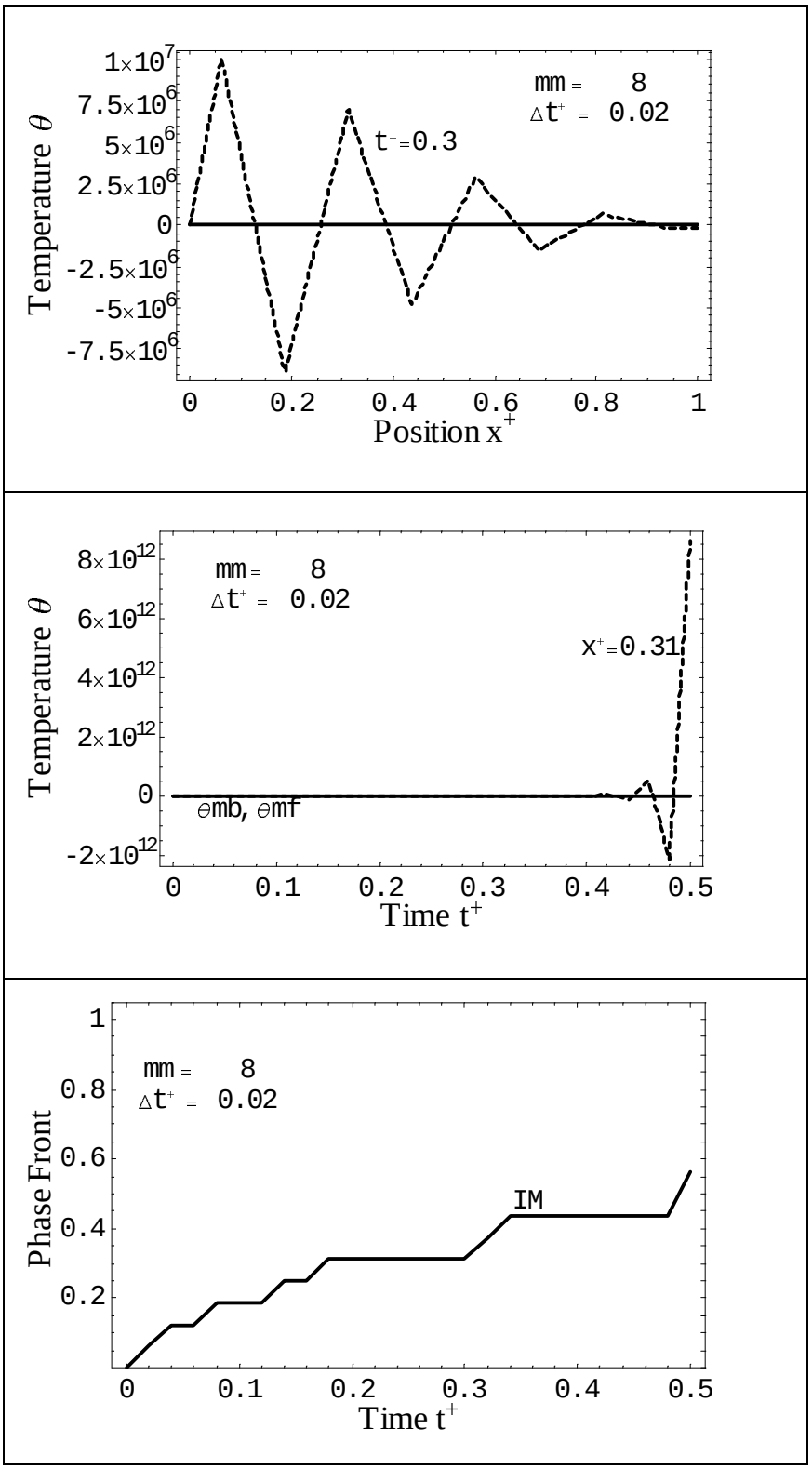

Fig. 4.2.3. Stability of implicit and explicit method for a homogeneous material, with a constant surface temperature $\theta_{sur}=0$ at $x^+=0$ and insulated at $x^+=1$,with $Cr=1,\quad Kr=1,\quad Ste=1$, ($Ex\Delta t^+_{crit}=0.00781$), (..... *Explicit,* —— *Implicit*).

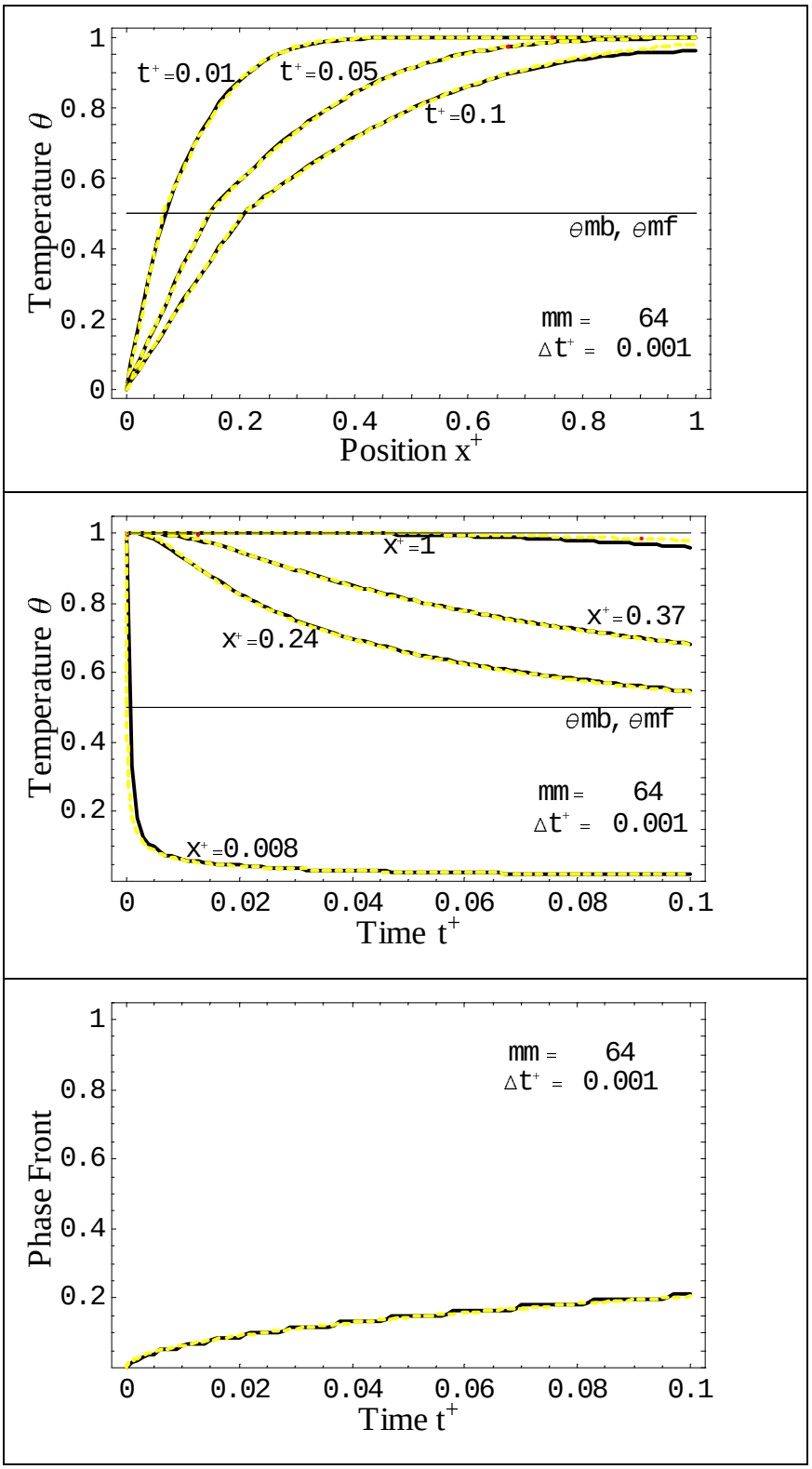

Fig. 4.2.4. Comparison of semi-infinite analytical solution with implicit method for a homogeneous material, with a constant surface temperature $\theta_{sur}=0$ at $x^+=0$, with $Cr=1$, $Kr=1$, $Ste=1$, (····· *Analytical*, —— *Implicit*).

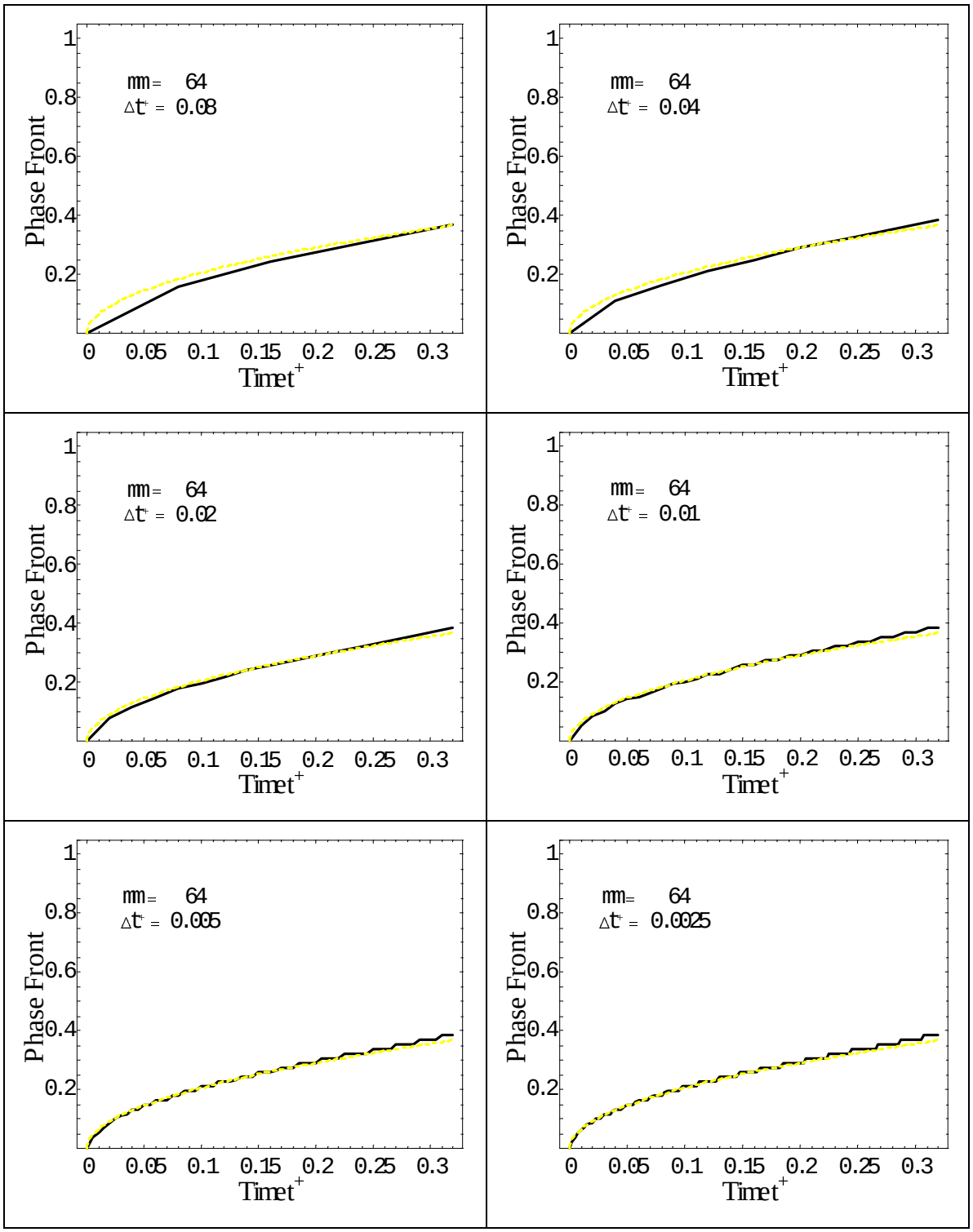

Fig. 4.2.5. Effect of Δt^+ on phase front vs. time for a homogeneous material, initially at $\theta_i = 1$ with a constant surface temperature $\theta_{sur} = 0$ at $x^+ = 0$ and insulated at $x^+ = 1$, with $Cr = 1$, $Kr = 1$, $Ste = 1$, and melting temperature $\theta mb = \theta mf = 0.5$.
(····· Analytical, —— Implicit)

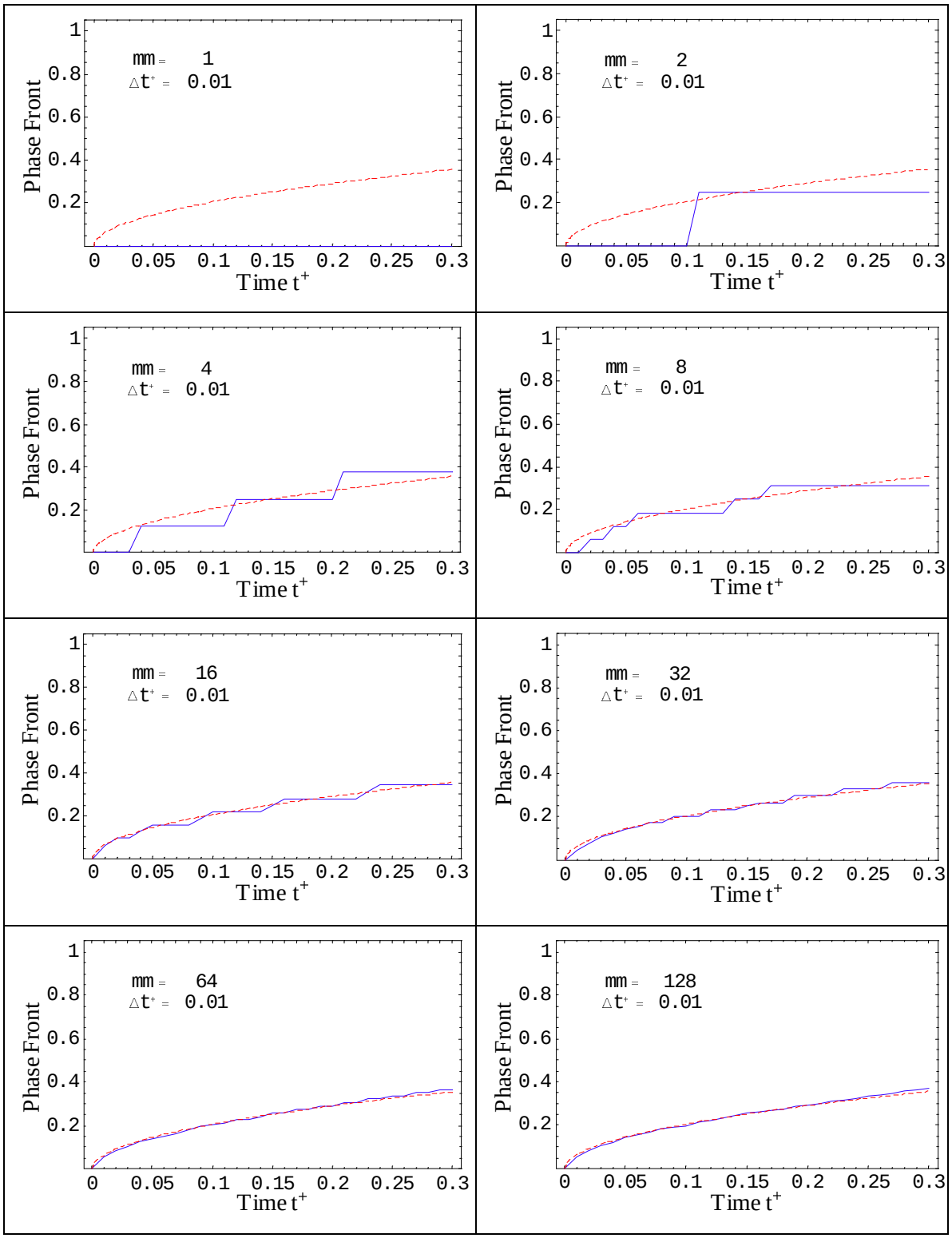

Fig. 4.2.6. Effect of Δx^+ on phase front vs. time for a homogeneous material, initially at $\theta_i = 1$ with a constant surface temperature $\theta_{sur} = 0$ at $x^+ = 0$ and insulated at $x^+ = 1$, with $Cr = 1$, $Kr = 1$, $Ste = 1$, and melting temperature $\theta mb = \theta mf = 0.5$.
(····· Analytical, —— Implicit)

4.2.4. Material Properties

The effects of material properties such as Stefan number, heat capacity ratio, conductivity ratio and melting temperature are investigated for a homogeneous material. In this investigation the homogeneous system is initially all liquid at temperature $\theta = 1$ with a constant surface temperature $\theta_{sur} = 0$ at $x^+ = 0$ and insulated at $x^+ = 1$. The number of control volumes is *64*, and $\Delta t^+ = 0.01$ is taken as the time step.

4.2.4.1. Stefan Number Effects

The Stefan number is a dimensionless group, which is the sensible energy divided by the latent energy. In this investigation the heat capacity ratio and conductivity ratio are *Cr=1* and *Kr=1*. Phase change occurs at a single melting temperature $\theta mb = \theta mf = 0.5$.

Figures 4.2.7 and 4.2.8 display respectively the temperature distributions at the various times and temperature histories at the different locations of the homogeneous material system for relatively low, medium and high Stefan number *Ste= 0.1, 1, 10*. Based on the definition of Stefan number, by decreasing the *Ste* the latent heat is increased, which means more energy must be released to complete phase change. Therefore, phase transition needs more time to be completed. The case of *Ste=10* is very close to the standard heat conduction problem with no phase change.

4.2.4.2. Heat Capacity Ratio Effects

The heat capacity ratio is a dimensionless group, which is the ratio of liquid heat capacity to the solid heat capacity. The solid thermal properties are chosen as reference quantities. In this investigation the Stefan number and conductivity ratio are *Ste=1* and *Kr=1*. Phase transition occurs at a single melting temperature $\theta mb = \theta mf = 0.5$.

Figures 4.2.9 displays the temperature distributions at the various times, and Fig 4.2.10 shows the temperature histories at the different locations of the homogeneous material system for relatively low, medium and high heat capacity ratio *Cr= 0.1, 1, 10*. These graphs demonstrate, by increasing the heat capacity ratio *Cr*, more energy has to be

released for the liquid material temperature to drop. As a result, each control volume needs more time to get to phase change at higher capacity ratio. On the other hand, when *Cr=0.1,* the temperature of the most control volumes drop very quickly to the phase transition temperature, therefore heat is transferred slowly through the control volumes because of the small control volumes temperature gradients.

4.2.4.3. Conductivity Ratio Effects

The conductivity ratio is a dimensionless group, which is the ratio of liquid conductivity to the solid conductivity. In this investigation the Stefan number and heat capacity ratio are *Ste=1* and C*r=1*. Phase transition occurs at a single melting temperature $\theta mb = \theta mf = 0.5$.

Figures 4.2.11 and 4.2.12 display respectively the temperature distributions at the various times and temperature histories at the different locations of the homogeneous material system for relatively low, medium and high conductivity ratio *Kr= 0.1, 1, 10*. These figures show, by increasing the conductivity ratio *Kr,* energy is transferred more easily through the liquid phase, therefore the temperature drops faster. On the other hand, when *Kr=10,* temperature of the most control volumes drop very quickly to the phase transition temperature.

4.2.4.4. Melting Temperature Effects

In pure materials the phase-change takes place at a discrete temperature, while in the other cases there is no discrete melting point temperature. Here a hypothetical material is considered which is changing phase in a linear way over an extended range of temperatures. In this investigation the heat capacity ratio, Stefan number and conductivity ratio are *Cr=1, Ste=1* and *Kr=1*.

Figures 4.2.13. and 4.2.14 display respectively the temperature and phase fraction histories at the different locations of the homogeneous system for a pure material and two hypothetical materials. For the pure material phase transition occurs at temperature *0.5,* while the hypothetical materials, one occurs over temperature *0.5-0.6* and the other one

occurs over temperature *0.5-0.7*. Since the systems are initially liquid, each system reaches phase transition at different times. Since the *Ste=1* for all the materials, the total energy to finish phase change is the same for each material. As a result, when phase change takes place over an extended range of temperatures, the system approaches the finishing phase transition temperature earlier. On the other hand, when phase transition happens very quickly the time difference is not noticeable.

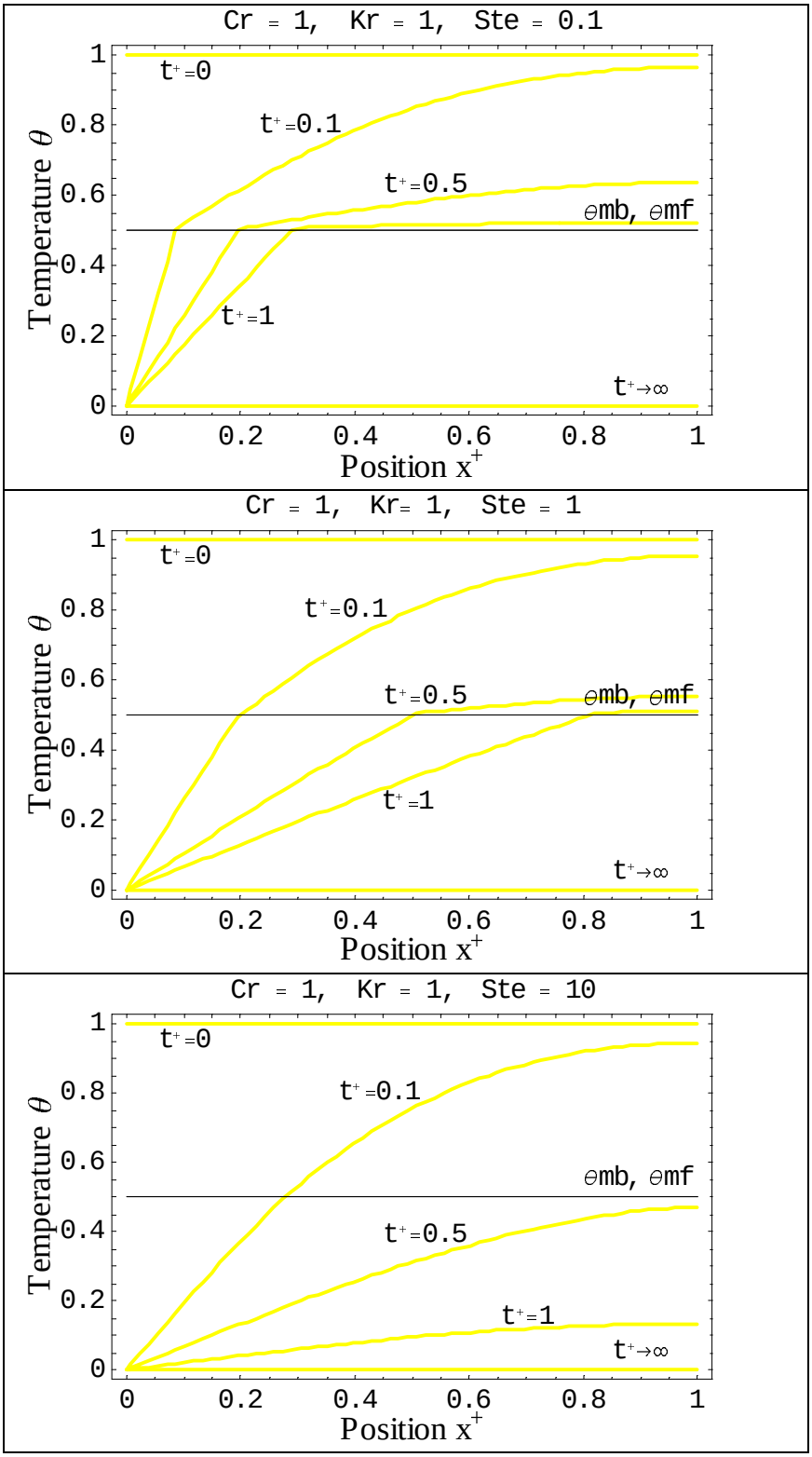

Fig. 4.2.7. Effect of Stefan number on temperature vs. position for a homogeneous material, with a constant surface temperature $\theta_{sur}=0$ at $x^+=0$and insulated at $x^+=1$, *(mm=64,* $\Delta t^+=0.01$*).*

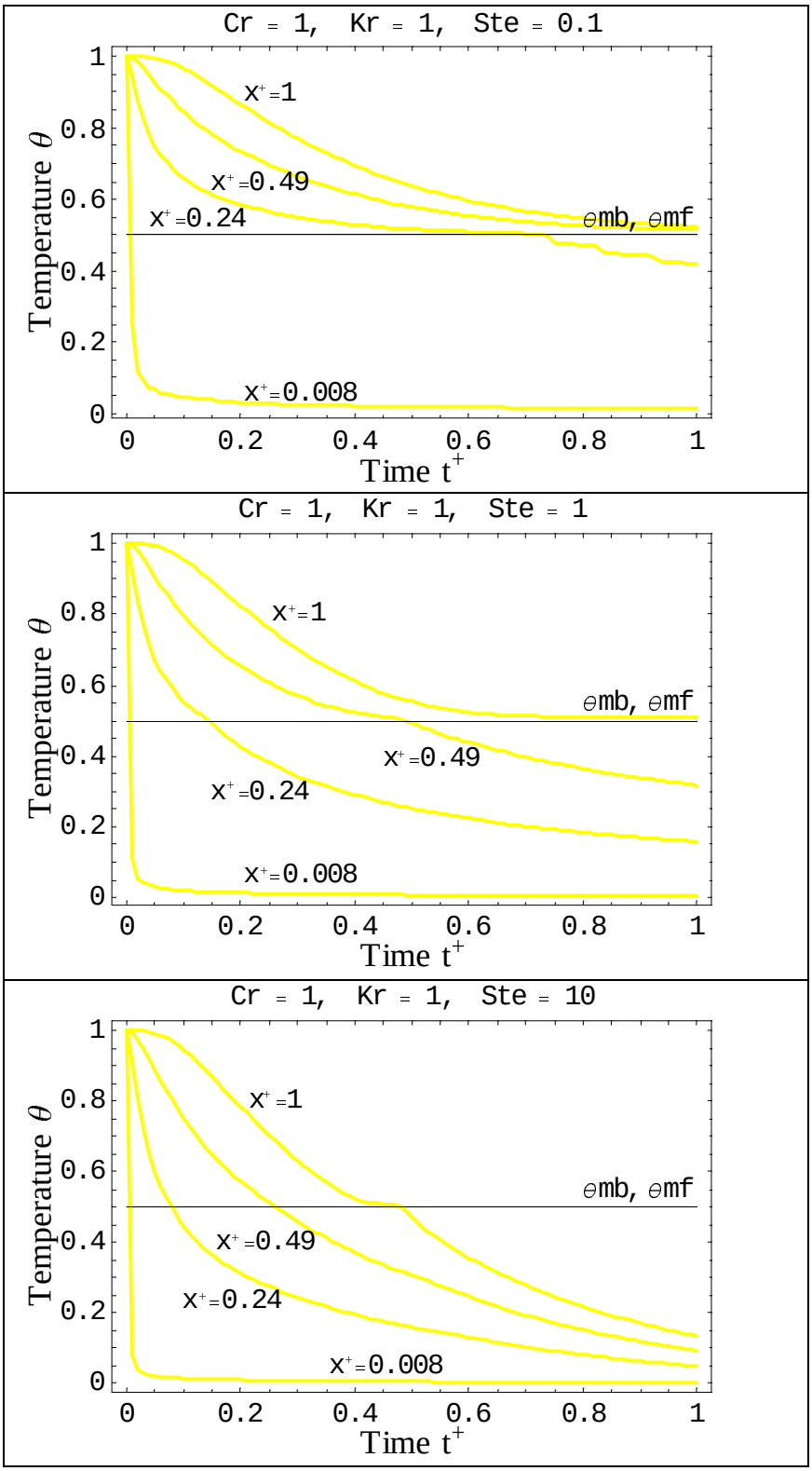

Fig. 4.2.8. Effect of Stefan number on temperature vs. time for a homogeneous material, with a constant surface temperature $\theta_{sur}=0$ at $x^+=0$ and insulated at $x^+=1$, *(mm=64,* $\Delta t^+=0.01$*).*

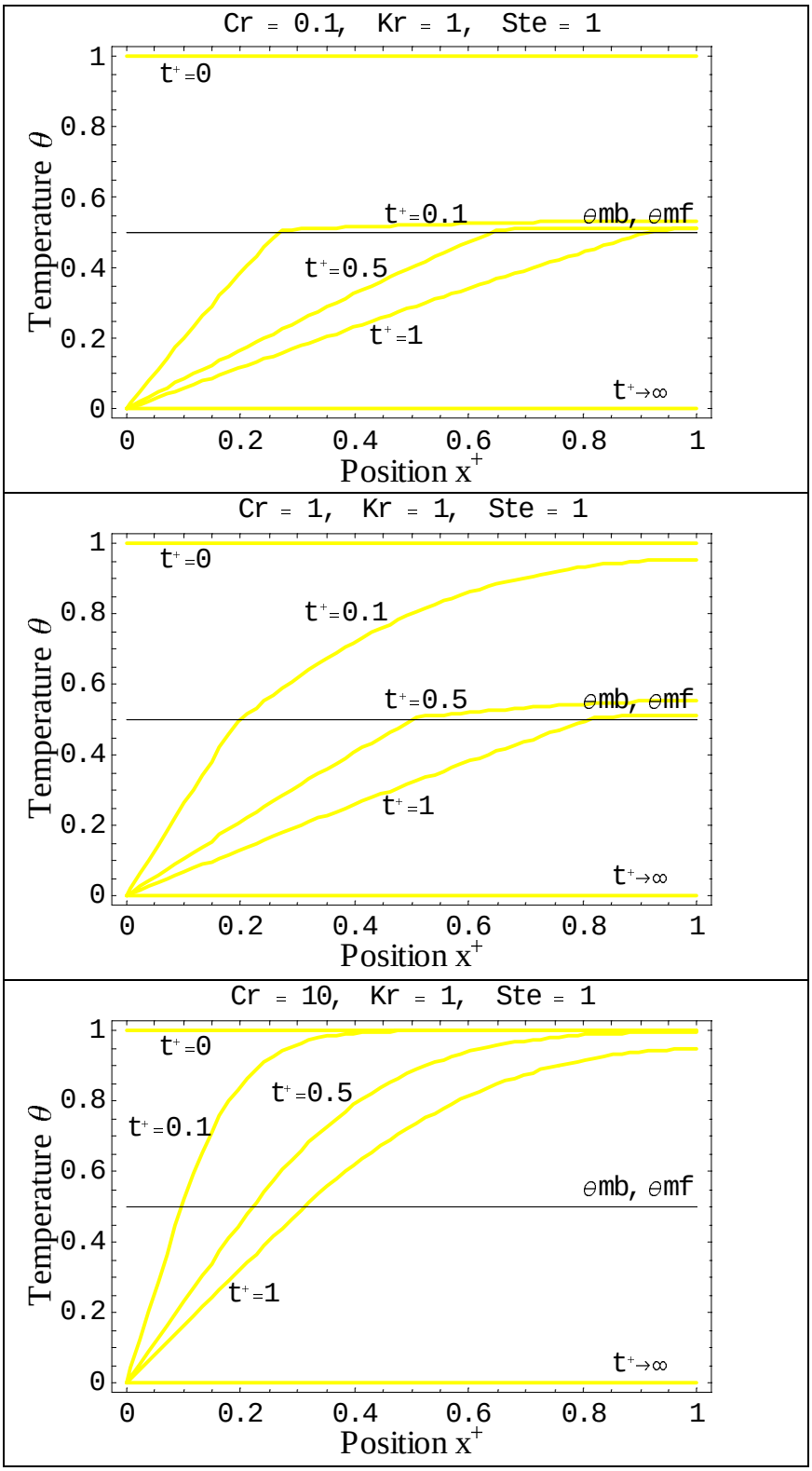

Fig. 4.2.9. Effect of heat capacity ratio on temperature vs. position for a homogeneous material, with a constant surface temperature $\theta_{sur}=0$ at $x^+=0$ and insulated at $x^+=1$, *(mm=64,* $\Delta t^+=0.01$*).*

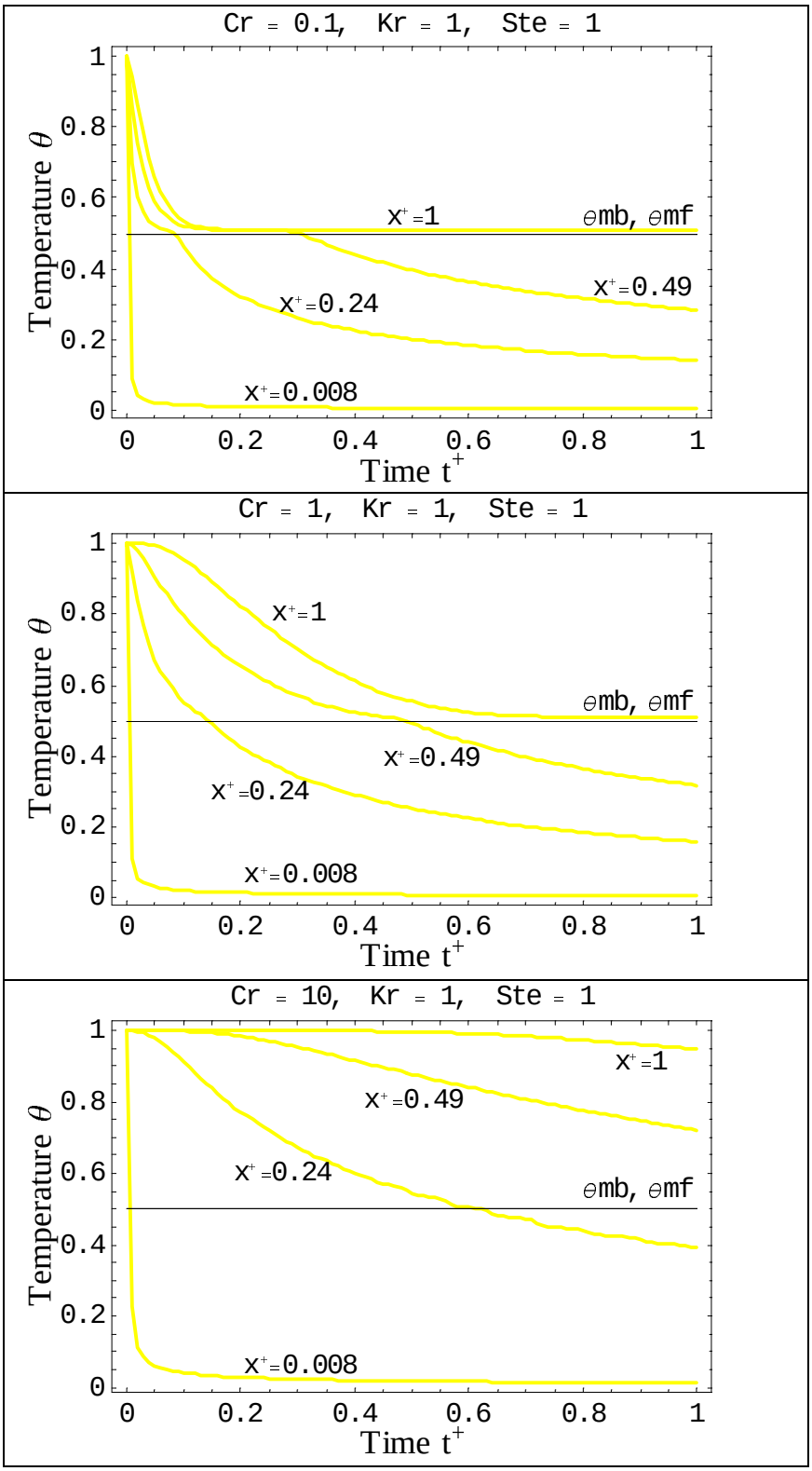

Fig. 4.2.10. Effect of heat capacity ratio on temperature vs. time for a homogeneous material, with a constant surface temperature $\theta_{sur}=0$ at $x^+=0$ and insulated at $x^+=1$, *(mm=64,* $\Delta t^+=0.01$*).*

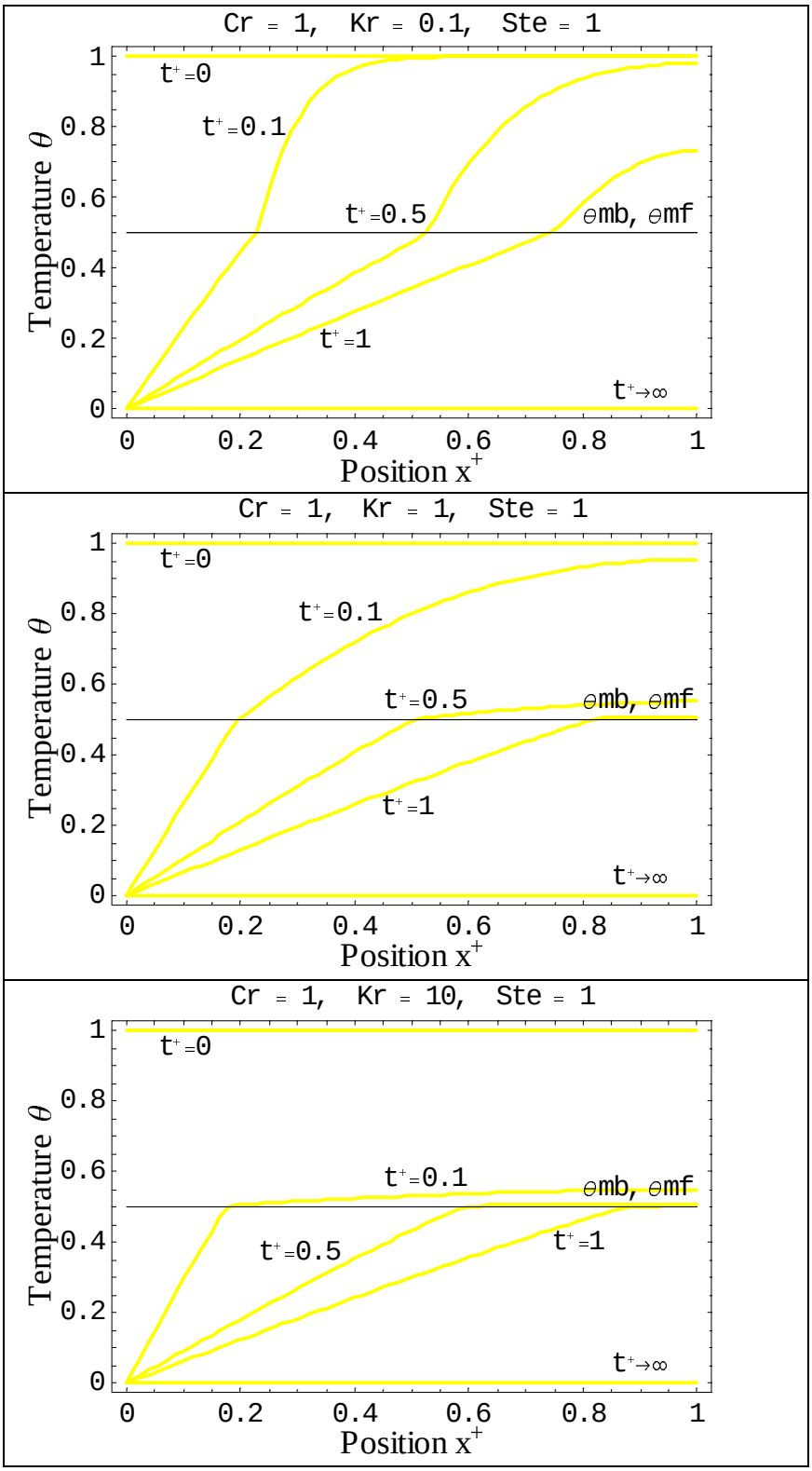

Fig. 4.2.11. Effect of conductivity ratio on temperature vs. position for a homogeneous material, with a constant surface temperature $\theta_{sur}=0$ at $x^+=0$ and insulated at $x^+=1$, *(mm=64,* $\Delta t^+=0.01$*).*

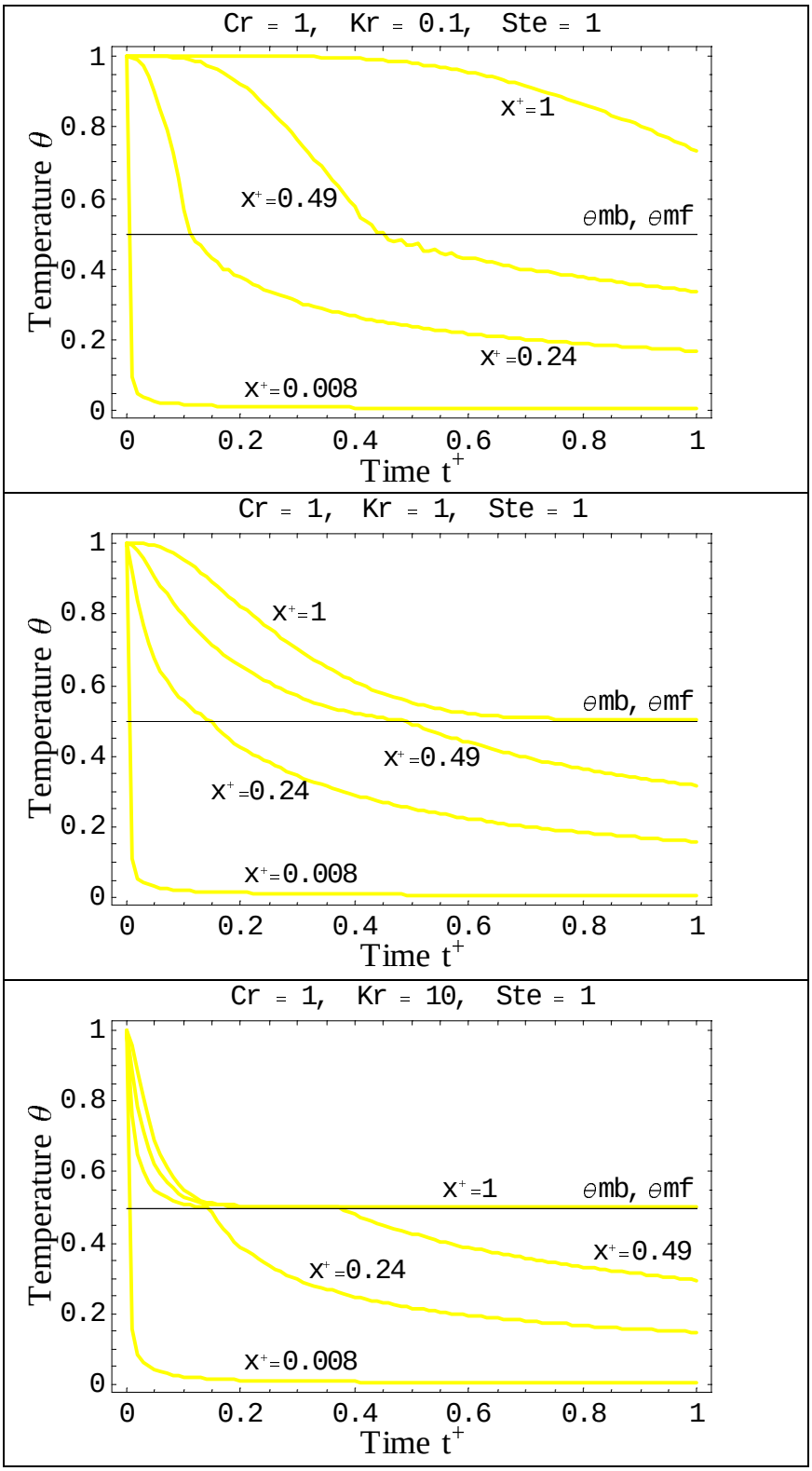

Fig. 4.2.12. Effect of conductivity ratio on temperature vs. time for a homogeneous material, with a constant surface temperature $\theta_{sur}=0$ at $x^+=0$ and insulated at $x^+=1$, *(mm=64,* $\Delta t^+=0.01$*).*

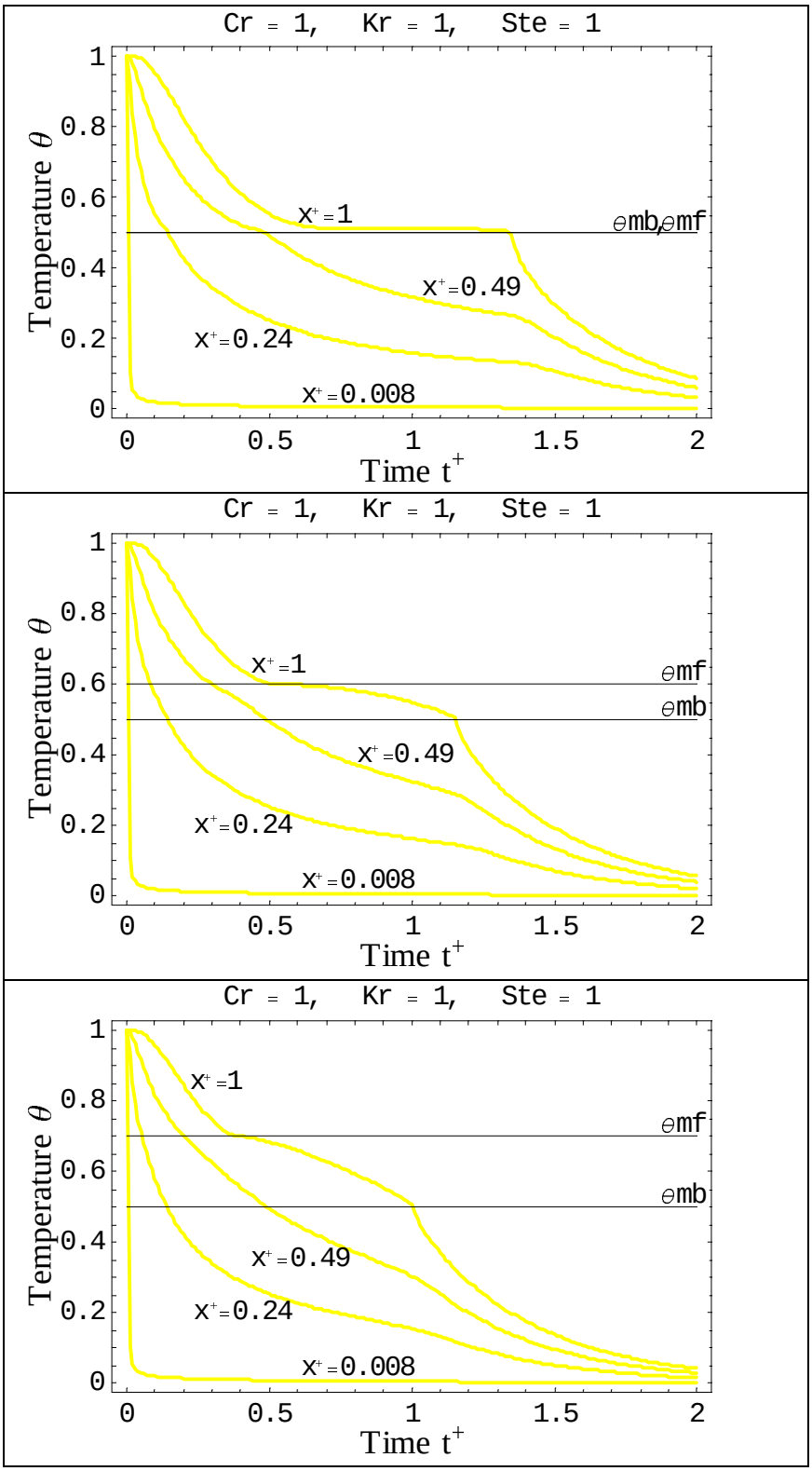

Fig. 4.2.13. Effect of melting temperature on phase fraction vs. time for a homogeneous material, with a constant surface temperature $\theta_{sur}=0$ at $x^+=0$ and insulated at $x^+=1$, *(mm=64,* $\Delta t^+=0.01$*).*

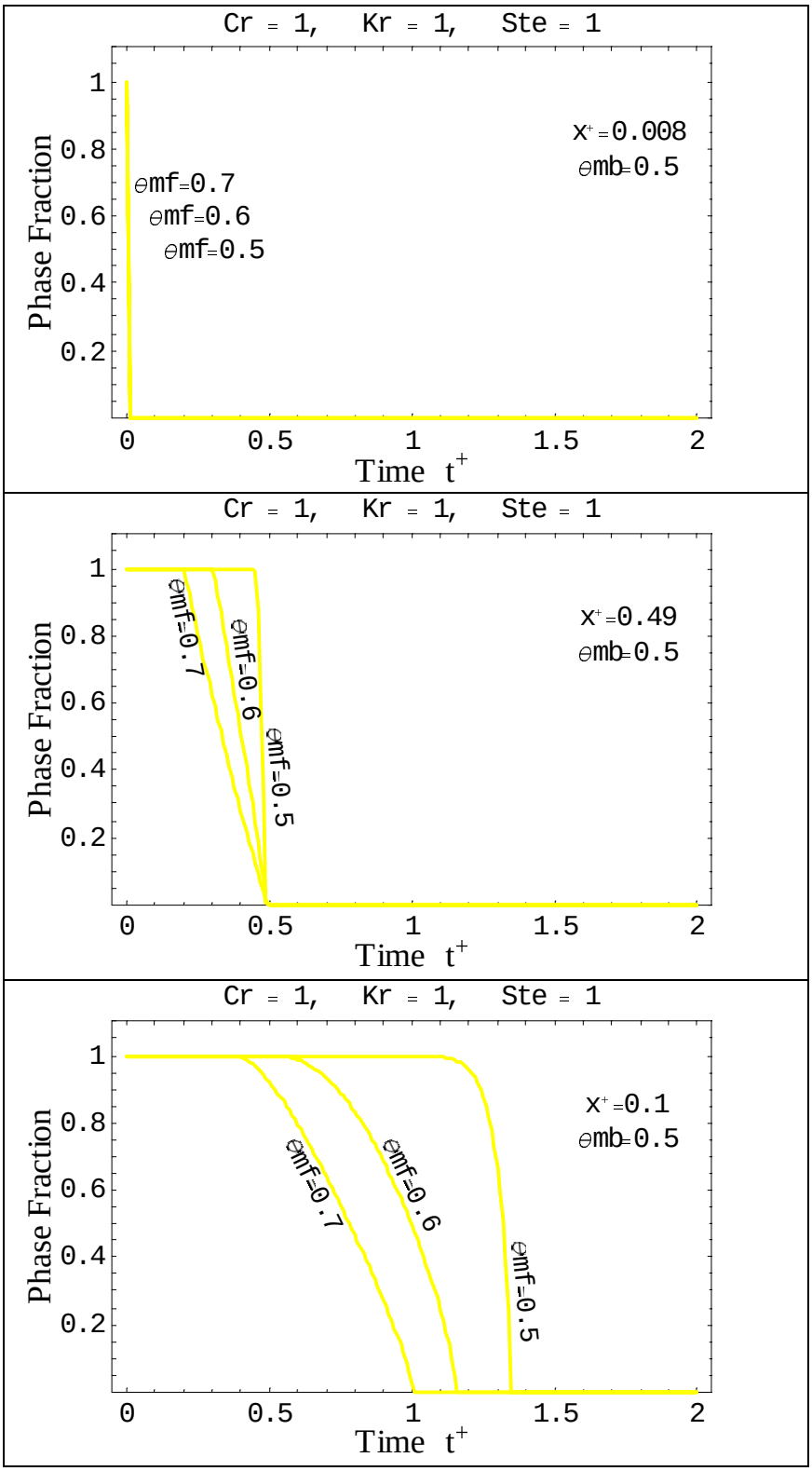

Fig. 4.2.14. Effect of melting temperature on phase fraction vs. time for a homogeneous material, initially at $\theta_i = 1$ with a constant surface temperature $\theta_{sur} = 0$ at $x^+ = 0$ and insulated at $x^+ = 1$, ($mm=64, \Delta t^+ = 0.01$).

4.2.5. Internal Sources

The effect of an internal source is investigated for a homogeneous material. In this investigation the homogeneous system is initially at temperature $\theta = 0$ with heat convection $\theta_\infty = 0$ and $h_\infty^+ = 5$ at $x^+ = 0$ and $x^+ = 1$. The heat capacity ratio, conductivity ratio, and Stefan number are *Cr=1*, *Kr=1*, and *Ste=1*. Phase transition occurs at a single melting temperature $\theta mb = \theta mf = 0.5$. The time step is taken as $\Delta t^+ = 0.01$ and 64 control volumes are used.

Figure 4.2.16 illustrates the temperature distributions at various times and Fig 4.2.17 shows the temperature histories at different locations of the homogeneous material system with a continuous localized heat source, which is located in the middle of the slab as shown on Fig 4.2.15. Since the total energy is the same for all cases, by increasing the region of application, the heat source strength gets weaker, as a result the temperature rises slower and phase change takes more time. In addition, the boundary conditions cause the temperature distributions of the control volumes near the surfaces to be similar for the different cases.

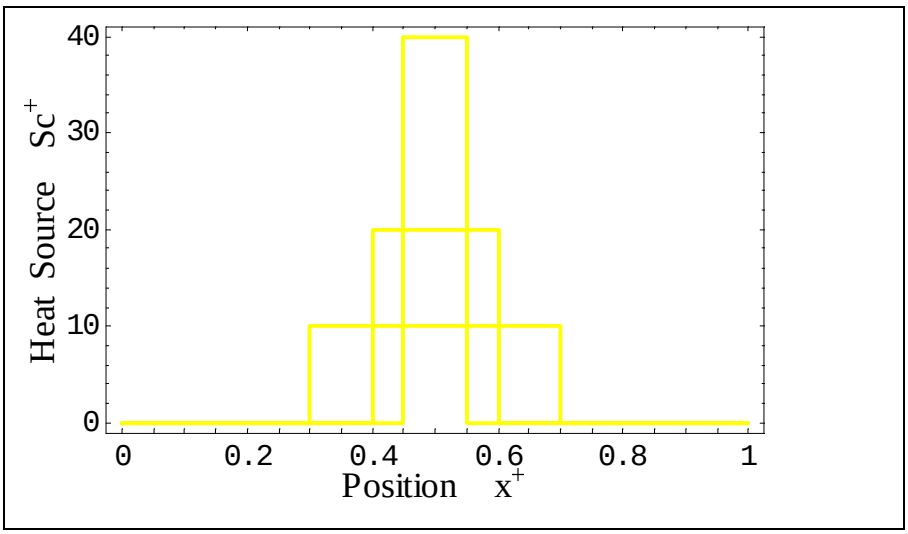

Fig. 4.2.15. Continuous localized volumetric heat source for a homogeneous material.

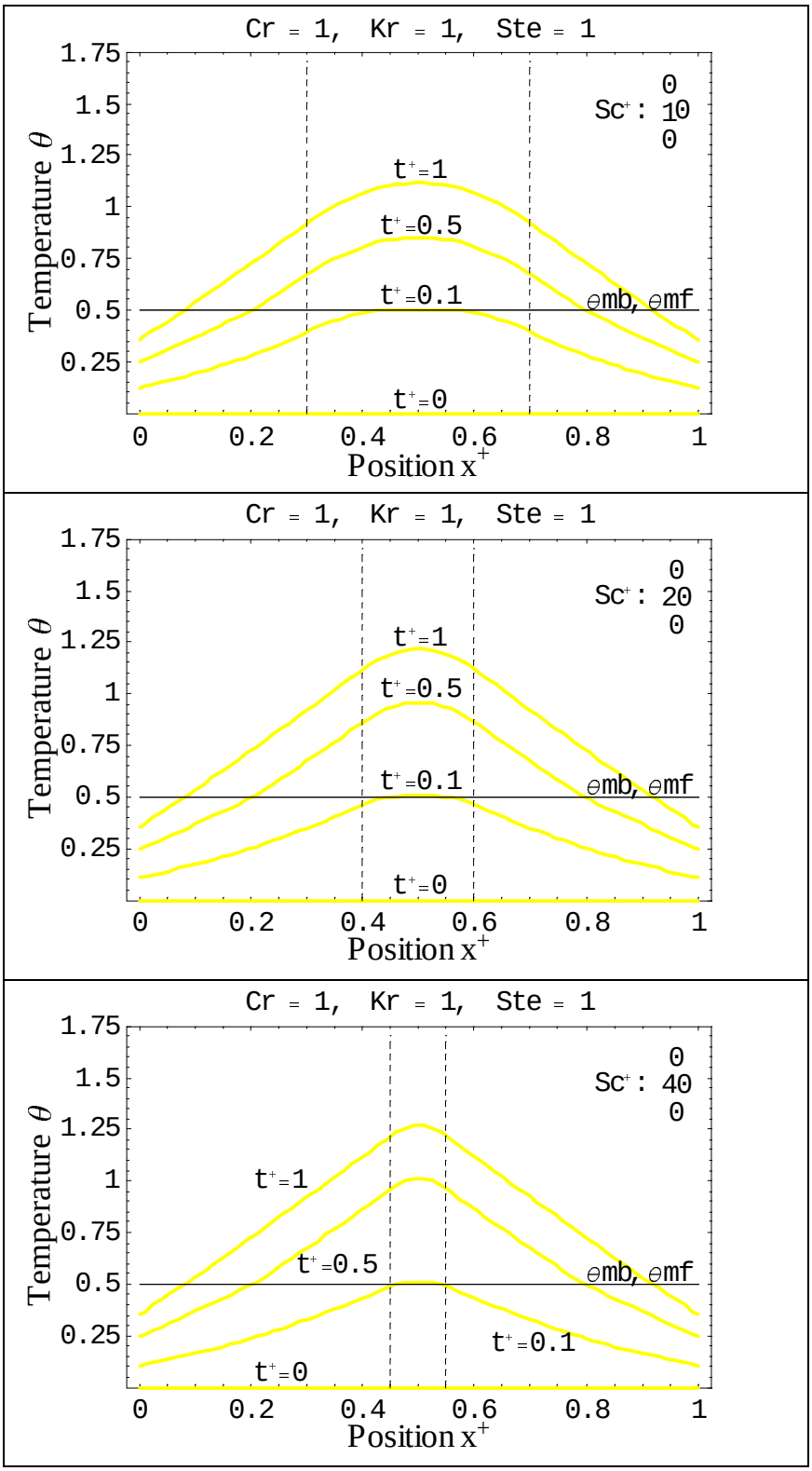

Fig. 4.2.16. Effect of heat source on temperature vs. position for a homogeneous material, with convection $\theta_\infty = 0$ and $h_\infty^+ = 5$ at $x^+ = 0$ and $x^+ = 1$, *(mm=64,* $\Delta t^+ = 0.01$*).*

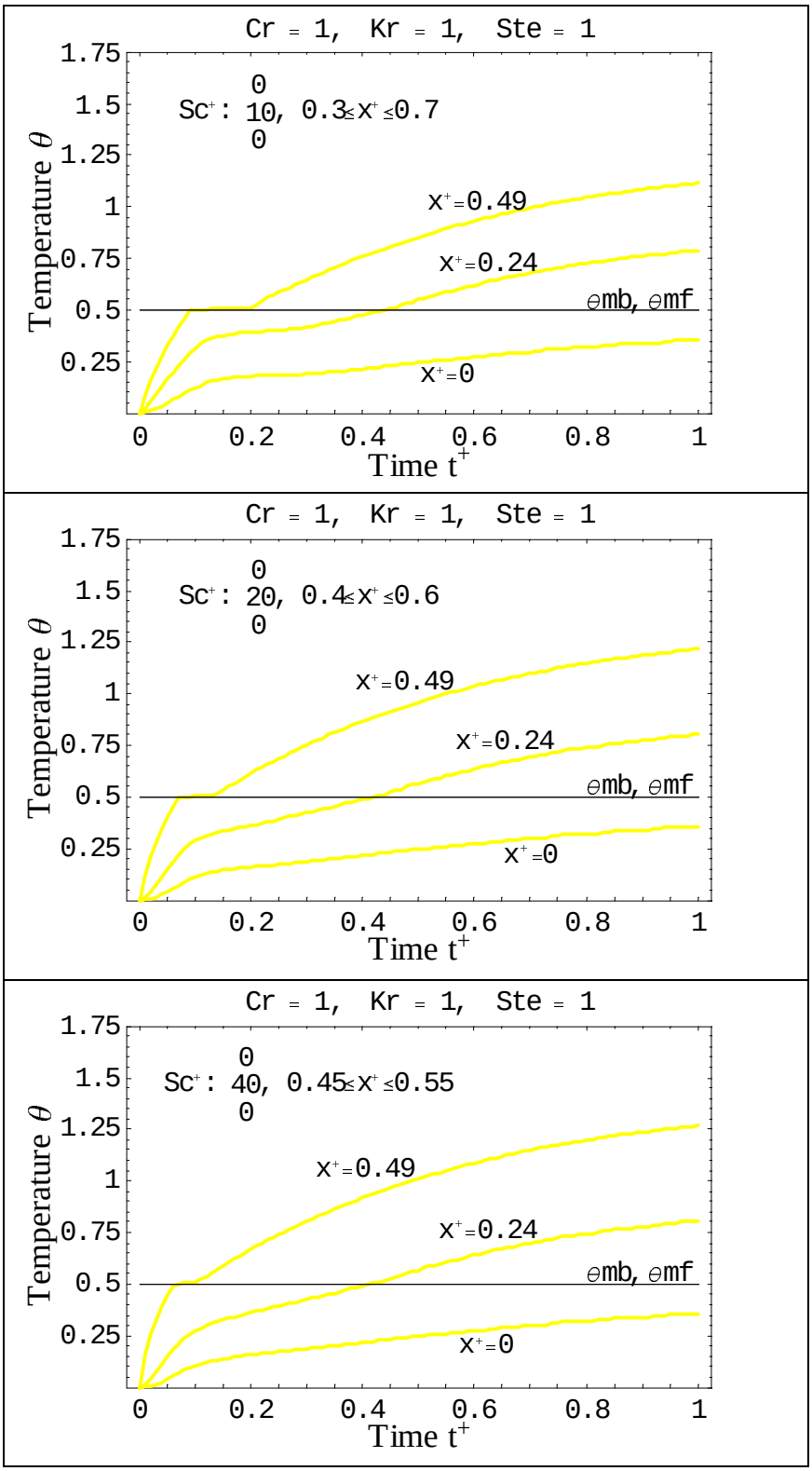

Fig. 4.2.17. Effect of heat source on temperature vs. time for a homogeneous material, with convection $\theta_\infty = 0$ and $h_\infty^+ = 5$ at $x^+ = 0$ and $x^+ = 1$,*(mm=64,* $\Delta t^+ = 0.01$*).*

4.2.6. External Sources

The effect of an external source is investigated by considering a pulsed surface heat flux at a surface for a homogeneous material. In this investigation the homogeneous system is initially all solid at temperature $\theta = 0$ with a pulsed heat flux at $x^+ = 0$ and insulated at $x^+ = 1$. The heat capacity ratio, conductivity ratio, and Stefan number are *Cr=1*, *Kr=1*, and *Ste=1*. Phase transition occurs at a single melting temperature $\theta mb = \theta mf = 0.5$. The number of control volumes is *64*, and $\Delta t^+ = 0.01$ is taken as the time step.

Figure 4.2.18 shows the pulsed surface heat flux at $x^+ = 0$ for three different time pulses. In each case, the total given energy is the same, but the time on is half, one-fourth, and one-eighth of the time pulse.

Figures 4.2.19 and 4.2.20 display respectively the temperature histories at different locations and temperature distributions at various times of the homogeneous material system. It is shown that the most noticeable effect of the pulsed heat flux occurs at the surface, $x^+ = 0$. Otherwise, the subsurfaces in middle of the slab or farther are similar for the different cases. In addition, during the heat flux time off, the surface temperature at $x^+ = 0$ drops severely, while there is no temperature drop for the subsurfaces in the middle of the slab or farther.

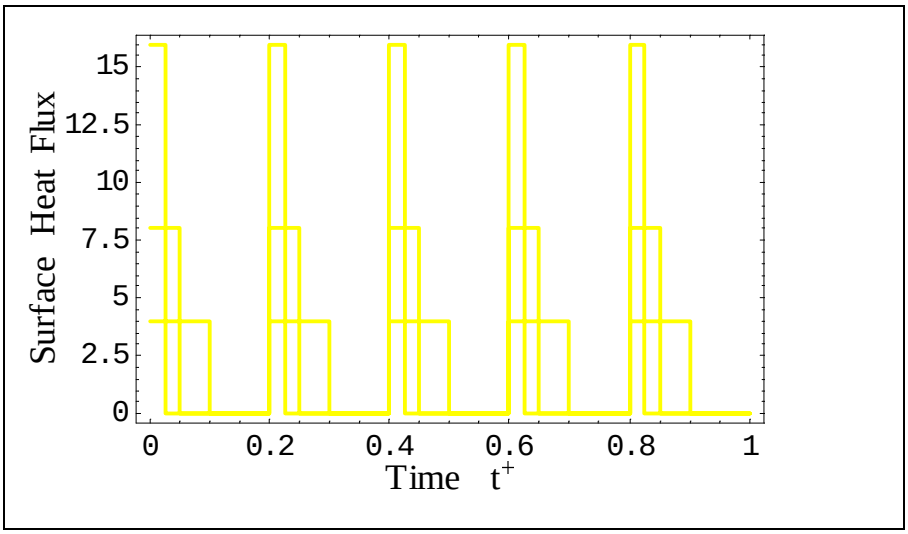

Fig. 4.2.18. Pulsed surface heat flux vs. time at $x^+ = 0$.

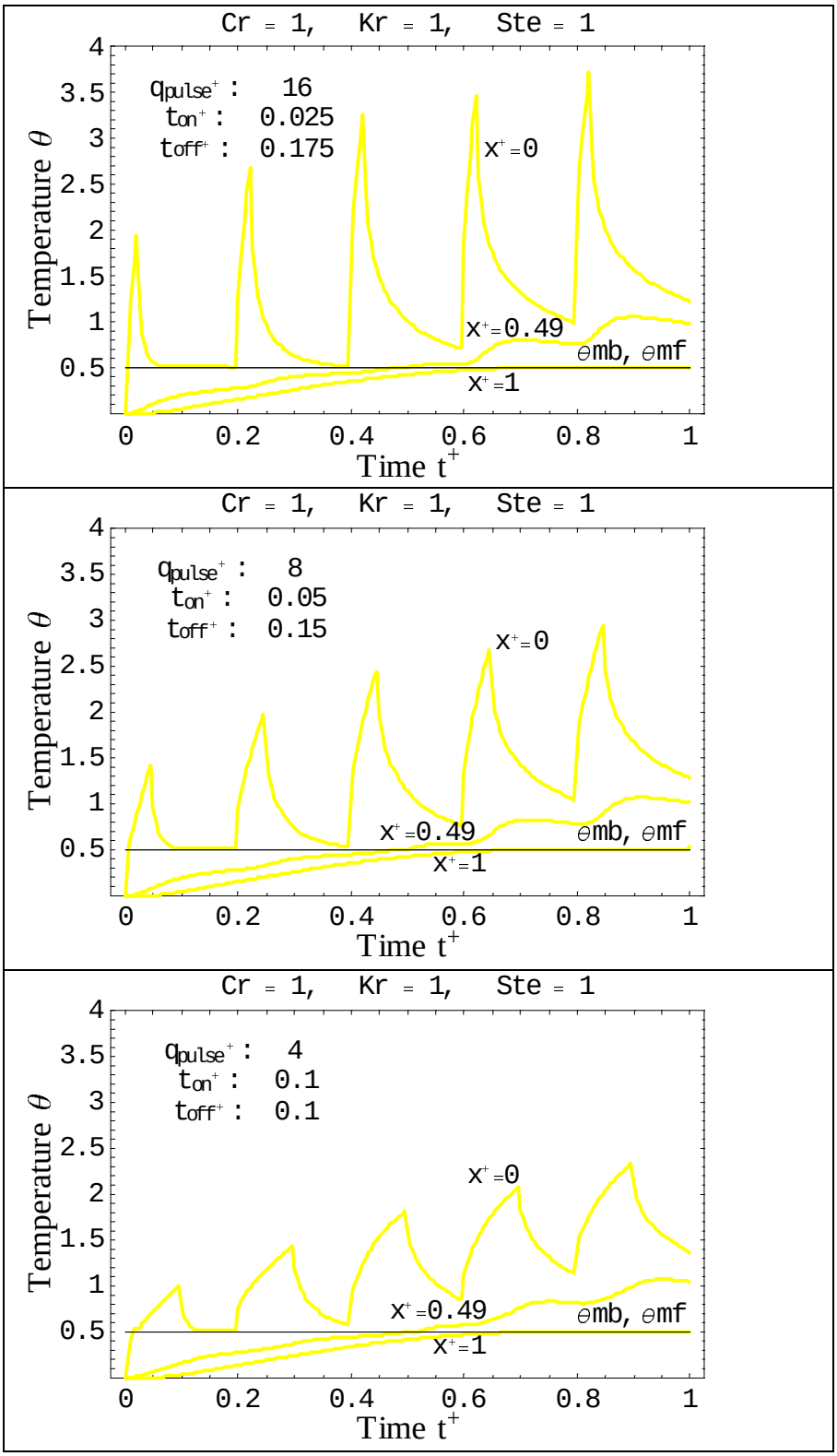

Fig. 4.2.19. Effect of pulsed surface heat flux on temperature vs. time for a homogeneous material, with a pulsed heat flux at $x^+=0$ and insulated at $x^+=1$, *(mm=64,* $\Delta t^+=0.01$*).*

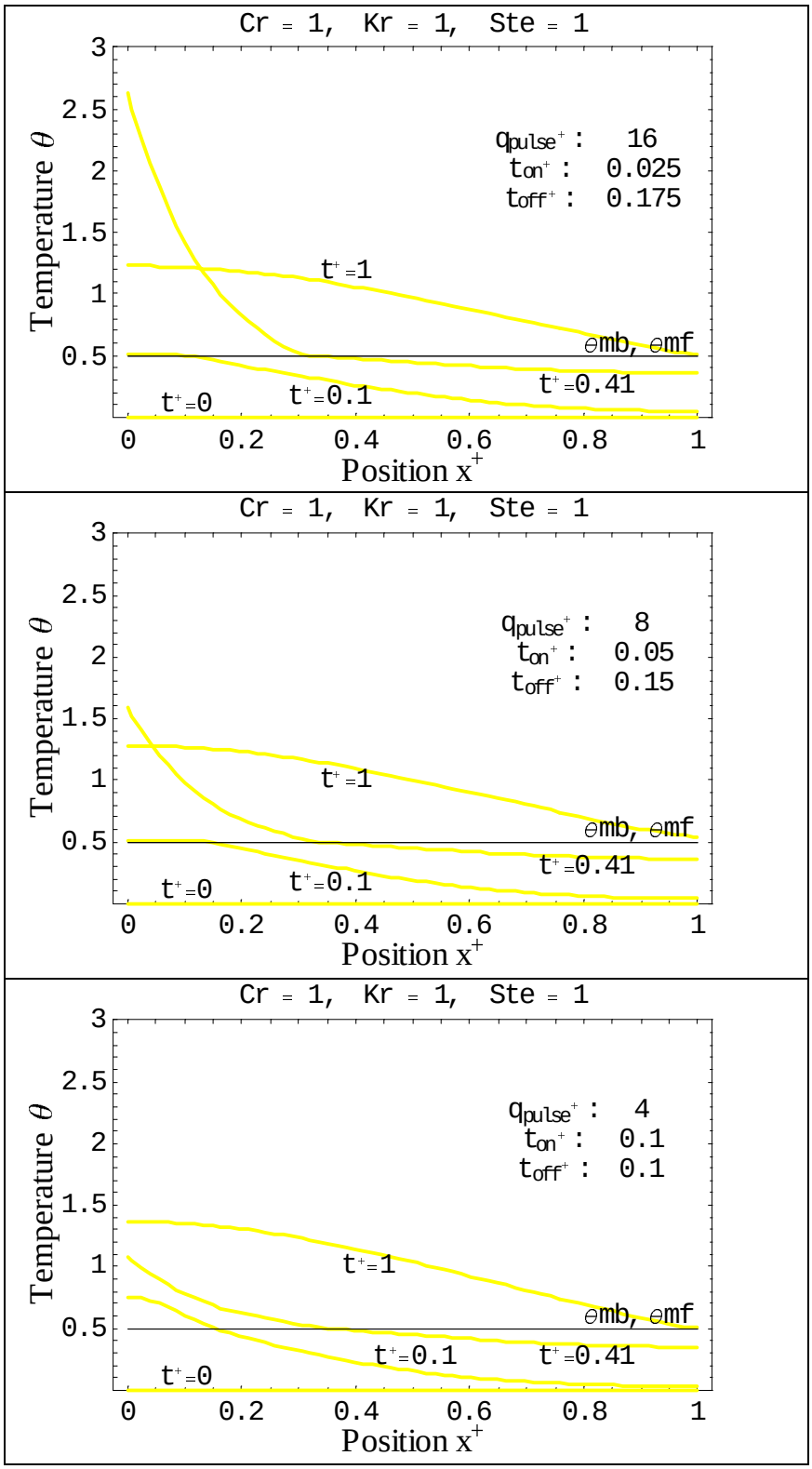

Fig. 4.2.20. Effect of Pulsed surface heat flux on temperature vs. position for a homogeneous material, with a pulsed heat flux at $x^+=0$ and insulated at $x^+=1$, *(mm=64,* $\Delta t^+=0.01$*).*

4.3. Heterogeneous Materials

The heterogeneous material, consisting of a matrix with relatively small particles embedded during melting or solidification is analyzed in this part. First, the effects of the time steps Δt and control volumes thickness Δx are examined. Next, the effects of the material properties such as Stefan number, heat capacity ratio, contact conductance, and melting temperature are investigated. Then, the effects of internal sources in the matrix and particles are studied. Last, the effects of the external sources are analyzed. Numerical results are presented in terms of the dimensionless variables.

4.3.1. Δt and Δx Effects

The effects of Δt^+ and Δx^+ on the implicit method are analyzed for a heterogeneous material, which is initially at temperature $\theta_i = 0$ with a constant surface heat flux $q^+_{sur} = 5$ at $x^+ = 0$ and insulated at $x^+ = 1$. Phase transition in the particles occurs at a single melting temperature $\theta mb = \theta mf = 0.5$. The Stefan number, particle heat capacity ratios, and contact conductance are $Ste = 1$, $Cr_l = Cr_s = 1$, and $\Gamma = 0.1$.

Table 4.3.1 displays the particle temperature at different times and locations, and Fig 4.3.1 demonstrates the particle phase front of the heterogeneous material with 16 control volumes for various Δt^+. They show that the smaller Δt^+ provides better results for the system. This means that by decreasing the Δt^+, the curves become more step-like and the results are more accurate. On the other hand, when the Δt^+ is small enough, negligible difference can be observed by decreasing the Δt^+.

Table 4.3.2 displays the surface temperature at different times, and Fig 4.3.2 shows the particle phase front of the heterogeneous material system with $\Delta t^+ = 0.003125$ for various control volumes. The figure shows the system with more control volumes provides more accurate results. This is because, by increasing the number of control volume, each control volume becomes smaller, as a result it is more realistic to be considered as a lumped capacity. Hence, it provides better results.

Table 4.3.1. Effect of Δt^+ on particle temperature in a heterogeneous material, initially at $\theta_i = 0$ with a constant surface heat flux $q^+_{sur} = 5$ at $x^+ = 0$ and insulated at $x^+ = 1$, with particle melting temperature $\theta m = 0.5$, *(mm=16).*

	Δt^+	$x^+ = 0.03$		$x^+ = 0.21$		$x^+ = 0.47$		$x^+ = 0.97$	
		Particle Temperature	***%Difference (next Δt^+)***	***Particle Temperature***	***%Difference (next Δt^+)***	***Particle Temperature***	***%Difference (next Δt^+)***	***Particle Temperature***	***%Difference (next Δt^+)***
$t^+ = 0.2$	0.025	2.32141	3.57587	1.32397	9.45305	0.5	0.	0.231992	16.6755
	0.0125	2.24127	1.88604	1.20963	4.23083	0.5	0.	0.198836	9.20666
	0.00625	2.19978	0.957436	1.16053	2.19905	0.5	0.	0.182073	4.84198
	0.003125	2.17892	0.484853	1.13555	1.0649	0.5	0.	0.173664	2.48888
	0.0015625	2.1684	--------	1.12359	-------	0.5	------	0.169447	-------
$t^+ = 0.6$	0.025	4.58525	1.07913	3.59523	1.39113	2.60473	1.98772	1.7503	3.38788
	0.0125	4.5363	0.540923	3.5459	0.698173	2.55397	1.00052	1.69295	1.74662
	0.00625	4.51189	0.270954	3.52132	0.349934	2.52867	0.502219	1.66388	0.886732
	0.003125	4.4997	0.135546	3.50904	0.175116	2.51603	0.251564	1.64926	0.447065
	0.0015625	4.49361	-------	3.5029	-------	2.50972	-------	1.64192	--------
$t^+ = 1$	0.025	6.58397	0.789896	5.5937	0.931747	4.60336	1.13711	3.75443	1.40315
	0.0125	6.53238	0.396475	5.54206	0.468016	4.55161	0.571797	3.70248	0.706615
	0.00625	6.50658	0.198626	5.51625	0.234551	4.52573	0.286715	3.6765	0.354576
	0.003125	6.49368	0.0994067	5.50334	0.117408	4.51279	0.143562	3.66351	0.177613
	0.0015625	6.48723	--------	5.49688	-------	4.50632	-------	3.65701	--------

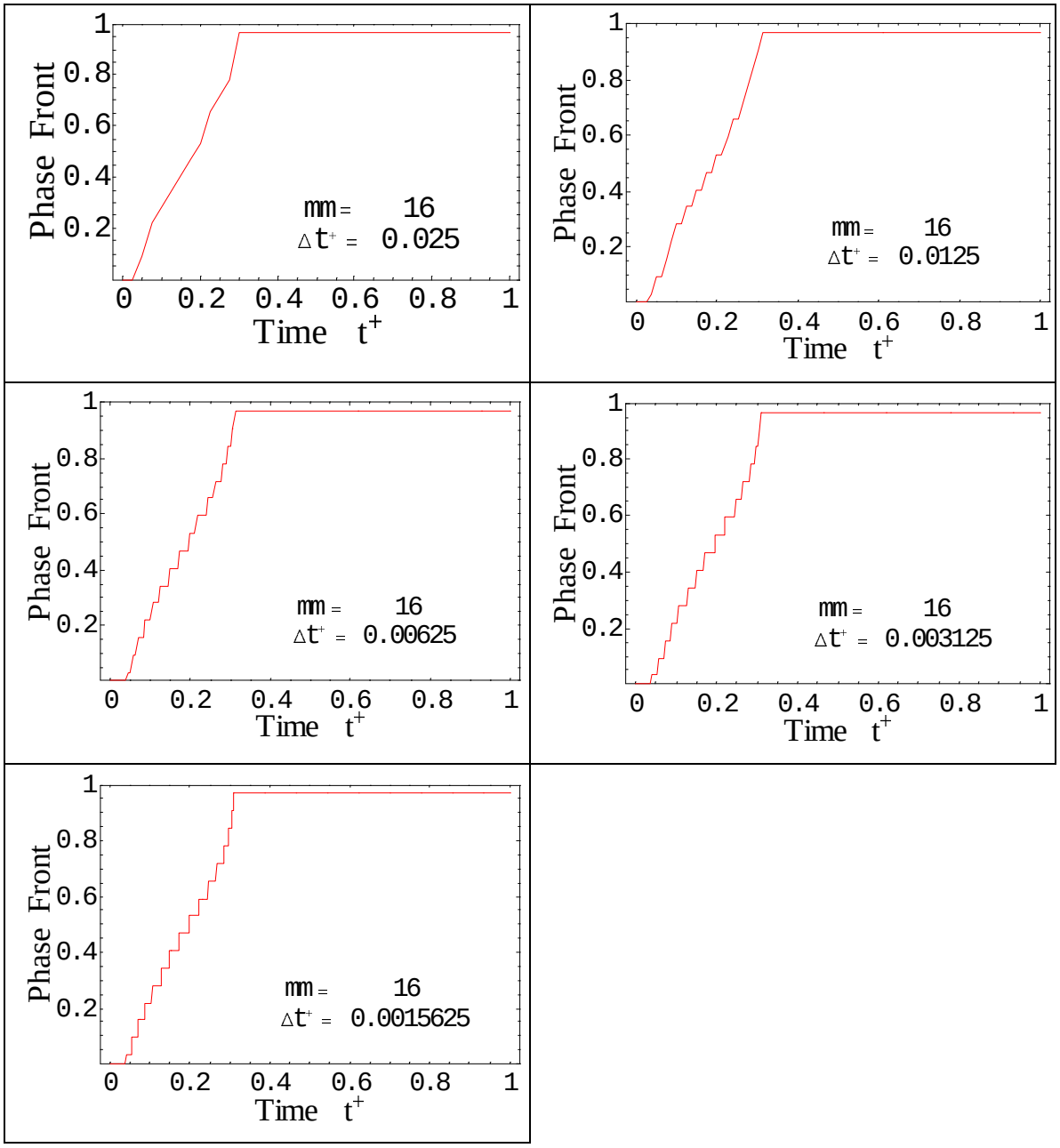

Fig. 4.3.1. Effect of Δt^+ on phase front vs. time for a heterogeneous material, initially at $\theta_i = 0$ with a constant surface heat flux $q^+_{sur} = 5$ at $x^+ = 0$ and insulated at $x^+ = 1$, with $Cr_l = Cr_s = 1$, $\Gamma = 0.1$, $Ste = 1$, and particle melting temp $\theta mb = \theta mf = 0.5$.

Table 4.3.2 Effect of Δx^+ on surface temperature for a heterogeneous material, initially at $\theta_i = 0$ with a constant surface heat flux $q^+_{sur} = 5$ at $x^+ = 0$ and insulated at $x^+ = 1$, with particle melting temperature $\theta m = 0.5$, ($\Delta t^+ = 0.003125$).

	$t^+ = 0.1$		$t^+ = 0.4$		$t^+ = 1.$	
# CVs	***Surface Temperature***	***%Difference (next #CVs)***	***Surface Temperature***	***%Difference (next #CVs)***	***Surface Temperature***	***%Difference (next #CVs)***
1	3.54975	47.1901	4.88043	18.7436	7.87992	10.5938
2	2.41168	16.9532	4.11006	4.62183	7.1251	2.71097
4	2.06209	4.61857	3.92849	1.12008	6.93704	0.683105
8	1.97105	0.908689	3.88498	0.279477	6.88998	0.171111
16	1.9533	0.238926	3.87415	0.0698239	6.87821	0.0427983
32	1.94865	0.0598099	3.87145	0.0174479	6.87526	0.0107011
64	1.94748	--------	3.87077	--------	6.87453	---------

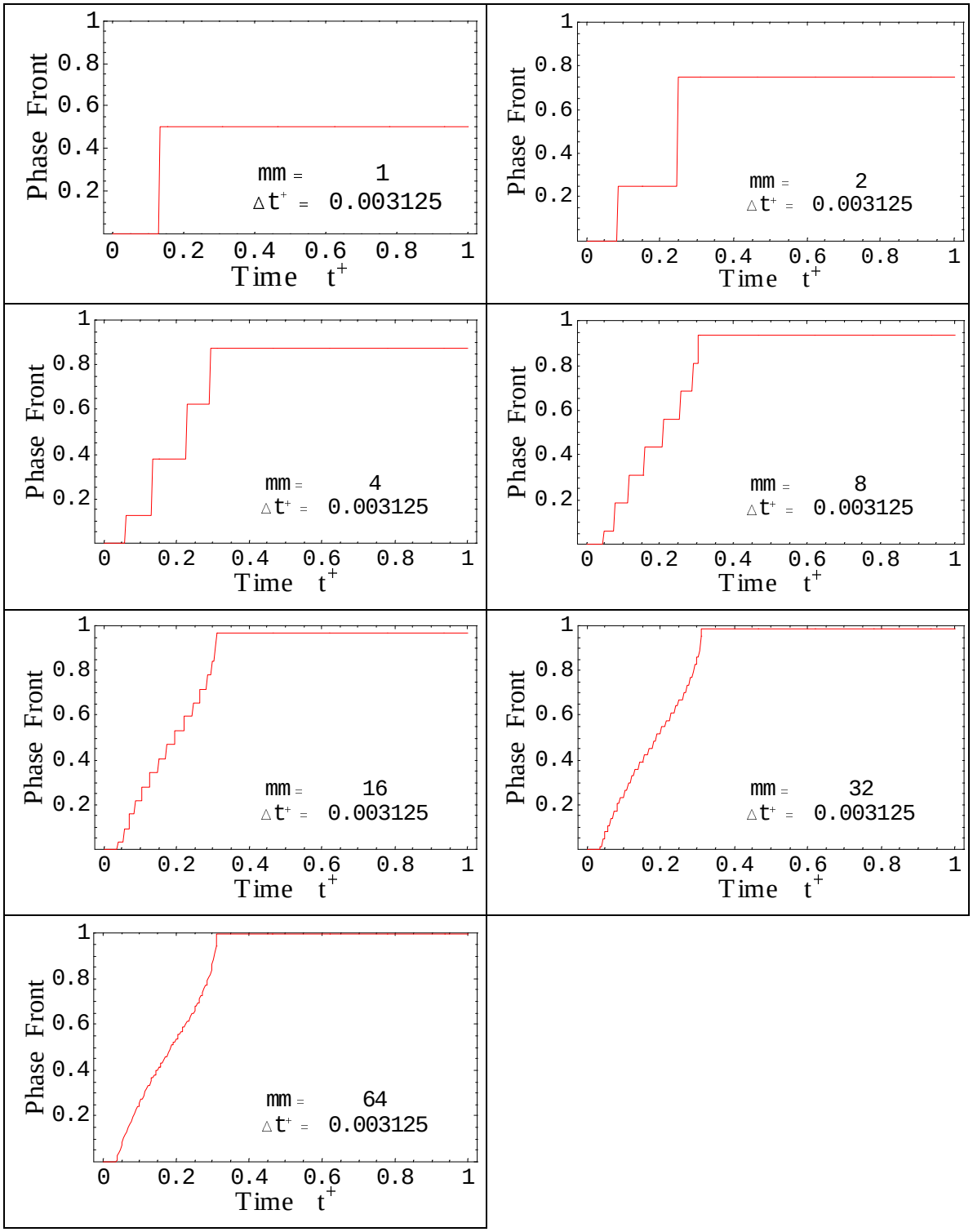

Fig. 4.3.2. Effect of Δx^+ on phase front vs. time for a heterogeneous material, initially at $\theta_i = 0$ with a constant surface heat flux $q^+_{sur} = 5$ at $x^+ = 0$ and insulated at $x^+ = 1$, with $Cr_l = Cr_s = 1$, $\Gamma = 0.1$, $Ste = 1$ and particle melting temp. $\theta mb = \theta mf = 0.5$.

4.3.2. Material Properties

The effects of material properties such as Stefan number, particle heat capacity ratio, contact conductance and melting temperature are investigated for a heterogeneous material. In this investigation the system is initially at temperature $\theta_i = 1$ with a constant surface temperature $\theta_{sur} = 0$ at $x^+ = 0$ and insulated at $x^+ = 1$. The number of control volumes is *16*, and $\Delta t^+ = 0.003125$ is taken as the time step.

4.3.2.1. Stefan Number Effects

The Stefan number is a dimensionless group, which is the sensible energy divided by the latent energy. In this investigation the particle heat capacity ratios and contact conductance are $Cr_l = Cr_s = 1$, and $\Gamma = 0.1$. Phase transition in the particles occurs at a single melting temperature $\theta mb = \theta mf = 0.5$.

Figures 4.3.3 and 4.3.4 display respectively the particle and matrix temperature distributions at the various times and particle and matrix temperature histories at the different locations of the heterogeneous material system for relatively low, medium and high Stefan number *Ste= 0.1, 1, 10*. According to the definition of Stefan number, by decreasing the *Ste* the latent heat is increased, which means more energy has to be released to finish the phase change process. Therefore, phase transition needs more time to be completed. During phase transition the lag between the particle and matrix temperatures increases, because the particle temperature stays at the melting temperature during the transient process. In addition, for *Ste=0.1* the matrix near the surface reaches the steady condition before the particles complete phase transition.

4.3.2.2. Particle Heat Capacity Ratio Effects

The particle heat capacity ratios are dimensionless groups. The particle liquid heat capacity ratio is the ratio of particle liquid heat capacity to the matrix solid heat capacity, while the particle solid heat capacity ratio is the ratio of particle solid heat capacity to the matrix solid heat capacity. The matrix solid thermal properties are chosen as reference quantities. In this investigation the Stefan number and contact conductance are *Ste=1* and

$\Gamma = 0.1$. Phase transition in the particle occurs at a single melting temperature $\theta mb = \theta mf = 0.5$.

Figure 4.3.5 displays the particle and matrix temperature distributions at the various times, while Fig 4.3.6 shows the particle and matrix temperature histories at the different locations of the heterogeneous material system for relatively low, medium and high particle heat capacity ratios $Cr_l = Cr_s = 0.1, 1, 10$. At the higher particle heat capacity ratios, the particle temperature drops more slowly because more energy has to be released for the particle temperature to drop. By increasing the particle heat capacity ratios, the lag between the particle and matrix temperature increases and during phase transition it becomes severe. The maximum temperature lag between the matrix and particle temperature occurs at the end of the phase transition except for the first control volume, because the first control volume matrix gets to the surface temperature very quickly.

4.3.2.3. Contact Conductance Effects

The heat exchange between the particle and matrix is characterized by a contact conductance. In this investigation the Stefan number and particle heat capacity ratios are *Ste=1* and $Cr_l = Cr_s = 1$. Phase transition occurs at a single melting temperature $\theta mb = \theta mf = 0.5$.

Figure 4.3.7 demonstrates the particle and matrix temperature distributions at the various times and Fig 4.3.8 shows the particle and matrix temperature histories at the different locations, while Fig 4.3.9 displays the matrix temperature vs. particle temperature for relatively low, medium and high contact conductance $\Gamma = 0.1, 1, 10$. By decreasing the contact conductance, the energy exchange mechanism between the matrix and particles is weaker. Therefore the particle temperature drops more slowly and, as a result, the lag between the particle and matrix temperature increases and during phase transition it becomes severe. The maximum temperature lag between the particle and matrix occurs at the first control volume because the first control volume matrix reaches the surface temperature very quickly.

4.3.2.4. Melting Temperature Effects

In pure materials the phase-change takes place at a discrete temperature, while in the other cases there is no discrete melting point temperature. Here a hypothetical material is considered for the particle, which changes phase in a linear way over an extended range of temperatures. In this investigation the particle heat capacity ratios, Stefan number and contact conductance are $Cr_l = Cr_s = 1$, Ste=1 and $\Gamma = 0.1$.

Figure 4.3.10 displays the particle and matrix temperature histories and Fig 4.3.11 shows the particle phase fraction histories at the different locations of the heterogeneous system for a pure material and two hypothetical materials. For the pure material phase transition occurs at temperature *0.5*, while the hypothetical materials, one occurs over temperature *0.5-0.6* and the other one occurs over temperature *0.5-0.7*. Since the systems are initially liquid, the particle of each system reaches phase transition at different times. Since the particle Stefan number of each system is *Ste=1*, the total energy to finish the phase transition is the same for each particle. As a result, when phase change takes place over an extended range of temperatures, the particle approaches the finishing phase transition temperature earlier. Phase transition in the first control volume particle happens quickly, therefore the time difference is not noticeable. In addition, during phase transition the temperature lag between the particle and matrix becomes severe.

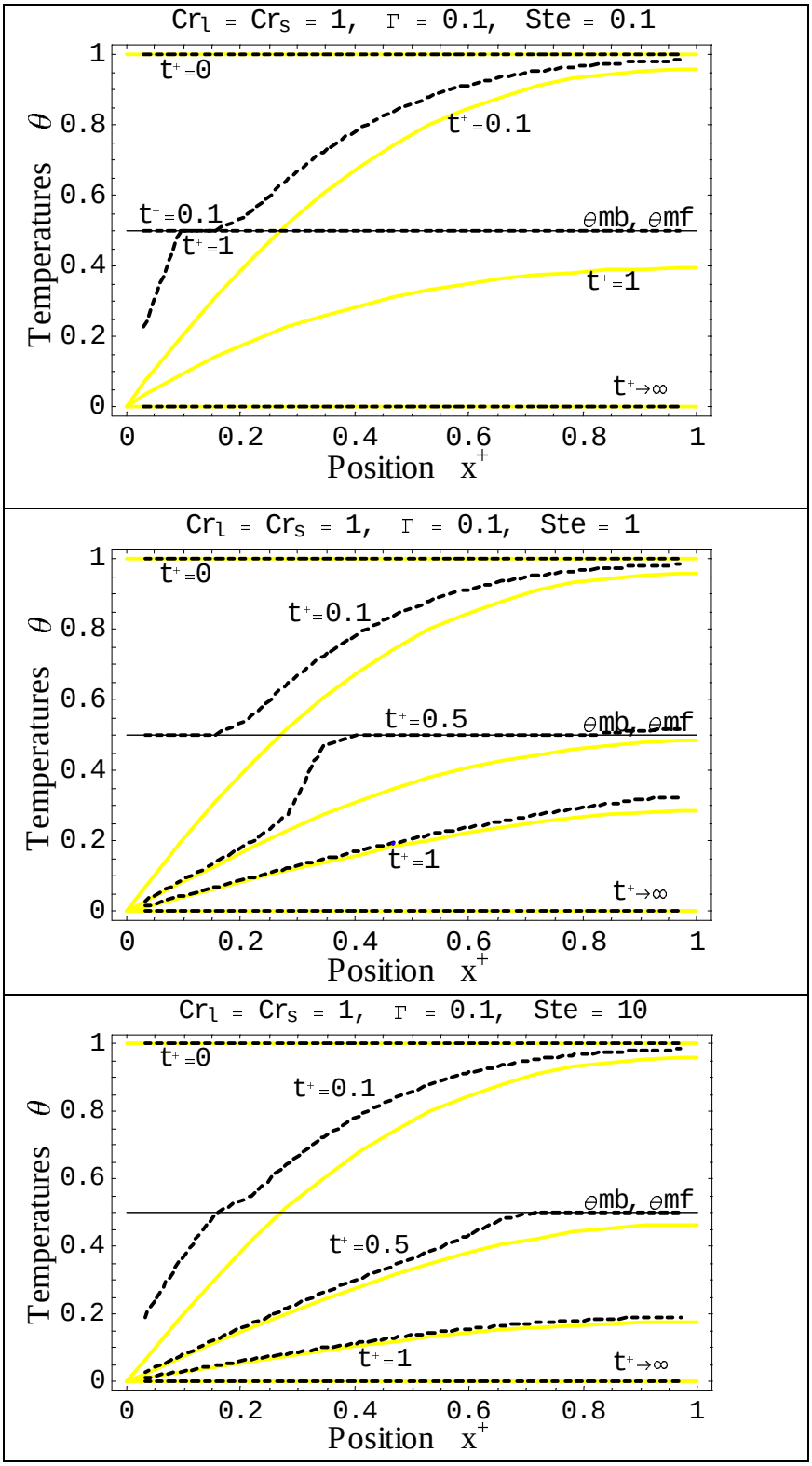

Fig. 4.3.3. Effect of particle Stefan number on temperature vs. position for a heterogeneous material, with a constant surface temperature $\theta_{sur}=0$ at $x^+=0$ and insulated at $x^+=1$, *(mm=16,* $\Delta t^+=0.003125$*), (—— Matrix, ... Particle).*

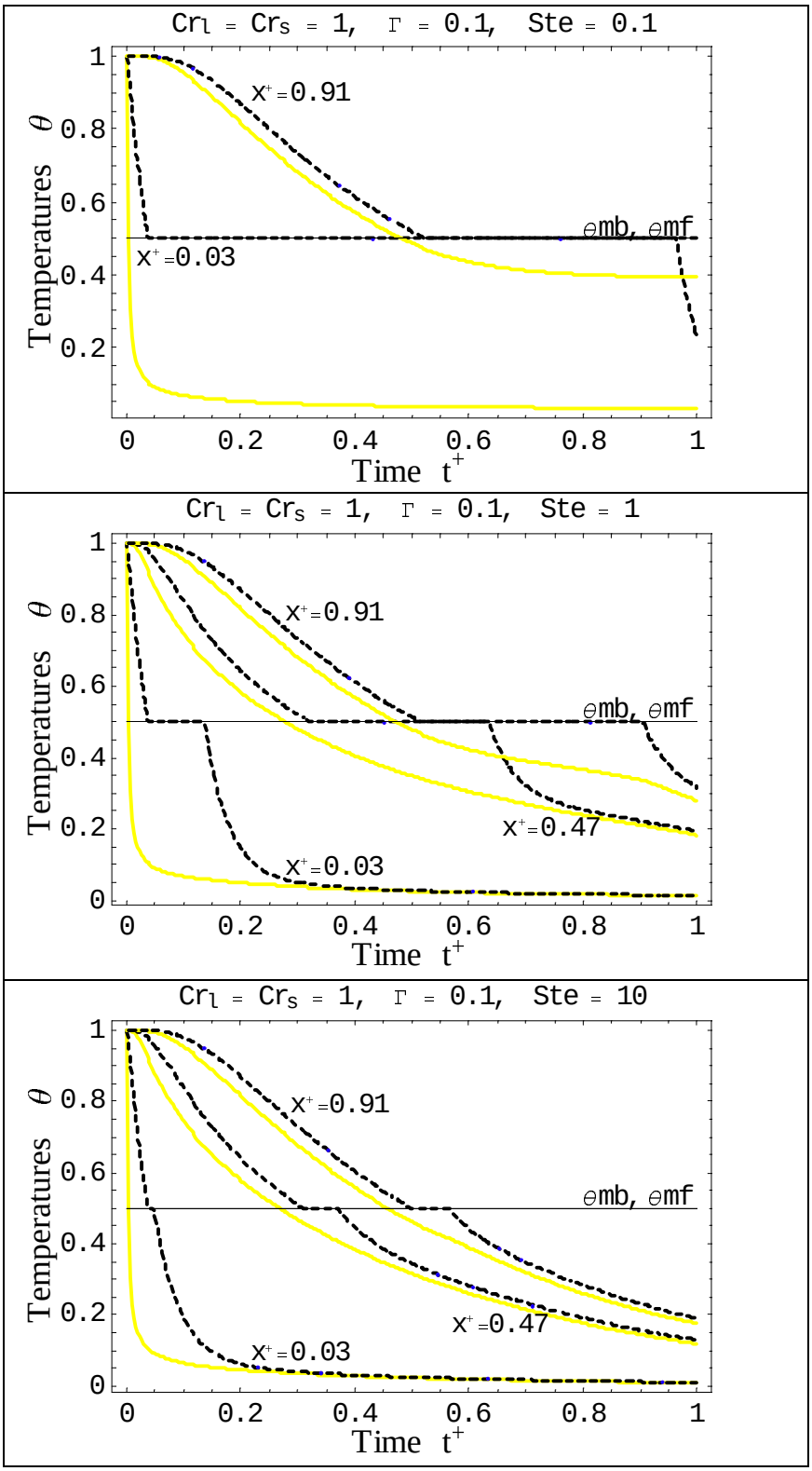

Fig. 4.3.4. Effect of particle Stefan number on temperature vs. time for a heterogeneous material, with a constant surface temperature $\theta_{sur}=0$ at $x^+=0$ and insulated at $x^+=1$, *(mm=16,* $\Delta t^+=0.003125$*), (* —— *Matrix,* ..... *Particle).*

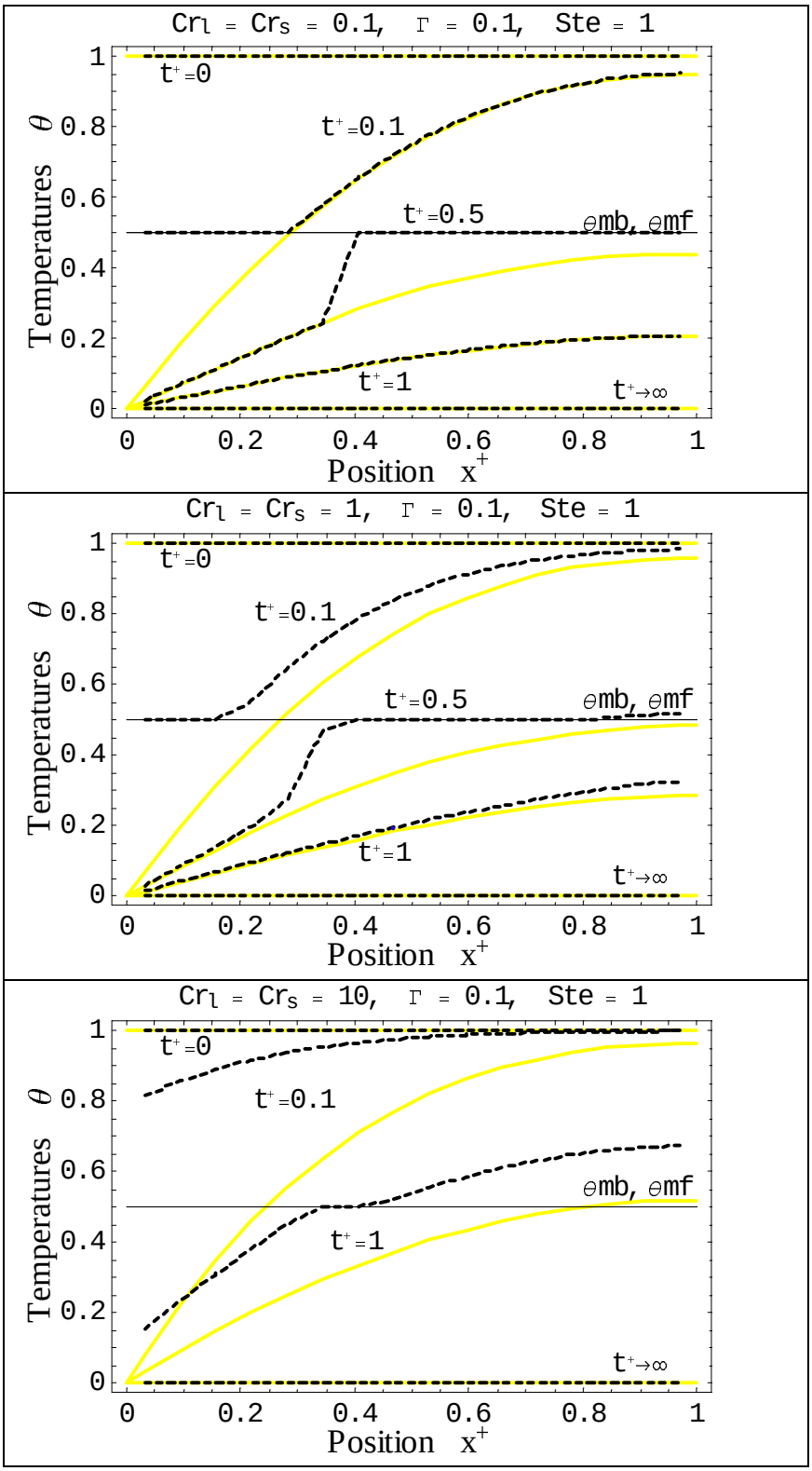

Fig. 4.3.5. Effect of particle heat capacity ratio on temperature vs. position for a heterogeneous material, with a constant surface temperature $\theta_{sur}=0$ at $x^+=0$ and insulated at $x^+=1$, *(mm=16,* $\Delta t^+=0.003125$*), (—— Matrix, ····· Particle).*

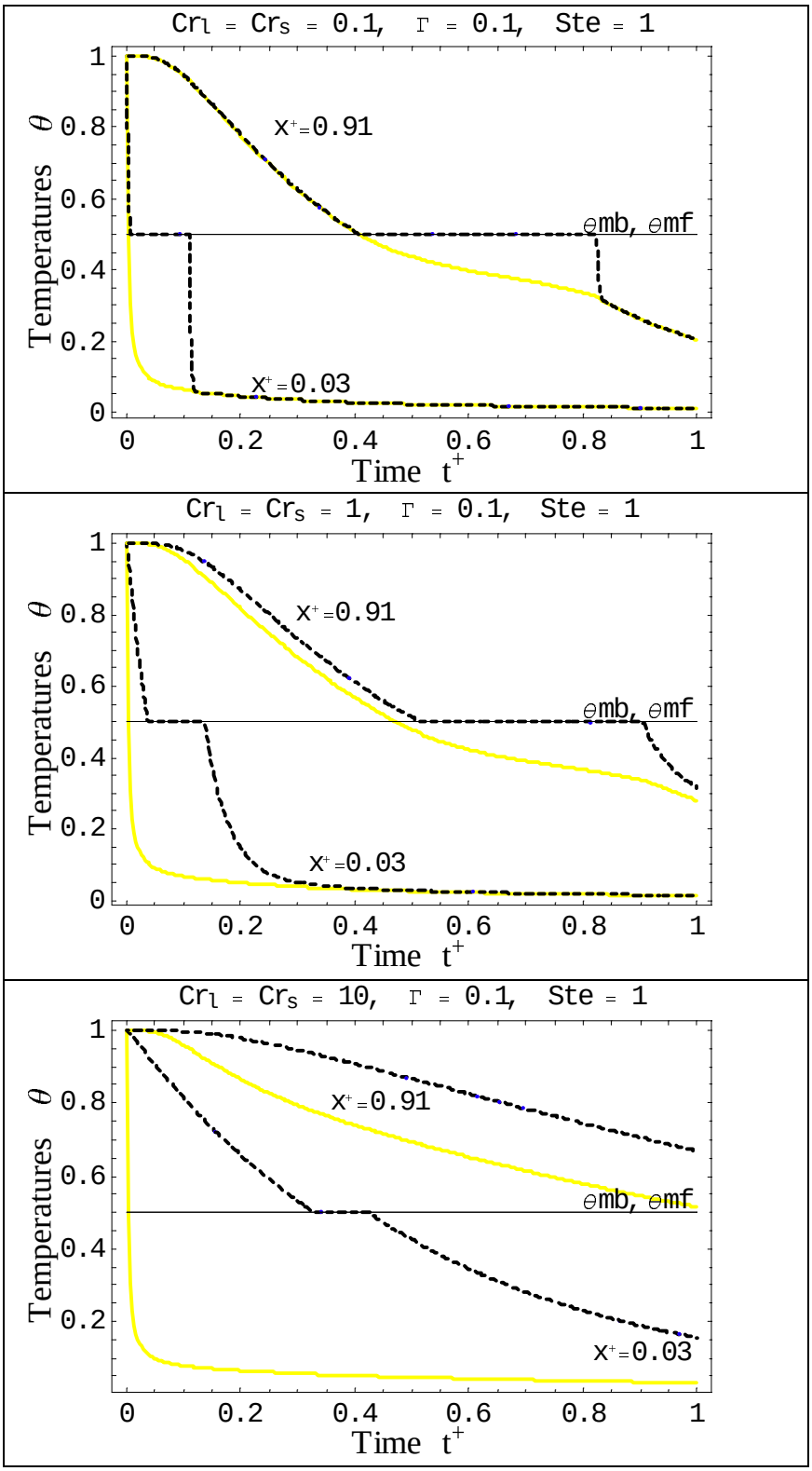

Fig. 4.3.6. Effect of particle heat capacity ratio on temperature vs. time for a heterogeneous material, with a constant surface temperature $\theta_{sur}=0$ at $x^+=0$ and insulated at $x^+=1$, *(mm=16,* $\Delta t^+=0.003125$*), (—— Matrix, ... Particle).*

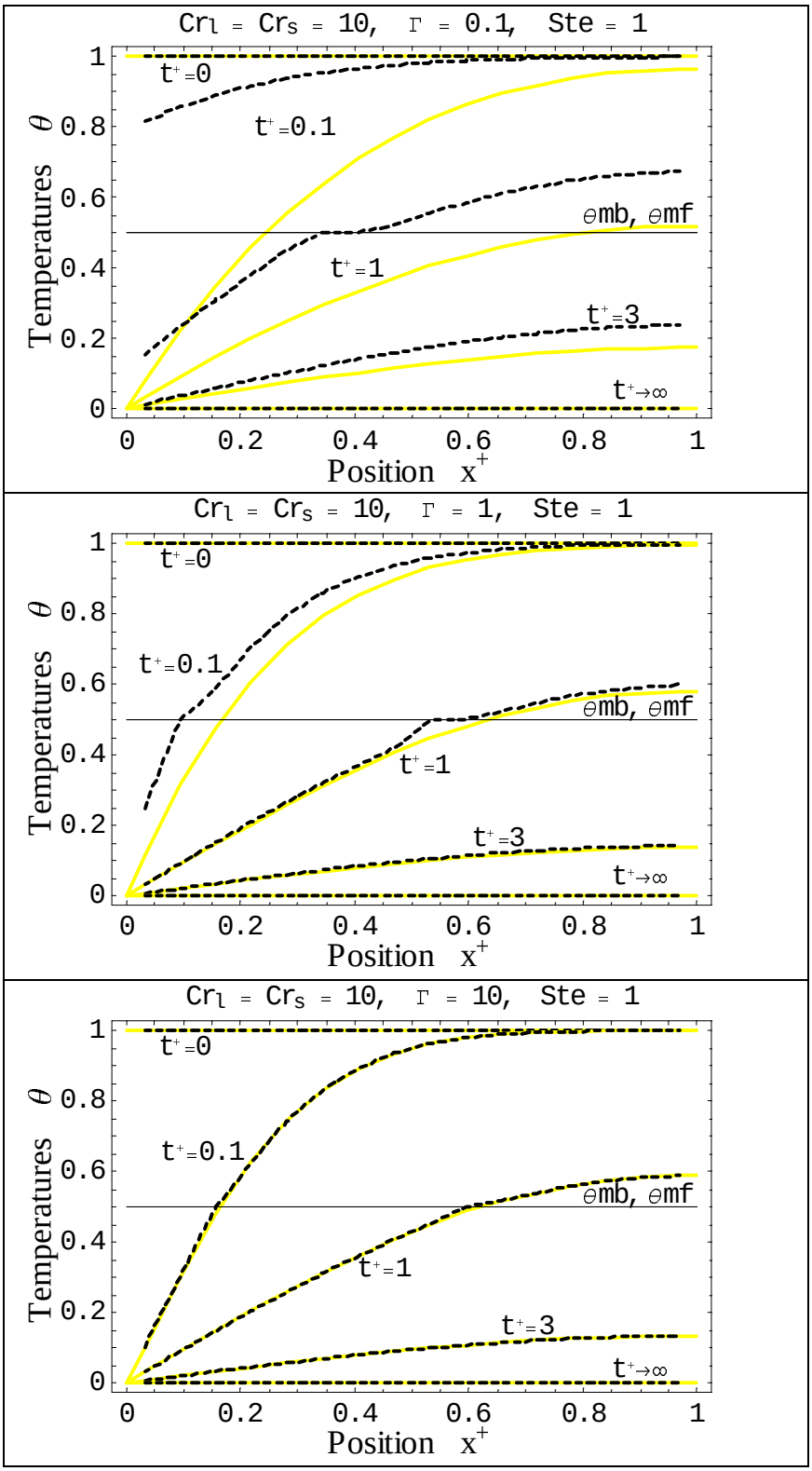

Fig. 4.3.7. Effect of particle contact conductance on temperature vs. position for a heterogeneous material, with a constant surface temperature $\theta_{sur}=0$ at $x^+=0$ and insulated at $x^+=1$, *(mm=16,* $\Delta t^+=0.003125$*), (—— Matrix, ····· Particle).*

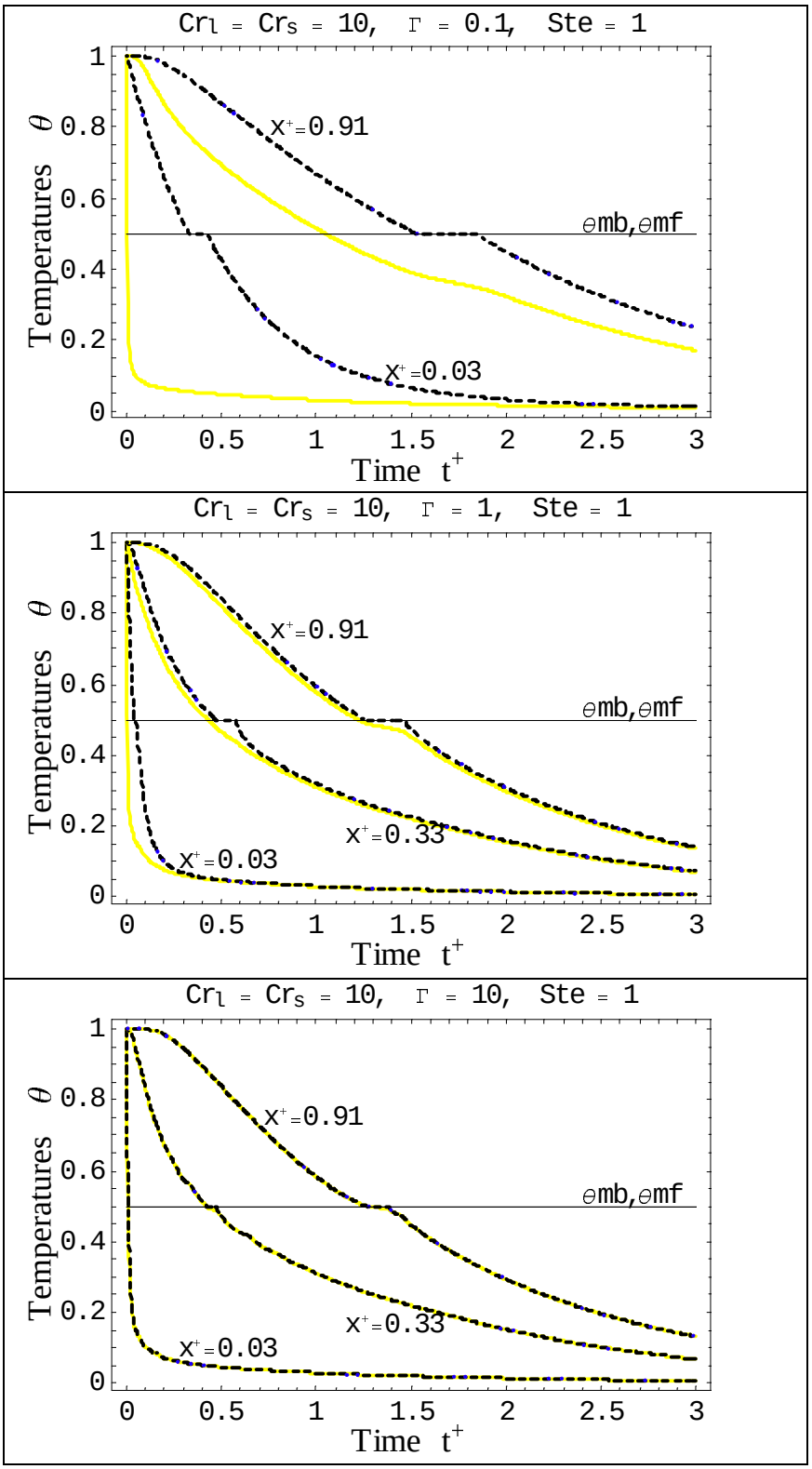

Fig. 4.3.8. Effect of particle contact conductance on temperature vs. time for a heterogeneous material, with a constant surface temperature $\theta_{sur}=0$ at $x^+=0$ and insulated at $x^+=1$, *(mm=16,* $\Delta t^+=0.003125$*), (—— Matrix, ····· Particle).*

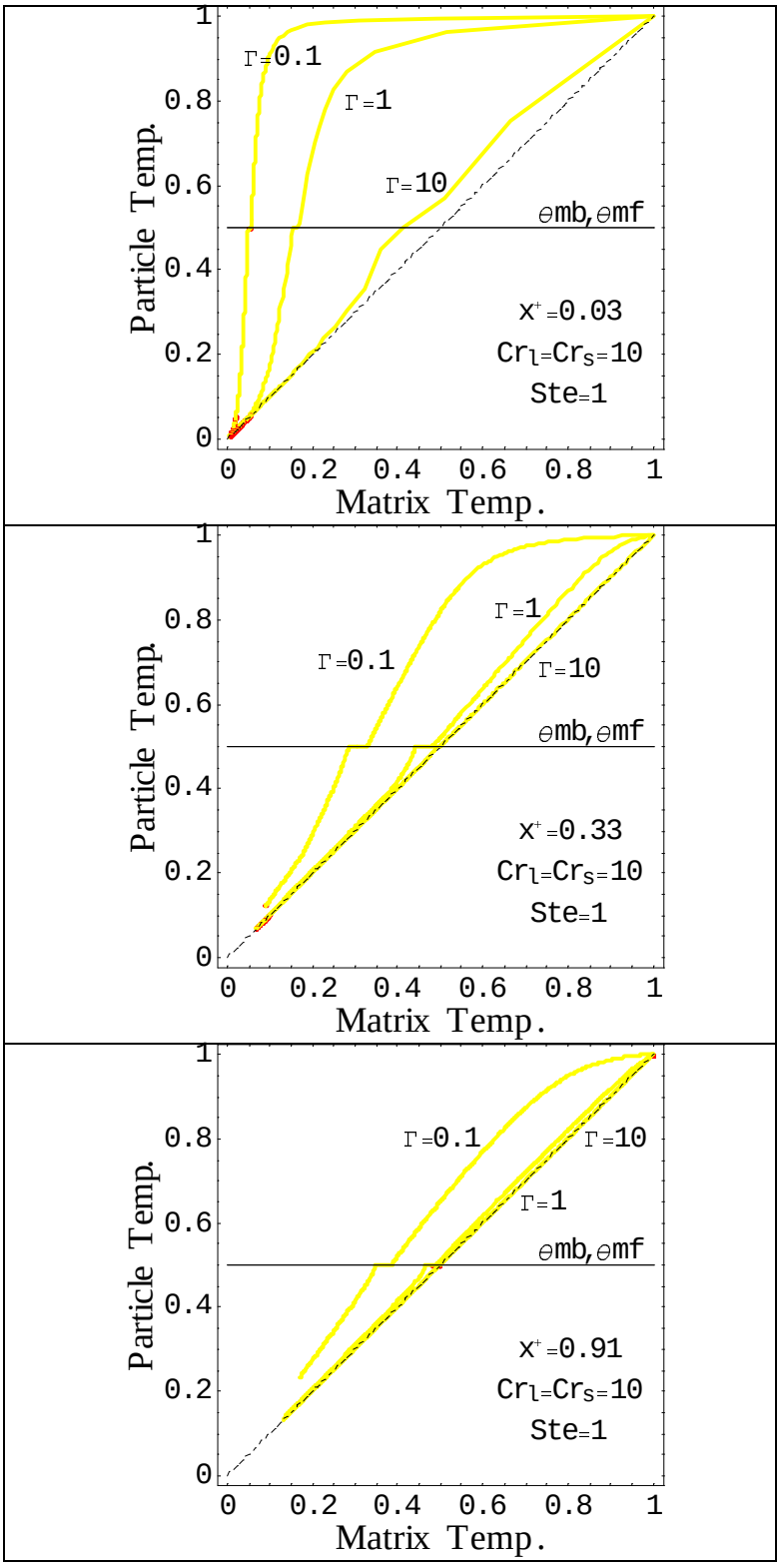

Fig. 4.3.9 Effect of particle contact conductance on particle temperature vs. matrix temperature for a heterogeneous material, initially at $\theta_i = 1$ with a constant surface temperature $\theta_{sur} = 0$ at $x^+ = 0$ and insulated at $x^+ = 1$, ($mm = 16, \Delta t^+ = 0.003125$).

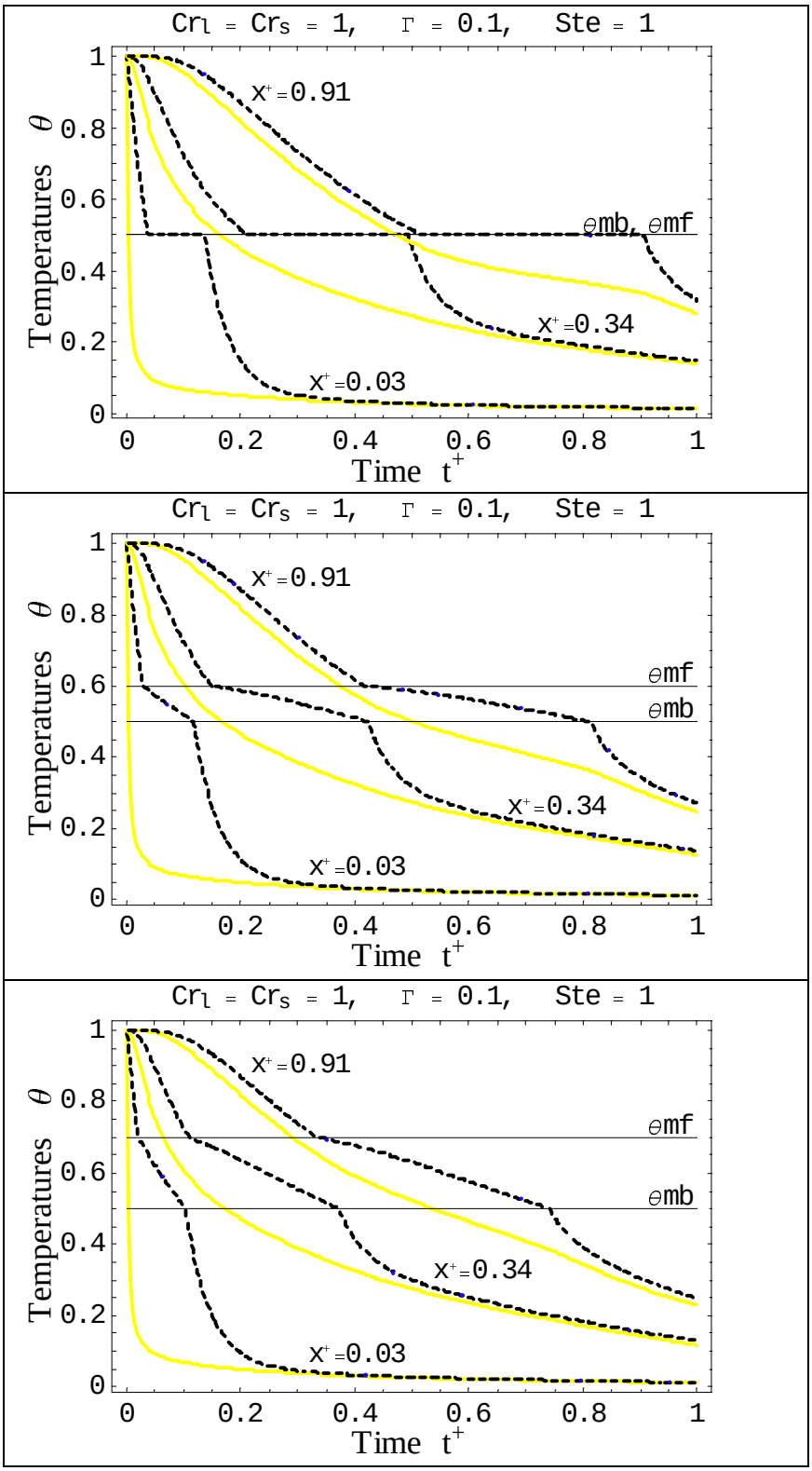

Fig. 4.3.10. Effect of particle melting temperature on phase fraction vs. time for a heterogeneous material, with a constant surface temperature $\theta_{sur}=0$ at $x^+=0$ and insulated at $x^+=1$, *(mm=16,* $\Delta t^+=0.003125$*), (—— Matrix, ····· Particle).*

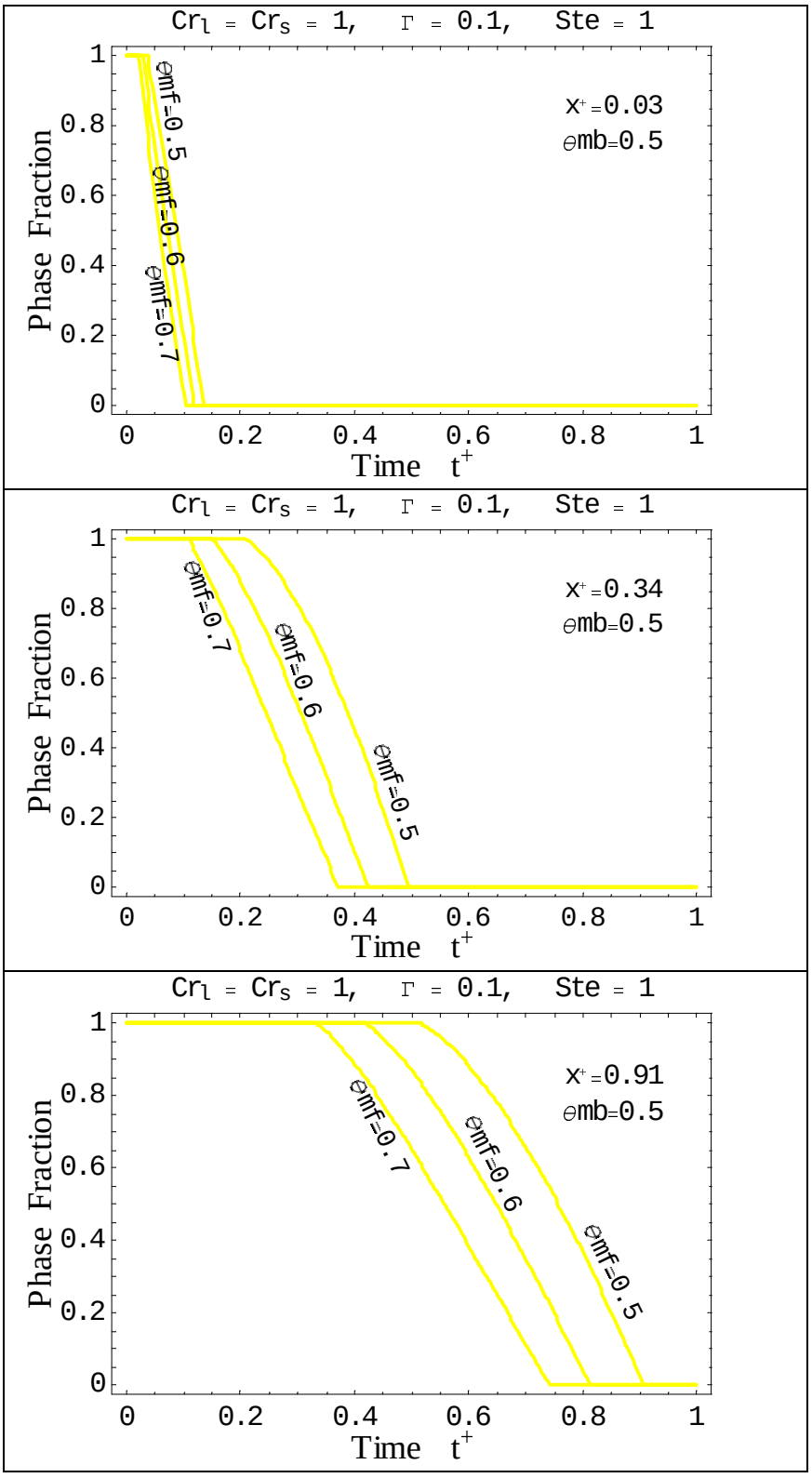

Fig. 4.3.11. Effect of particle melting temperature on phase fraction vs. time for a heterogeneous material, initially at $\theta_i = 1$ with a constant surface temperature $\theta_{sur} = 0$ at $x^+ = 0$ and insulated at $x^+ = 1$, ($mm=16, \Delta t^+ = 0.003125$).

4.3.3. *Internal Sources*

The effect of the internal source is investigated for a heterogeneous material, which is initially at temperature $\theta_i = 0$ with heat convection $\theta_\infty = 0$ and $h_\infty^+ = 5$ at $x^+ = 0$ and $x^+ = 1$. The particle heat capacity ratios and Stefan number are $Cr_l = Cr_s = 1$ and $Ste = 1$. Phase change occurs at a single melting temperature $\theta mb = \theta mf = 0.5$ and $\Delta t^+ = 0.003125$ is taken as the time step.

4.3.3.1. *Matrix Heat Source Intensity Effects*

In the matrix heat source intensity effect investigation, the contact conductance is $\Gamma = 0.1$ and 64 control volumes are used.

Figures 4.3.14 and 4.3.15 display respectively the particle and matrix temperature distributions at various times and particle and matrix temperature histories at different locations in the heterogeneous material system with relatively low, medium and high values of the continuous localized matrix heat source $Sc^+ = 1,\ 4,\ and\ 16$ located in the middle of the slab as shown on Fig 4.3.12. The effect of the internal source can be observed before, during and after phase transition. When $Sc^+ = 1$ the generated energy is not enough to let the particles get to the phase change, and the particles and matrix temperature increase very slowly. In the other case with $Sc^+ = 4$ the energy is enough to let only the particles of a few control volumes in the middle of the slab get to the phase change, but phase transition happens very slowly and it takes a long time to finish the process. On the other hand when $Sc^+ = 16$ the generated energy is so high that all control volumes are able to finish phase change. The particles in the middle control volumes get to the saturation temperature very quickly and they complete the phase transition process in a short time and their temperature goes up fast. In addition, the temperature lag between the particle and matrix temperature increases during the phase change process, because the particle temperature stays at melting temperature during the transient process. When steady conditions are reached the temperature lag disappears. The system approaches the steady condition approximately at $t^+ = 1$ for the different cases.

4.3.3.2. Matrix Heat Source Distribution Effects

In the matrix heat source distribution effect investigation, the contact conductance coefficient is $\Gamma = 0.1$ and the number of control volumes is *64*.

Figures 4.3.16 and 4.3.17 illustrate respectively the particle and matrix temperature distributions at various times and particle and matrix temperature histories at different locations in the heterogeneous material system with a continuous localized matrix heat source, which is located in the middle of the slab as shown on Fig 4.3.13. Since the total energy is same for all cases, by increasing the region, the heat source strength gets weaker, as a result the temperature rise gets slower and the particle phase transition takes more time. On the other hand, the boundary conditions cause the particle and matrix temperature distributions of the control volumes near the surfaces to be similar for the different cases. In addition, since the particle temperature stays at melting temperature during phase transition, the lag between particle and matrix temperature increases during the transient process. When the steady states are reached the temperature lag disappears. The system reaches the steady condition approximately at $t^+ = 1$ for the different cases.

4.3.3.3. Particles Heat Source Effects

In the particle heat source investigation, the contact conductance coefficient is $\Gamma = 1$ and the number of control volumes is *64*.

Figures 4.3.18 and 4.3.19 display respectively the particle and matrix temperature distributions at various times and particle and matrix temperature histories at different locations in the heterogeneous material system with relatively low, medium and high values of uniform particle heat source $Scpt^+$=1, 4, and 16 in the entire slab. When $Scpt^+ = 1$ the generated energy is not enough to heat the particles to the phase change temperature, and the particle and matrix temperature increase very slowly. In the other case with $Scpt^+ = 4$ the energy is enough to let all the particles reach the phase transition temperature, but because of the boundary conditions, the matrix and particle temperature of the control volumes near the surfaces rise more slowly and phase change takes more

time. On the other hand when $Scpt^{+} = 16$, the generated energy is so high that the particles get to the saturation temperature very quickly and they complete the phase transition process in a very short time. In addition, because of the relatively high particle heat capacity ratios a noticeable temperature lag exists between the particle and matrix temperature. The lag between the particle and matrix temperature decreases during the transient process as the particle temperature stays at the melting temperature.

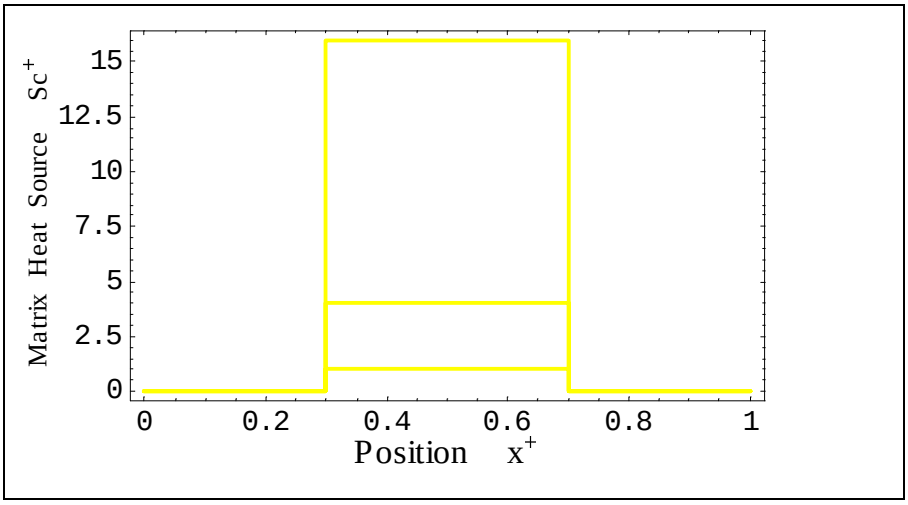

Fig. 4.3.12. Continuous localized volumetric matrix heat source for a heterogeneous material (Intensity Effects).

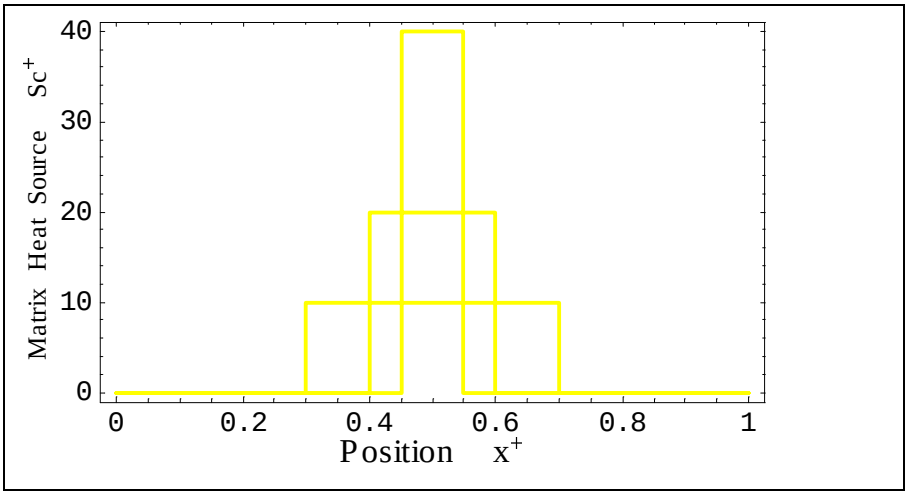

Fig. 4.3.13. Continuous localized volumetric matrix heat source for a heterogeneous material (Distribution Effects).

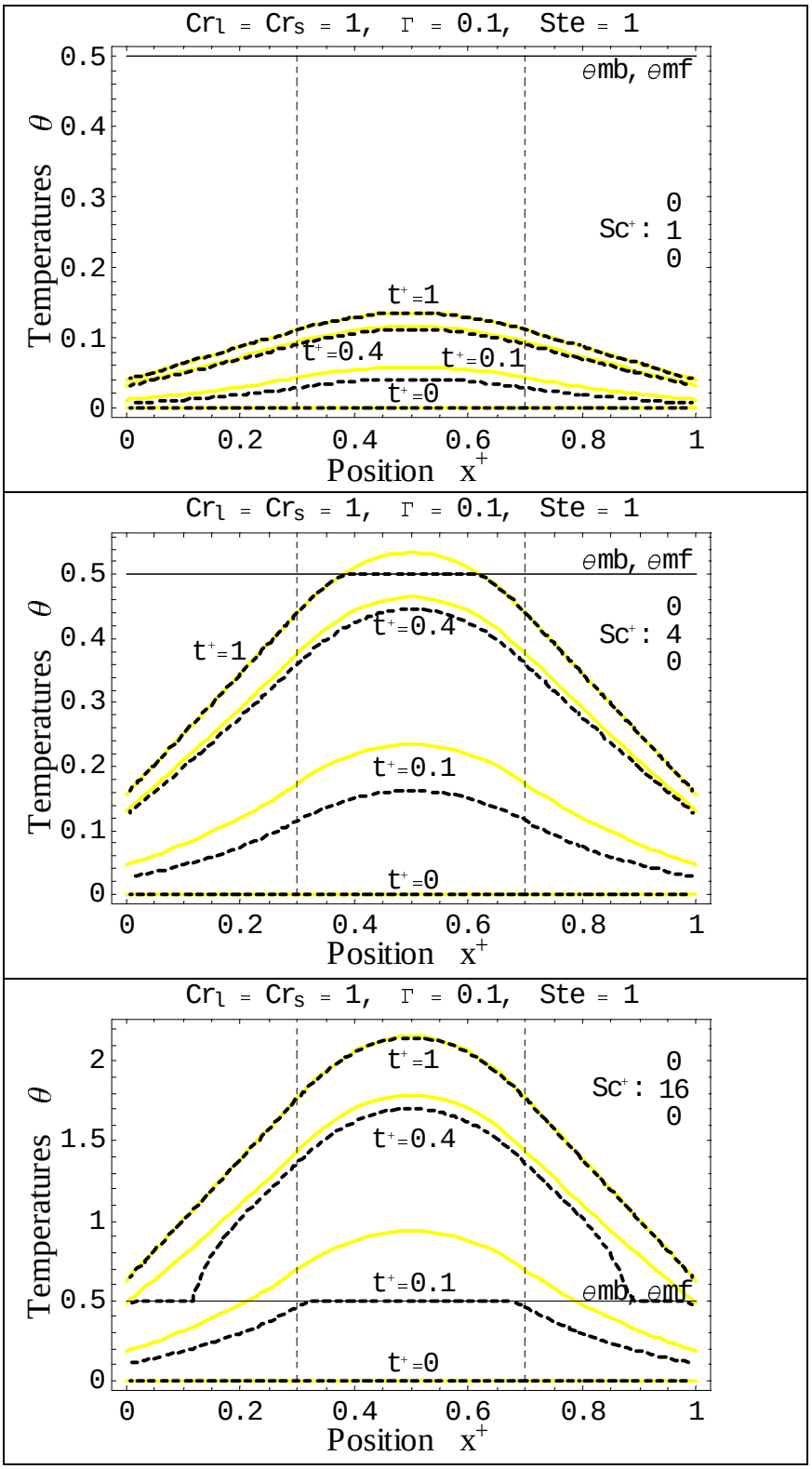

Fig. 4.3.14. Effect of matrix heat source intensity on temperature vs. position for a heterogeneous material, with convection $\theta_\infty = 0$ and $h_\infty^+ = 5$ at $x^+ = 0$ and $x^+ = 1$, *(mm=64, $\Delta t^+ = 0.003125$), (—— Matrix, ····· Particle).*

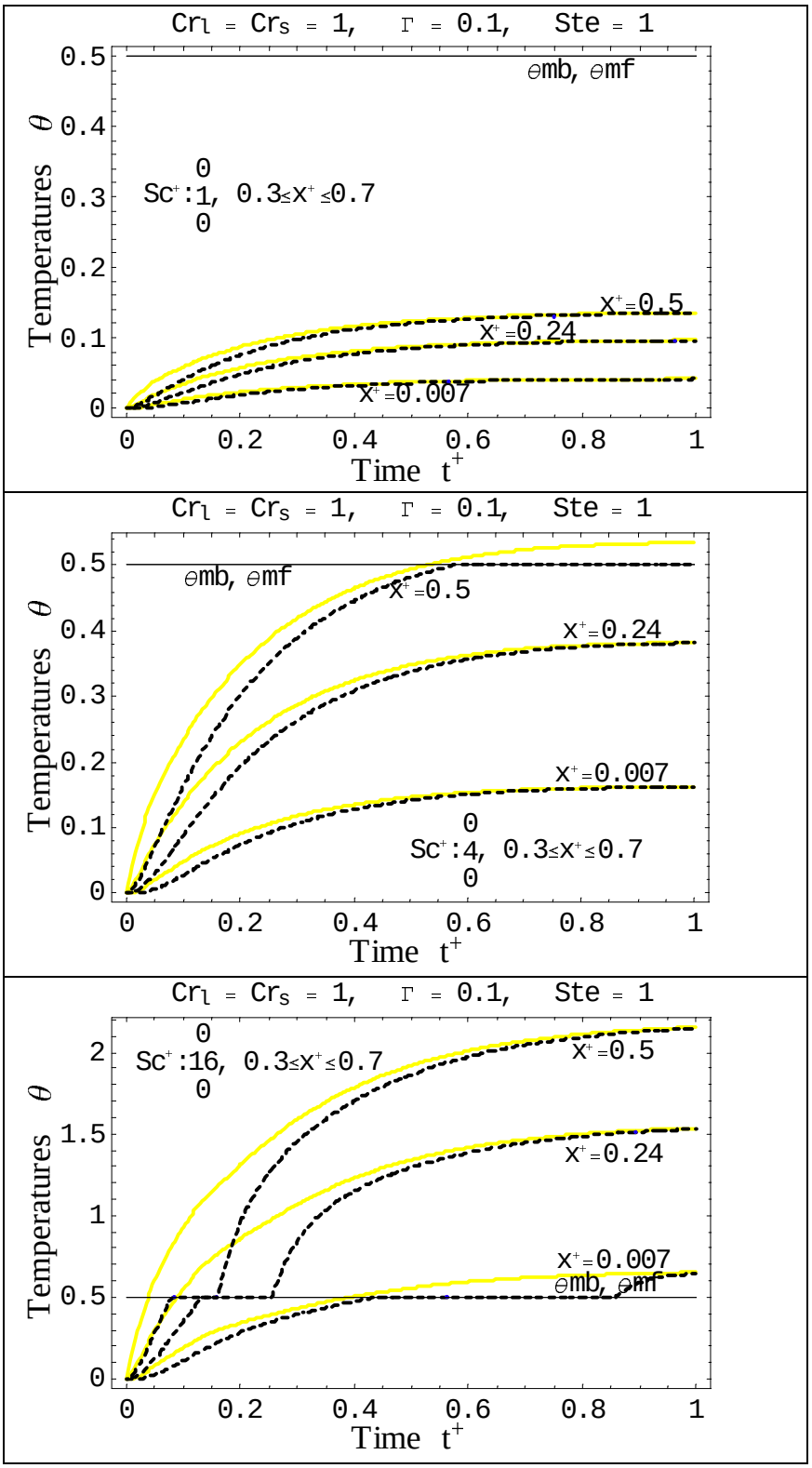

Fig. 4.3.15. Effect of matrix heat source intensity on temperature vs. time for a heterogeneous material, with convection $\theta_\infty = 0$ and $h_\infty^+ = 5$ at $x^+ = 0$ and $x^+ = 1$, *(mm=64,* $\Delta t^+ = 0.003125$*),(—— Matrix, ····· Particle).*

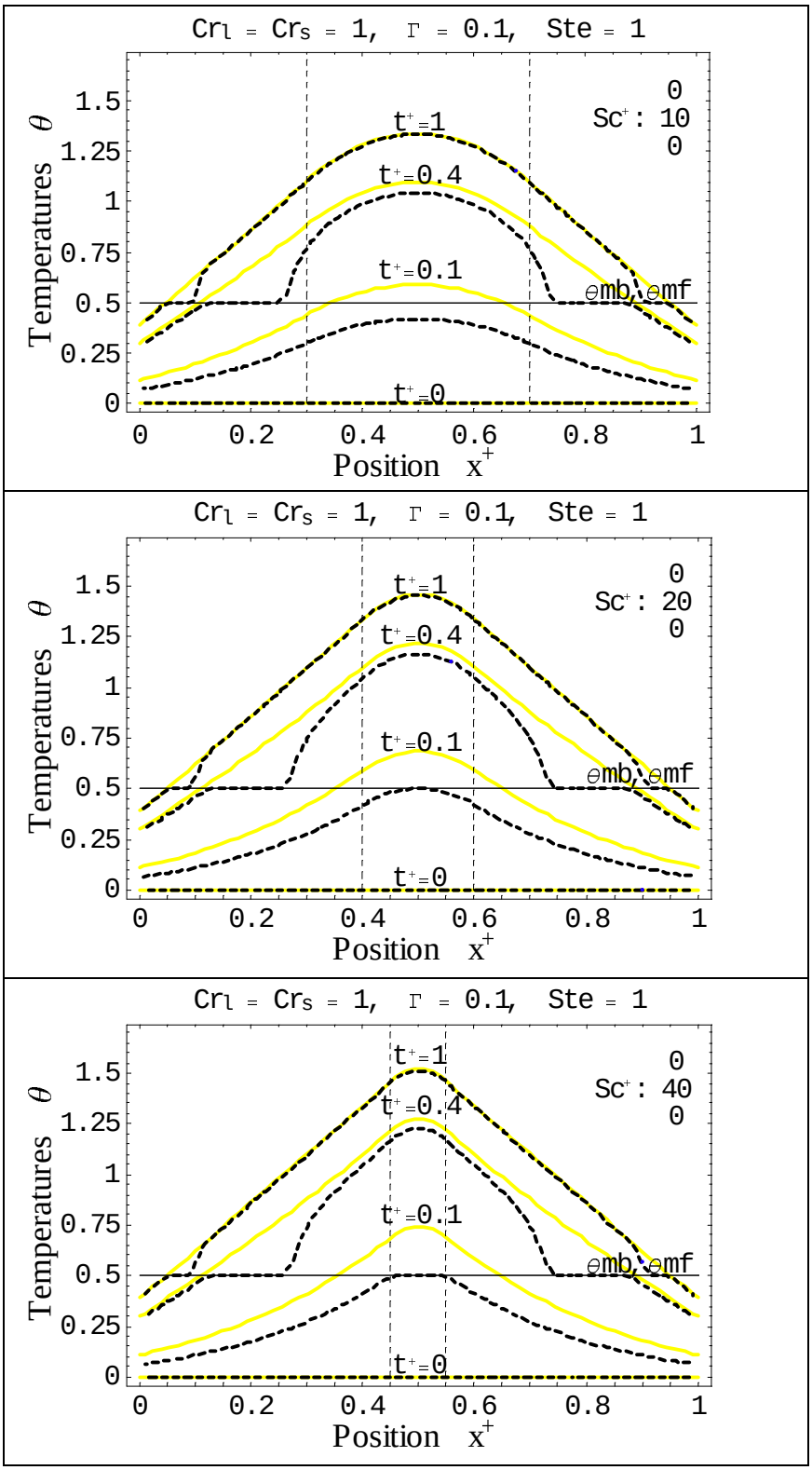

Fig. 4.3.16. Effect of matrix heat source distribution on temperature vs. position for a heterogeneous material, with convection $\theta_\infty = 0$ and $h_\infty^+ = 5$ at $x^+ = 0$ and $x^+ = 1$, *(mm=64,* $\Delta t^+ = 0.003125$*), (* —— *Matrix,* ..... *Particle).*

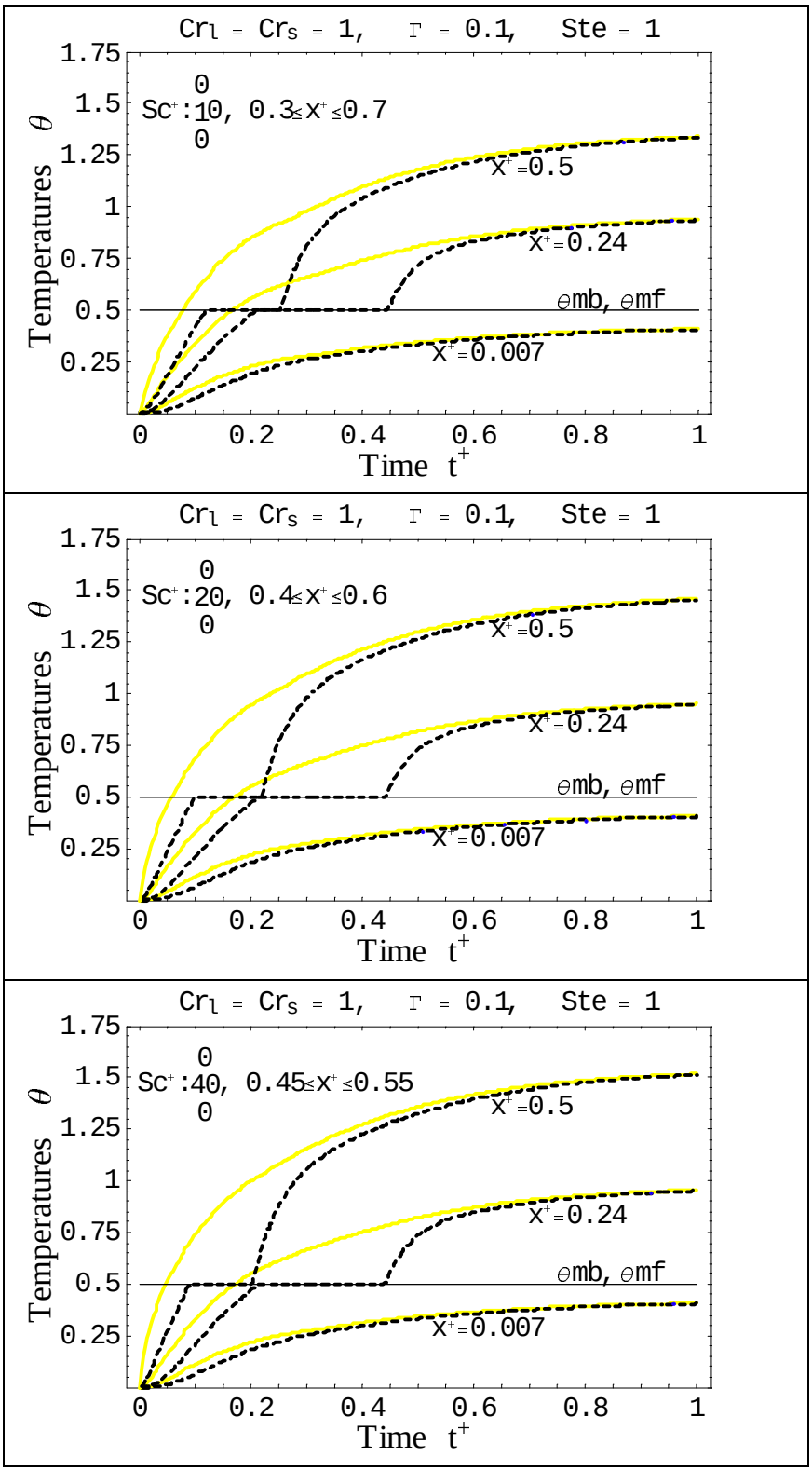

Fig. 4.3.17. Effect of matrix heat source distribution on temperature vs. time for a heterogeneous material, with convection $\theta_\infty = 0$ and $h_\infty^+ = 5$ at $x^+ = 0$ and $x^+ = 1$, *(mm=64,* $\Delta t^+ = 0.003125$*), (—— Matrix, ····· Particle).*

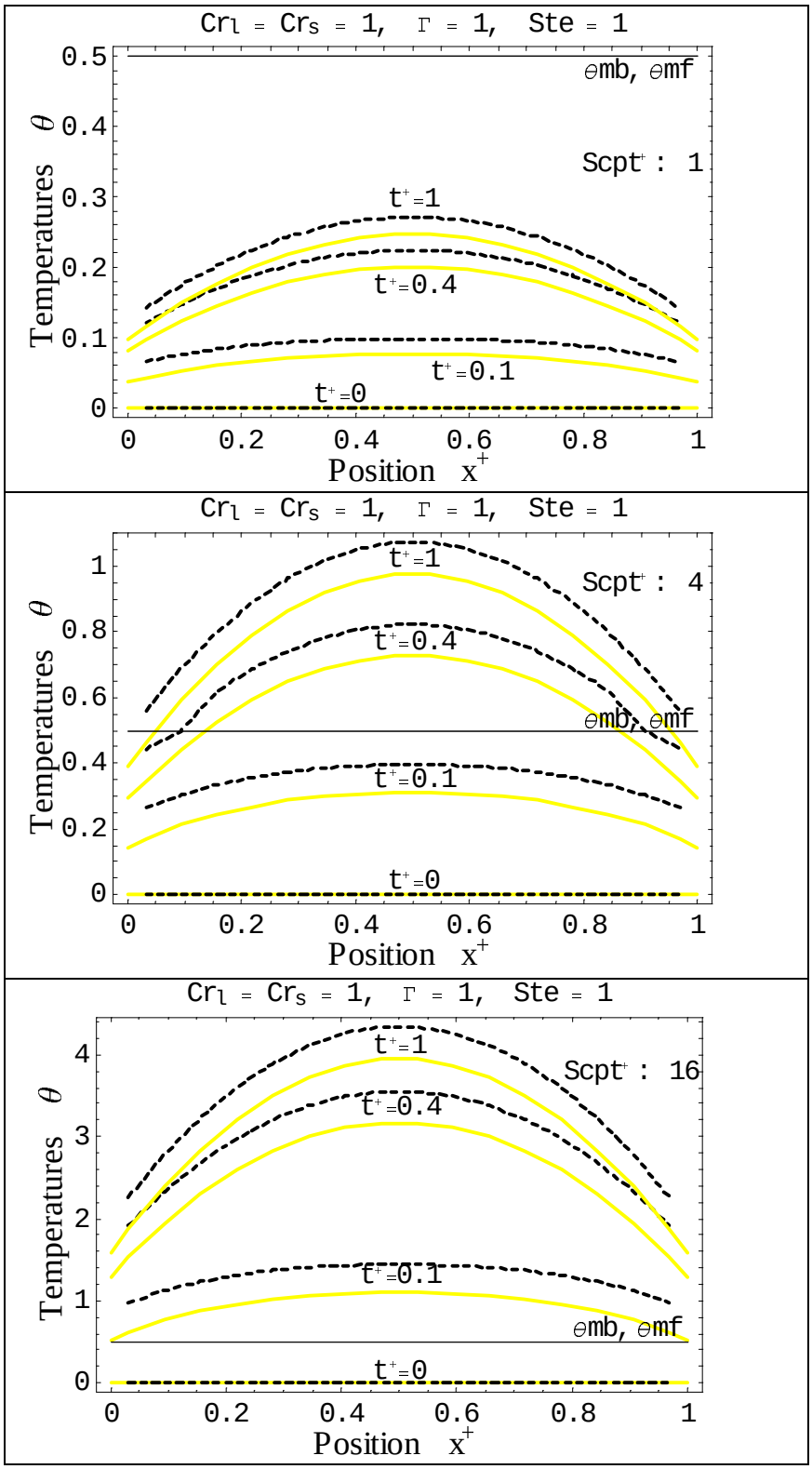

Fig. 4.3.18. Effect of particle heat source on temperature vs. position for a heterogeneous material, with convection $\theta_\infty = 0$ and $h_\infty^+ = 5$ at $x^+ = 0$ and $x^+ = 1$, *(mm=16,* $\Delta t^+ = 0.003125$*), (* —— *Matrix,* ..... *Particle).*

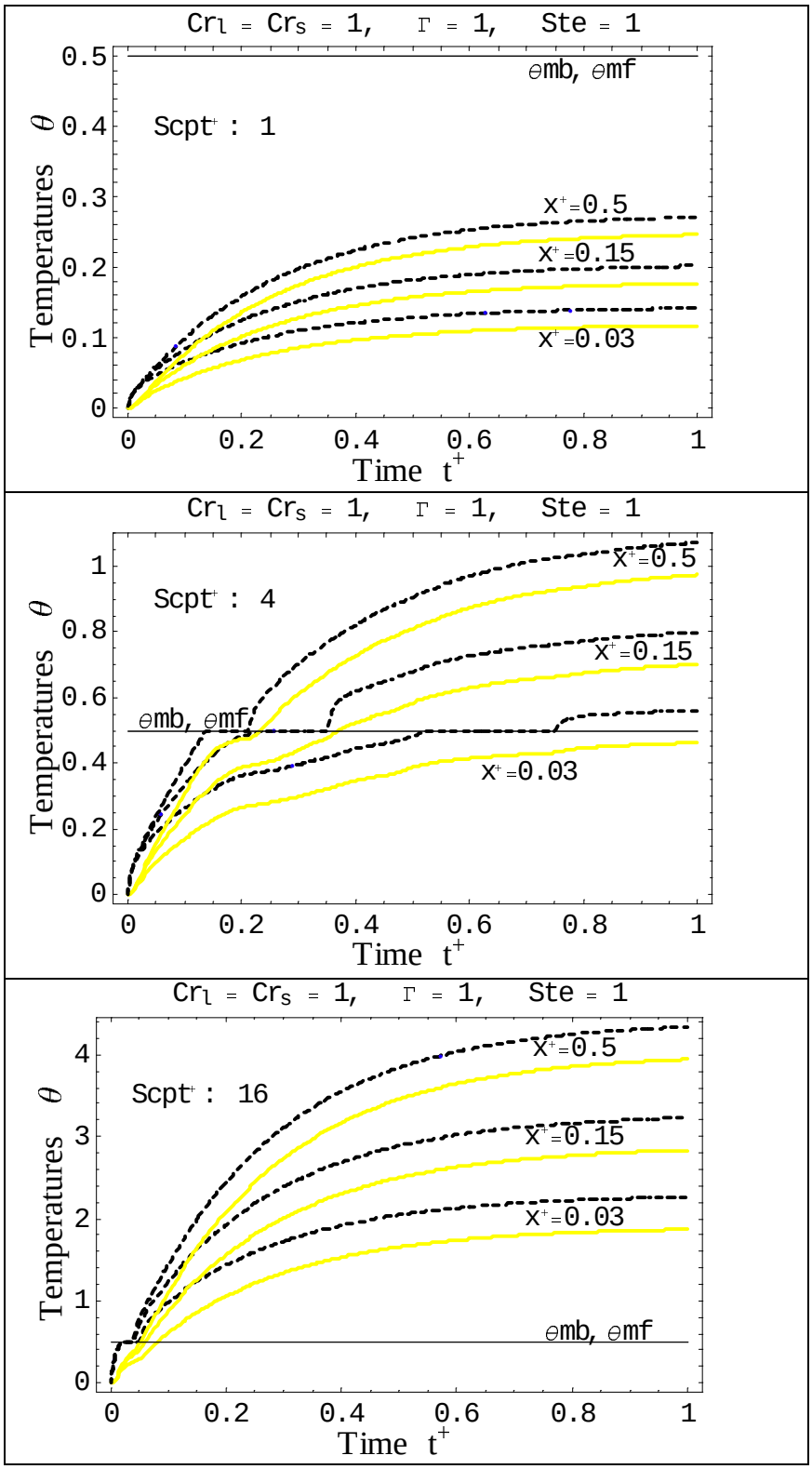

Fig. 4.3.19. Effect of particle heat source on temperature vs. time for a heterogeneous material, with convection $\theta_\infty = 0$ and $h_\infty^+ = 5$ at $x^+ = 0$ and $x^+ = 1$, *(mm=16,* $\Delta t^+ = 0.003125$*), (* —— *Matrix,* ..... *Particle).*

4.3.4. *External Sources*

The effect of external sources is investigated by investigating a pulsed surface heat flux at a surface for a heterogeneous material. In this investigation, the system is initially all solid at temperature $\theta_i = 0$ with a pulsed heat flux at $x^+ = 0$ and insulated at $x^+ = 1$. The particle heat capacity ratios, Stefan number and contact conductance coefficient are $Cr_l = Cr_s = 1$, $Ste = 1$ and $\Gamma = 0.1$. Phase transition occurs at a single melting temperature $\theta mb = \theta mf = 0.5$. The number of control volumes is *16,* and $\Delta t^+ = 0.003125$ is taken as the time step.

4.3.4.1. *Pulsed Surface Heat Flux: Intensity Effects*

Figure 4.3.20 illustrates the pulsed surface heat flux at $x^+ = 0$ for three different cases. In all cases, the time on for the pulse is the same but the heat flux intensity is different.

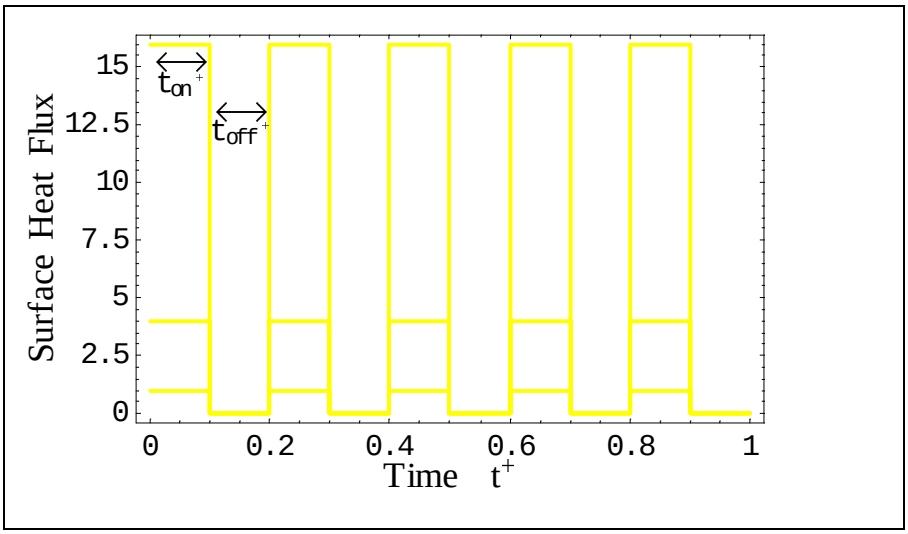

Fig. 4.3.20. Pulsed surface heat flux vs. time at $x^+ = 0$ (Heat Flux Intensity Effects).

Figures 4.3.22 and 4.3.23 demonstrate respectively the particle and matrix temperature histories at different locations and the particle and matrix temperature distributions at various times in the heterogeneous material system for relatively low, medium and high intensity pulsed surface heat flux $q^+_{pulse} = 1,\ 4,\ and\ 16$. It is shown that the most noticeable effect of the pulsed form of the heat flux occurs at the first control volume.

During the heat flux off time, temperature of the first control volume particle and matrix drop severely, while there is no temperature drop for the matrix or particle in middle of the slab or farther. The poor contact conductance causes the temperature lag between the matrix and particle temperature. The temperature lag increases during phase transition, because the particle temperature stays at the melting temperature. Also the weak contact conductance causes the matrix temperatures to drop below the particle temperatures towards the end of the off periods. In addition, When $q^{+}_{pulse} = 1$ the particle and matrix temperatures increase slowly and only the particles of a few control volumes near the surface get to the phase transition temperature. In the other case with $q^{+}_{pulse} = 4$ the given energy is enough to let the particles of all control volumes complete phase change. On the other hand, when $q^{+}_{pulse} = 16$ the energy is so high that the particles of all control volumes reach the saturation temperature very quickly and they complete the transient process in a short time.

4.3.4.2. Pulsed Surface Heat Flux: Pulse Duration Effects

Figure 4.3.21 shows the pulsed surface heat flux at $x^{+} = 0$ for three different time pulses. In each case, the total given energy is the same, but the time on for the pulse is different.

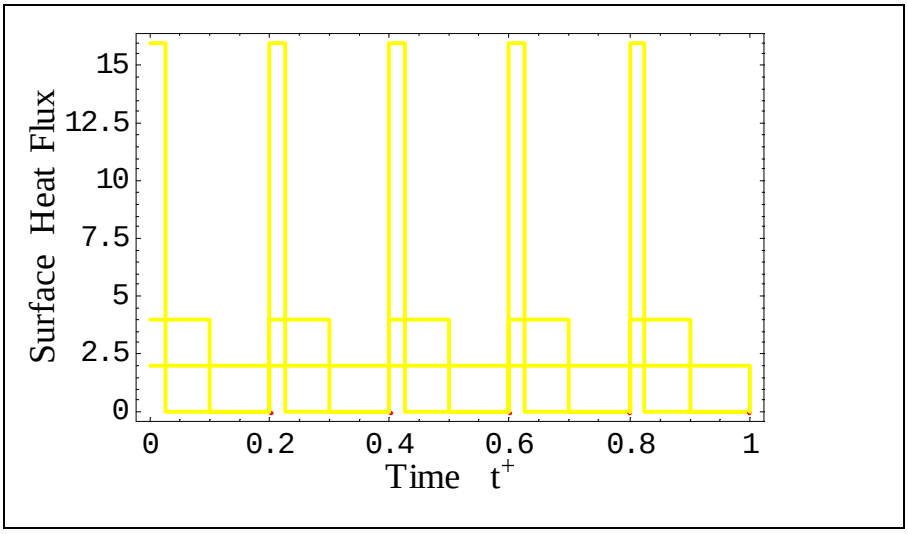

Fig. 4.3.21. Pulsed surface heat flux vs. time at $x^{+}=0$ (Pulse Duration Effects).

Figures 4.3.24 and 4.3.25 demonstrate respectively the matrix and particles temperature histories at different locations and the matrix and particle temperature distributions at various times in the heterogeneous material system. It is shown that the most noticeable effect of the pulsed form of the heat flux occurs at the first control volume. During the heat flux off time, the temperature of the first control volume particle and matrix drop severely, while there is no temperature drop for the matrix or particle in middle of the slab or farther. The particle and matrix temperature histories of the control volumes in middle of the slab or farther are similar for the different cases. The weak contact conductance causes the temperature lag between the matrix and particle temperature. The temperature lag increases during phase transition, because the particle temperature stays at the melting temperature. In addition, the poor contact conductance causes the matrix temperatures to drop below the particle temperatures towards the end of the off periods.

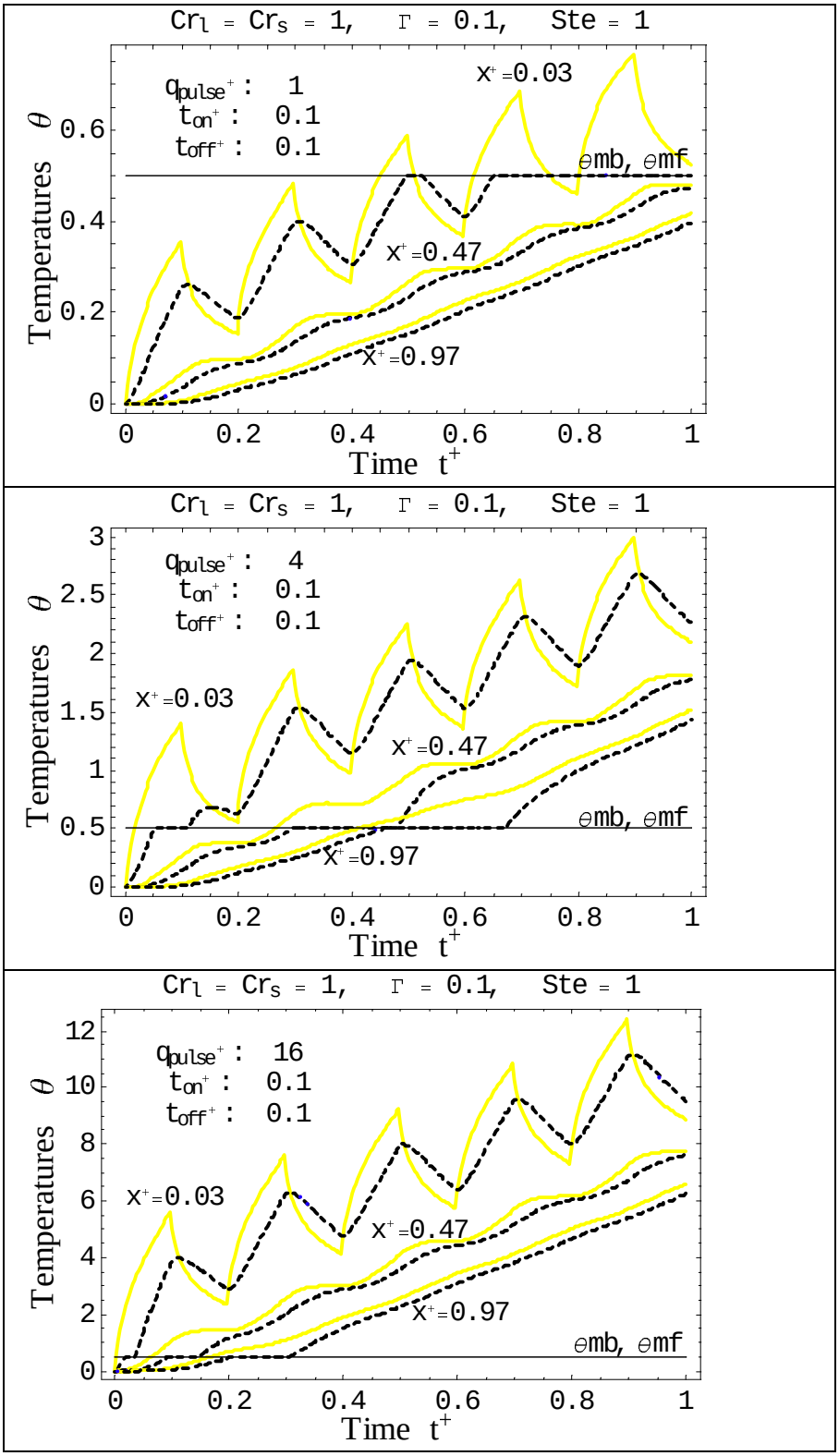

Fig. 4.3.22. Effect of pulsed surface heat flux on temperature vs. time for a heterogeneous material, with a pulsed heat flux at $x^+=0$ and insulated at $x^+=1$, *(mm=16,* $\Delta t^+=0.003125$*), (—— Matrix, ····· Particle).*

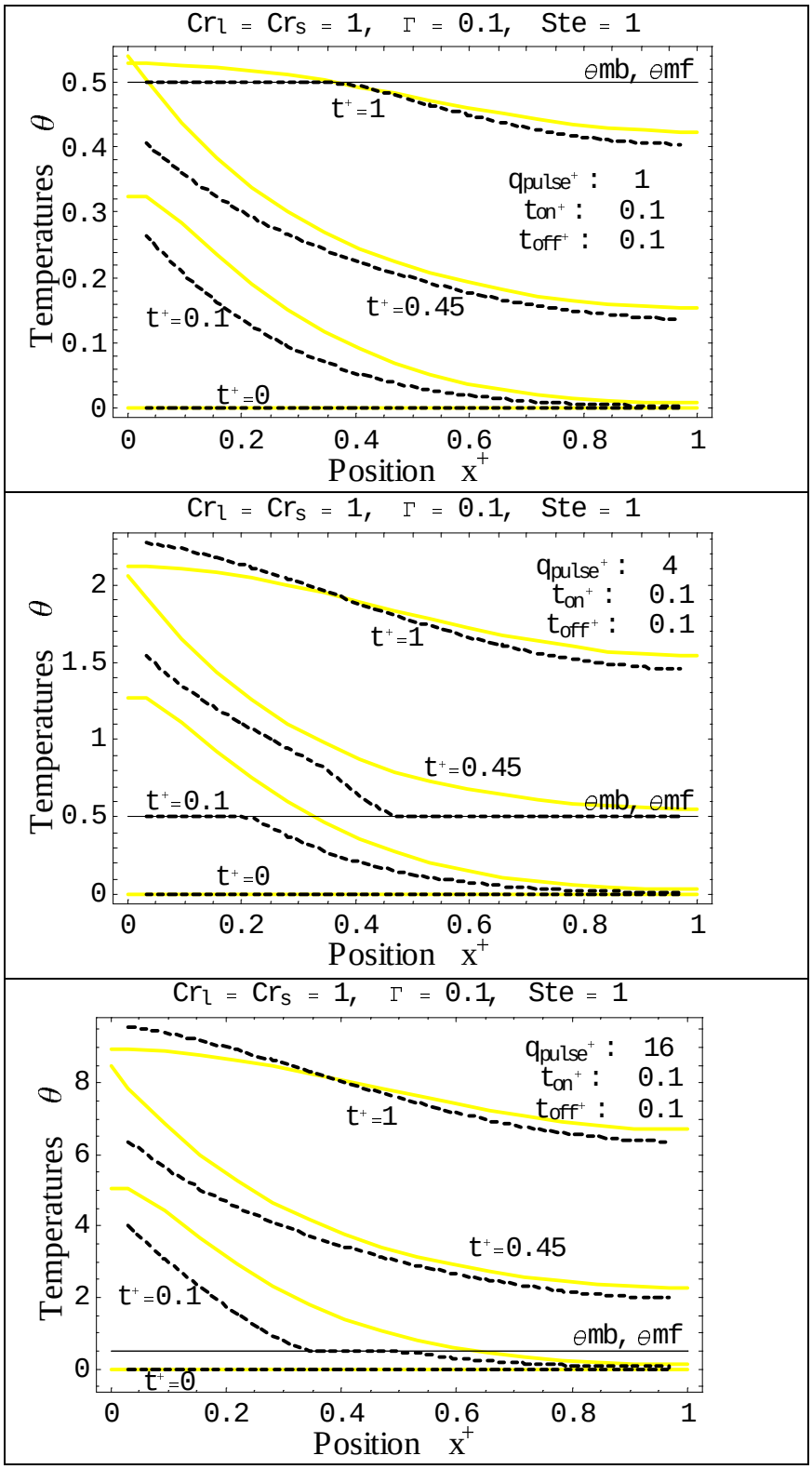

Fig. 4.3.23. Effect of Pulsed surface heat flux on temperature vs. position for a heterogeneous material, with a pulsed heat flux at $x^+=0$ and insulated at $x^+=1$, *(mm=16,* $\Delta t^+=0.003125$*), (—— Matrix, ····· Particle).*

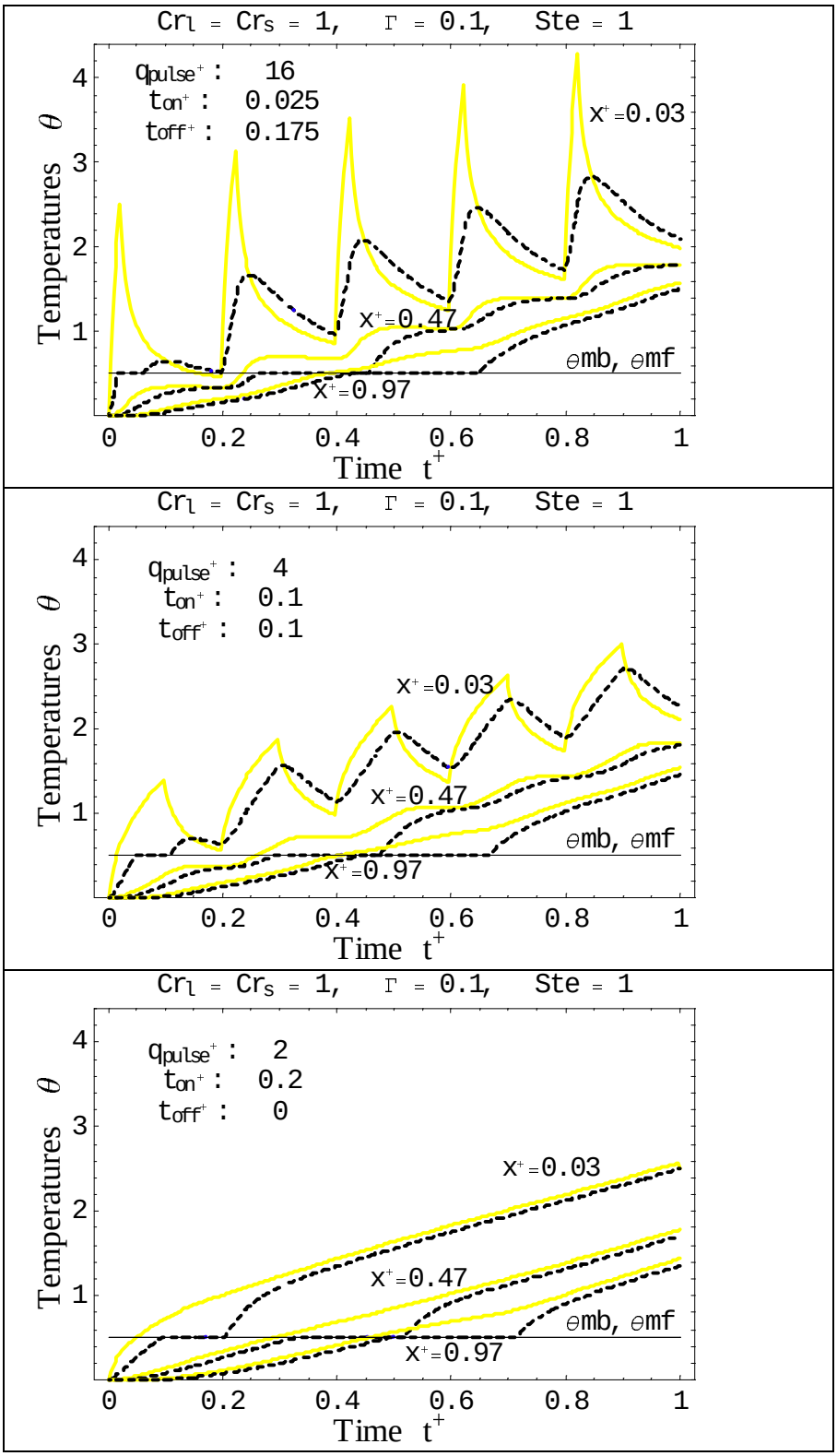

Fig. 4.3.24. Effect of pulsed surface heat flux on temperature vs. time for a heterogeneous material, with a pulsed heat flux at $x^+=0$ and insulated at $x^+=1$, *(mm=16,* $\Delta t^+=0.003125$*), (—— Matrix, ····· Particle).*

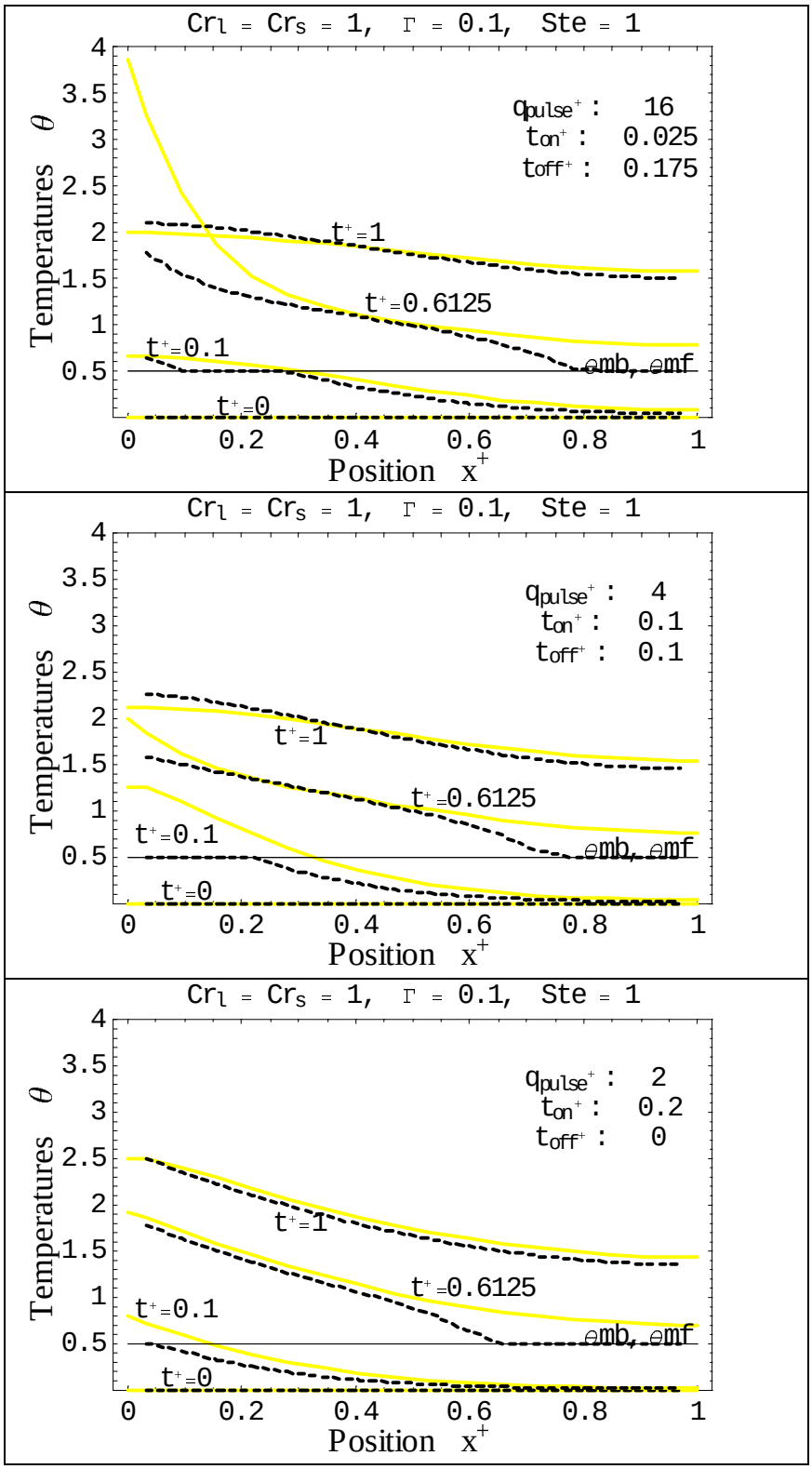

Fig. 4.3.25. Effect of Pulsed surface heat flux on temperature vs. position for a heterogeneous material, with a pulsed heat flux at $x^+=0$ and insulated at $x^+=1$, *(mm=16,* $\Delta t^+=0.003125$*), (—— Matrix, ····· Particle).*

CHAPTER 5
CONCLUSIONS AND FUTURE WORK

5.1. Summary and Conclusions

The main part of this thesis is the investigation of a heterogeneous material consisting of a matrix with relatively small particles embedded during melting or solidification. This investigation is conducted in several phases using a building block approach. First, a lumped capacity system during phase transition is studied, then a one-dimensional homogeneous material during phase change is investigated, and finally the one-dimensional heterogeneous material is analyzed.

Lumped Capacity System: In this thesis a physical model of a lumped capacity system is investigated and the problem formulations for both dimensional and non-dimensional are provided for this model. A numerical solution based on the finite difference method is developed both for the implicit and explicit schemes. In addition, computer programs, using Mathematica, are developed for both the implicit and explicit methods to analyze the thermal behavior of the system by visualizing graphically the transient temperature, phase fraction and energy of the system at any time in the process. These programs are flexible enough to accept any material properties such as liquid and solid density, liquid and solid heat capacity, latent heat, and beginning and finishing melting temperature. Also phase transition can occur at a single melting temperature like a pure material or take place over an extended range of temperatures with a linear function of the energy-temperature relationship. The process can be divided into several time periods and each period can have individual lengths and number of time steps. The system initially can be all solid, liquid or at saturation temperature with specified phase fraction. The boundary condition can change during the process, and the heat source can vary with time. In this thesis by using this program the effects of the time step, internal source, heat transfer coefficient, material properties such as heat capacity ratio, Stefan number, and melting temperature are investigated.

Homogeneous Materials: A one-dimensional homogenous material is analyzed and the dimensional and non-dimensional problem formulations are provided for this system. A numerical solution based on the finite difference method is developed both for the implicit and explicit schemes. In addition, computer programs are developed for both the implicit and explicit methods to investigate the thermal behavior of the system by visualizing graphically the transient and spatial temperature, phase fraction and energy at any time in the process or any location in the system. These programs allow for the inclusion of any system with different zones, and each zone can have individual length, number of control volumes and material properties. Phase transition can occur at a single melting temperature like a pure material or take place over an extended range of temperatures with a linear function of the energy-temperature relationship. The process can be divided into several time periods and each period can have different lengths and number of time steps. The system initially can be all solid, liquid or at phase transition temperature with specified phase fraction. The boundary conditions individually can be either specified temperature or heat flux with heat convection and are allowed to change during the process. The heat source can be applied in any zone and vary with time. Eventually, by applying the computer programs the effects of the time step, control volumes thickness, internal source, external source, material properties such as heat capacity ratio, Stefan number, conductivity ratio, and melting temperature are analyzed.

Heterogeneous Materials: A model of a one-dimensional heterogeneous material consisting of a matrix and small separated spherical particles is investigated and dimensional and non-dimensional problem formulations are provided for this system. A numerical solution based on the finite difference method is developed. A computer program is developed to investigate the thermal behavior of the system by visualizing graphically the transient and spatial particle and matrix temperature, particle phase fraction and particle energy at any time in the process or any location in the system. This program accepts any system with different zones, where each zone is allowed to have individual lengths, number of control volumes and matrix properties. Particle phase transition can occur at a single melting temperature like a pure material or take place over an extended range of temperatures with a linear function of the energy-temperature

relationship. The process can be divided into several time periods and each period is allowed to have individual lengths and number of time steps. The system initially can be all solid, liquid or at particle phase transition temperature with specified particle phase fraction. The boundary conditions individually can be either specified temperature or heat flux with heat convection and are allowed to change during the process. The heat source inside the particles can vary with time, and the heat source inside the matrix can be localized in any zone and change during the process. Finally, in this thesis by using the computer program the effects of the time steps, control volumes thickness, internal sources in the matrix and particles, external sources, material properties such as heat capacity ratio, Stefan number, contact conductance, and particle melting temperature are investigated. According to the results, the weak contact conductance and large heat capacity ratio cause the temperature lag between the matrix and particle temperature, and during the particle phase transition this temperature lag increases. These results are significant in that an increased understanding of this phenomenon could allow for enhanced thermal modeling in a variety of heterogeneous materials and the exploitation of the thermal lag effect in the design of thermal systems and processes.

5.2. Future work

This thesis has demonstrated the concept of lumped capacity system for particles. For more general use, this work needs to be enhanced for larger particles with temperature gradients inside. In this thesis the matrix is not allowed to get involve with phase change, it would be useful to extend this work by eliminating this assumption. In this thesis particle phase transition can occur over an extended range of temperatures with a linear function of the energy-temperature relationship, which is a hypothetical assumption. Therefore a nonlinear function assumption is more realistic to be considered for future work. The other consideration for future work is the concept of varying particle properties with position instead of uniform particle properties. In particular, the significant future research and development have been realized in the following five areas:

1. Multidimensional formulations and numerical solution.
2. Large separated particles without the lumped capacity restriction.

3. Phase transition in the matrix.
4. Nonlinear function of the energy-temperature relationship during phase change.
5. Varying particle properties with position.

REFERENCES

[Colvin and Bryant, 1998] Colvin, D. and Y. Bryant, 1998, "Protective Clothing Containing Encapsulated Phase Change Materials," ASME HTD-Vol. 362/BED Vol. 40, *Advances in Heat and Mass Transfer in Biotechnology*.

[Crank, 1972] Crank, J. and R. S. Gupta,1972, "A Method of Solving Moving Boundary Problems in Heat Flow Using Cubic Splines or Polynomials," *J. Inst. Maths. Applies*, Vol. 10, pp. 296-304.

[Crank, 1981] Crank, J., 1981, "How to Deal with Moving Boundaries in Thermal Problems," in *Numerical Methods in Heat Transfer* (R. W. Lewis and K. Morgan, Eds.), John Wiley & Sons, New York.

[Date, 1991] Date, A., 1991, "A Strong Enthalpy Formulation for the Stefan Problem," *Int. J. Heat Mass Transfer*, Vol. 34, No. 9, pp. 2231-2235.

[Date, 1992] Date, A., 1992, "Novel Strongly Implicit Enthalpy Formulation for Multidimensional Stefan Problem," *Numerical Heat Transfer*, Part B, Vol. 21, pp. 231-251.

[Fomin and Saitoh, 1999] Fomin, S. and T. S. Saitoh, 1999, "Melting of Unfixed Material in Spherical Capsule with Non-Isothermal Wall," *Int. J. Heat Mass Transfer*, Vol. 42, pp. 4197-4205.

[Furmanski, 1992] Furmanski, P., 1992, "Effective Macroscopic Description for Heat Conduction in Heterogeneous Materials," *Int. J. Heat Mass Transfer*, Vol. 35, pp.3047-3058.

[Furmanski, 1994] Furmanski, P., 1994, "Wall Effects in Heat Conduction through a Heterogeneous Material," *Int. J. Heat Mass Transfer*, Vol. 37, No. 13, pp. 1945-1955

[Gupta, 1974] Gupta, R. S., 1974, "Moving Grid Method without Interpolations," *Comp. Meth. Appl. Mech. Engng.*, Vol. 4, pp. 143-152.

[Gupta and Kumar, 1980] Gupta, R. S. and D. Kumar, 1980, "A Modified Variable Time Step Method for One-Dimensional Stefan Problem," *Comp. Meth. Appl. Mech. Engng.*, Vol. 23, pp. 101-109.

[Hsiao, 1985] Hsiao, J., 1985, "An Efficient Algorithm for Finite-Difference Analysis of Heat Transfer with Melting and Solidification," *Numerical Heat Transfer*, Vol. 8, pp. 653-666.

[Ketkar, 1999] Ketkar, P. S., 1999, "*Numerical Thermal Analysis*," ASME, New York.

[Kim and Kaviany, 1990] Kim, C. J., M. Kaviany, 1990, "A Numerical Method for Phase-Change Problems," *Int. J. Heat Mass Transfer*, Vol. 33, No. 12, pp. 2721-2734.

[Langhaar, 1983] Langhaar, L. H., 1983, "*Dimensional Analysis and Theory of Models*," Robert E. Krieger Publishing Company, Florida.

[Colvin and Bryant, 1996] Colvin, D., Y. Bryant, 1996, "Microencapsulated Phase-Change Material Suspensions for Heat Transfer in Spacecraft Thermal Systems," *J. Spacecraft and Rockets*, Vol. 33, No. 2, pp. 278-284.

[Ozisik, 1993] Ozisik, N. M., 1993, "*Heat Conduction*," 2nd ed., John Wiley & Sons, New York.

[Ozisik, 1994] Ozisik, N. M., 1994, "*Finite Difference Methods in Heat Transfer*," CRC Press, Florida.

[Patankar, 1980] Patankar, S. V., 1980, "*Numerical Heat Transfer and Fluid Flow*," McGraw-Hill, New York.

[Pham, 1985] Pham, Q., 1985, "A Fast Unconditionally Stable Finite-Difference Scheme for Heat Conduction with Phase Change," *Int. J. Heat Mass Transfer*, Vol. 28, pp. 2079-2084.

[Pham, 1987] Pham, Q., 1987, "A Note on Some Finite-Difference Methods for Heat Conduction with Phase Change," *Numerical Heat Transfer*, Vol. 11, pp. 353-359.

[Poirier, 1988] Poirier, D., 1988, "On Numerical Methods Used in Mathematical Modeling of Phase Change in Liquid Metals," *J. Heat Transfer*, Vol. 110, pp. 562-570.

[Shamsundar and Sparrow, 1975] Shamsundar, N. and E. M. Sparrow, 1975, "Analysis of Multidimensional Conduction Phase Change Via the Enthalpy Model," *J. Heat Transfer*, Vol. 97, pp. 333-340.

[Tacke, 1985] Tacke, K. H., 1985, "Discretization of the Explicit Enthalpy Method for Planar Phase Change," *Int. J. Num. Methods in Eng.*, Vol. 21, pp. 543-554.

[Vick and Scott, 1998] Vick, B. and P. Scott, 1998, "Heat Transfer in a Matrix with Embedded Particles," *Int. Mech. Engng. Congress and Exposition*, Anaheim, California.

APPENDICES
A. COEFFICIENTS

Step Function:

$$A_n = H[eGuess_n - eo_n] * H[eo_n + \lambda_n - eGuess_n]$$
$$B_n = H[eo_n - eGuess_n]$$
$$C_n = H[eGuess_n - eo_n - \lambda_n]$$

Coefficients:

$$(cW)_n = \frac{k_W}{\Delta x_W} * \left(\left(\frac{Tm_{f,n-1} - Tm_{b,n-1}}{\lambda_{n-1}} \right) * A_{n-1} + \frac{1}{Cp_{s,n-1}} * B_{n-1} + \frac{1}{Cp_{l,n-1}} * C_{n-1} \right)$$

$$(cE)_n = \frac{k_E}{\Delta x_E} * \left(\left(\frac{Tm_{f,n+1} - Tm_{b,n+1}}{\lambda_{n+1}} \right) * A_{n+1} + \frac{1}{Cp_{s,n+1}} * B_{n+1} + \frac{1}{Cp_{l,n+1}} * C_{n+1} \right)$$

$$c_n = -(\rho_n * \Delta x_n) / \Delta t_j - \left(\frac{k_W}{\Delta x_W} + \frac{k_E}{\Delta x_E} + Sp_n{}^j * \Delta x_n \right) * \left(\left(\frac{Tm_{f,n} - Tm_{b,n}}{\lambda_n} \right) * A_n + \frac{1}{Cp_{s,n}} * B_n + \frac{1}{Cp_{l,n}} * C_n \right)$$

$$d_n = -(\rho_n * \Delta x_n) / \Delta t_j * e_n^{j-1} - Sc_n^j * \Delta x_n +$$
$$\frac{k_W}{\Delta x_W} * \left(\left(A_{n-1} * \left(-Tm_{b,n-1} + \left(\frac{Tm_{f,n-1} - Tm_{b,n-1}}{\lambda_{n-1}} \right) * eo_{n-1} \right) \right) + \left(B_{n-1} * \left(-Tm_{b,n-1} + \frac{1}{Cp_{s,n-1}} * eo_{n-1} \right) \right) + \left(C_{n-1} * \left(-Tm_{f,n-1} + \frac{1}{Cp_{l,n-1}} * (eo_{n-1} + \lambda_{n-1}) \right) \right) \right) +$$
$$\frac{k_E}{\Delta x_E} * \left(\left(A_{n+1} * \left(-Tm_{b,n+1} + \left(\frac{Tm_{f,n+1} - Tm_{b,n+1}}{\lambda_{n+1}} \right) * eo_{n+1} \right) \right) + \left(B_{n+1} * \left(-Tm_{b,n+1} + \frac{1}{Cp_{s,n+1}} * eo_{n+1} \right) \right) + \left(C_{n+1} * \left(-Tm_{f,n+1} + \frac{1}{Cp_{l,n+1}} * (eo_{n+1} + \lambda_{n+1}) \right) \right) \right) -$$
$$\left(\frac{k_W}{\Delta x_W} + \frac{k_E}{\Delta x_E} + Sp_n^j * \Delta x_n \right) * \left(\left(A_n * \left(-Tm_{b,n} + \left(\frac{Tm_{f,n} - Tm_{b,n}}{\lambda_n} \right) * eo_n \right) \right) + \left(B_n * \left(-Tm_{b,n} + \frac{1}{Cp_{s,n}} * eo_n \right) \right) + \left(C_n * \left(-Tm_{f,n} + \frac{1}{Cp_{l,n}} * (eo_n + \lambda_n) \right) \right) \right)$$

Boundary Coefficients at x=0:

Specified Temperature Tx0

$$(cE)_0 = 0$$

$$c_0 = \left(\left(\frac{Tm_{f,0} - Tm_{b,0}}{\lambda_0} \right) * A_0 + \frac{1}{Cp_{s,0}} * B_0 + \frac{1}{Cp_{l,0}} * C_0 \right) + (\rho_0 * \Delta x_0) / \Delta t_j$$

$$d_0 = Tx0 + \left(\left(A_0 * \left(-Tm_{b,0} + \left(\frac{Tm_{f,0} - Tm_{b,0}}{\lambda_0} \right) * eo_0 \right) \right) + \left(B_0 * \left(-Tm_{b,0} + \frac{1}{Cp_{s,0}} * eo_0 \right) \right) + \left(C_0 * \left(-Tm_{f,0} + \frac{1}{Cp_{l,0}} * (eo_0 + \lambda_0) \right) \right) \right)$$

Specified Heat Flux qx0 with Convection hx0 and Tx0$_\infty$

$$(cE)_0 = -\frac{2\,k_1}{\Delta x_1} * \left(\left(\frac{Tmf_{,1} - Tmb_{,1}}{\lambda_1} \right) * A_1 + \frac{1}{Cps_{,1}} * B_1 + \frac{1}{Cpl_{,1}} * C_1 \right)$$

$$c_0 = \left(\frac{2\,k_1}{\Delta x_1} + hx0 \right) * \left(\left(\frac{Tmf_{,0} - Tmb_{,0}}{\lambda_0} \right) * A_0 + \frac{1}{Cps_{,0}} * B_0 + \frac{1}{Cpl_{,0}} * C_0 \right) +$$

$$(\rho_0 * \Delta x_0) \Big/ \Delta t_j$$

$$d_0 = qx0 + hx0 * Tx0_\infty +$$

$$\left(\frac{2\,k_1}{\Delta x_1} + hx0 \right) *$$

$$\left(\left(A_0 * \left(-Tmb_{,0} + \left(\frac{Tmf_{,0} - Tmb_{,0}}{\lambda_0} \right) * eo_0 \right) \right) + \right.$$

$$\left(B_0 * \left(-Tmb_{,0} + \frac{1}{Cps_{,0}} * eo_0 \right) \right) +$$

$$\left. \left(C_0 * \left(-Tmf_{,0} + \frac{1}{Cpl_{,0}} * (eo_0 + \lambda_0) \right) \right) \right) -$$

$$\frac{2\,k_1}{\Delta x_1} * \left(\left(A_1 * \left(-Tmb_{,1} + \left(\frac{Tmf_{,1} - Tmb_{,1}}{\lambda_1} \right) * eo_1 \right) \right) + \right.$$

$$\left(B_1 * \left(-Tmb_{,1} + \frac{1}{Cps_{,1}} * eo_1 \right) \right) +$$

$$\left. \left(C_1 * \left(-Tmf_{,1} + \frac{1}{Cpl_{,1}} * (eo_1 + \lambda_1) \right) \right) \right)$$

Boundary Coefficients at x=L

Specified Temperature TxL

$$(cW)_{nn+1} = 0$$

$$c_{nn+1} =$$

$$\left(\left(\frac{Tmf_{,nn+1} - Tmb_{,nn+1}}{\lambda_{nn+1}} \right) * A_{nn+1} + \frac{1}{Cps_{,nn+1}} * B_{nn+1} + \frac{1}{Cpl_{,nn+1}} * C_{nn+1} \right) +$$

$$(\rho_{nn+1} * \Delta x_{nn+1}) \Big/ \Delta t_j$$

$$d_{nn+1} = TxL + \left(\left(A_{nn+1} * \left(-Tm_{b,nn+1} + \left(\frac{Tm_{f,nn+1} - Tm_{b,nn+1}}{\lambda_{nn+1}} \right) * eo_{nn+1} \right) \right) + \left(B_{nn+1} * \left(-Tm_{b,nn+1} + \frac{1}{Cp_{s,nn+1}} * eo_{nn+1} \right) \right) + \left(C_{nn+1} * \left(-Tm_{f,nn+1} + \frac{1}{Cp_{l,nn+1}} * (eo_{nn+1} + \lambda_{nn+1}) \right) \right) \right)$$

Specified Heat Flux qxL with Convection hxL and TxL_∞

$$(cw)_{nn+1} = -\frac{2\,k_{nn}}{\Delta x_{nn}} * \left(\left(\frac{Tm_{f,nn} - Tm_{b,nn}}{\lambda_{nn}} \right) * A_{nn} + \frac{1}{Cp_{s,nn}} * B_{nn} + \frac{1}{Cp_{l,nn}} * C_{nn} \right)$$

$$c_{nn+1} = \left(\frac{2\,k_{nn}}{\Delta x_{nn}} + hxL \right) * \left(\left(\frac{Tm_{f,nn+1} - Tm_{b,nn+1}}{\lambda_{nn+1}} \right) * A_{nn+1} + \frac{1}{Cp_{s,nn+1}} * B_{nn+1} + \frac{1}{Cp_{l,nn+1}} * C_{nn+1} \right) + (\rho_{nn+1} * \Delta x_{nn+1}) \Big/ \Delta t_j$$

$$d_{nn+1} = qxL + hxL * TxL_\infty + \left(\frac{2\,k_{nn}}{\Delta x_{nn}} + hxL \right) * \left(\left(A_{nn+1} * \left(-Tm_{b,nn+1} + \left(\frac{Tm_{f,nn+1} - Tm_{b,nn+1}}{\lambda_{nn+1}} \right) * eo_{nn+1} \right) \right) + \left(B_{nn+1} * \left(-Tm_{b,nn+1} + \frac{1}{Cp_{s,nn+1}} * eo_{nn+1} \right) \right) + \left(C_{nn+1} * \left(-Tm_{f,nn+1} + \frac{1}{Cp_{l,nn+1}} * (eo_{nn+1} + \lambda_{nn+1}) \right) \right) \right) - \frac{2\,k_{nn}}{\Delta x_{nn}} * \left(\left(A_{nn} * \left(-Tm_{b,nn} + \left(\frac{Tm_{f,nn} - Tm_{b,nn}}{\lambda_{nn}} \right) * eo_{nn} \right) \right) + \left(B_{nn} * \left(-Tm_{b,nn} + \frac{1}{Cp_{s,nn}} * eo_{nn} \right) \right) + \left(C_{nn} * \left(-Tm_{f,nn} + \frac{1}{Cp_{l,nn}} * (eo_{nn} + \lambda_{nn}) \right) \right) \right)$$

B. HETEROGENEOUS MATERIAL COMPUTER PROGRAM

B.1. Partly Implicit Method

Problem Description

A model of a one-dimensional heterogeneous material consisting of a matrix and small separated spherical particles is investigated. The computer program is developed to investigate the thermal behavior of the system by visualizing graphically the transient and spatial particle and matrix temperature, particle phase fraction and particle energy at any time in the process or any location in the system. This program accepts any system with different zones, where each zone is allowed to have individual lengths, number of control volumes and matrix properties. Particle phase transition can occur at a single melting temperature like a pure material or take place over an extended range of temperatures with a linear function of the energy-temperature relationship. The process can be divided into several time periods and each period is allowed to have individual lengths and number of time steps. The system initially can be all solid, liquid or at particle phase transition temperature with specified particle phase fraction. The boundary conditions individually can be either specified temperature or heat flux with heat convection and are allowed to change during the process. The heat source inside the particles can vary with time, and the heat source inside the matrix can be localized in any zone and change during the process.

Inputs:

PART ONE

Overal Geometery

```
NZones = 1;
LZone[1] = 1.;

L = 1.;(* m *)
AreaTotal = 1. (* m^2 *)
```

Microstructure

```
(* Particle Density *)

NumberParticles = 20000 ;
ParticleDiameter = 1. / 1 * In2M ;
```

```
(* Contact Conductance *)

h = 1.; (* W/m^2 K *)
```

Grid

```
NCVZone [1] = 16;
mm1 = 16;(* number of CV's in x *)
```

Material Properties

```
(* Matrix *)

kMatrixZone [1] = 1.;
αMatrixZone [1] = 1.;
ρCMatrixZone [1] = kMatrixZone [1] / αMatrixZone [1];
(* Particles *)

TmParticleb1 = 0.5;
TmParticlef1 = 0.5;
λParticle1 = 1.;

ρParticleliq1 = 1.;
CpParticleliq1 = 1.;
ρCParticleliq1 = ρParticleliq1 * CpParticleliq1 ;

ρParticlesol1 = 1.;
CpParticlesol1 = 1.;
ρCParticlesol1 = ρParticlesol1 * CpParticlesol1 ;
```

Stability Condition

```
StabilityCondition ;
```

PART TWO

Time Discretization

```
NPeriods = 1;
Lper = 0.05 ;
Table [LPeriod [per] = Lper , {per , NPeriods }];
Table [NTimeStepsPeriod [per] = 20, {per , NPeriods }];
```

Initial Temperature

```
Tinitial = 0.
finitial = 0.
e0 = 0;
PhF0 = 0;
ConvergenceRatio = 0.001;
MaxNiter = 20;
```

Boundary Condition

```
(* BC at x=0 *)
BCx0 = 2;

Table[
  {Tx0Period[per] = 0.,
   qx0Period[per] = 2.,
   hx0Period[per] = 0.,
   T∞x0Period[per] = 0.},
  {per, NPeriods}
 ];
(* BC at x=L *)
BCxL = 2;

Table[
  {TxLPeriod[per] = 0.,
   qxLPeriod[per] = 0.,
   hxLPeriod[per] = 0.,
   T∞xLPeriod[per] = 0.},
  {per, NPeriods}
 ];
```

Heat Sources in the CV's

```
(* Matrix *)
Table[ScZonePeriod[i, per] = 0. * Random[Integer],
  {per, NPeriods},
  {i, NZones}];

Table[SZonePeriod[i, per] = 0.,
  {per, NPeriods},
  {i, NZones}];
```

```
(*  Particles   *)
Table[ScptPeriod[per] = 0. * Random[Integer],
  {per, NPeriods}];

Table[SptPeriod[per] = 0.,
  {per, NPeriods}];
```

Compute Solution:

Record Solution

```
RecordSolution :=
 Module[{m, p},
  MatrixTempData = Table[T_{m,p}, {p, 0, pmax}, {m, 0, mm + 1}];
  MaxMatrixTemp = Max[MatrixTempData];
  MinMatrixTemp = Min[MatrixTempData];
  ParticleTempData = Table[Tpt_{m,p}, {p, 0, pmax}, {m, 1, mm}];
  MaxParticleTemp = Max[ParticleTempData];
  MinParticleTemp = Min[ParticleTempData];
  ParticlePhaseFractionData = Table[fpt_{m,p}, {p, 0, pmax}, {m, 0, mm + 1}];
 ]
StartTime = TimeUsed[];
mm = mm1;
ComputeSolution;
RecordSolution;
EndTime = TimeUsed[];
RunTime = EndTime - StartTime
```

Functions to Generate Results

Spatial Temperature Distribution Plots

```
MatrixTempDistPlot[p_] :=
ListPlot[Table[{x_m, T_{m,p}}, {m, 0, mm + 1}],
  PlotRange → {MinMatrixTemp, MaxMatrixTemp},
  PlotLabel →
   FontForm[StringJoin["t⁺=", ToString[t_p], "   CVs=",
     ToString[mm], "   Δt⁺=", ToString[t_1]], {"Times", 14}],
  FrameLabel →
   {StyleForm["Position  x⁺", FontSize → 14],
    StyleForm["Matrix  Temp  Θ", FontSize → 14]}]
```

```
PartTempDistPlot [p_] :=
 ListPlot [Table [{x_m, Tpt_{m,p}}, {m, 1, mm}],
  PlotRange → {MinParticleTemp , MaxParticleTemp },
  PlotLabel →
   FontForm [StringJoin ["t⁺=", ToString [t_p], "   CVs=",
     ToString [mm], "   Δt⁺=", ToString [t_1]], {"Times", 14}],
  FrameLabel →
   {StyleForm ["Position  x⁺", FontSize → 14],
    StyleForm ["Particle  Temp  θ", FontSize → 14]}]


MatrixPartTempDistPlot [p_] :=
 MultipleListPlot [Table [{x_m, T_{m,p}}, {m, 0, mm + 1}],
  Table [{x_m, Tpt_{m,p}}, {m, 1, mm}],
  PlotRange → {MinParticleTemp , MaxMatrixTemp },
  PlotLabel →
   FontForm [StringJoin ["t⁺=", ToString [t_p], "   CVs=",
     ToString [mm], "   Δt⁺=", ToString [t_1]], {"Times", 14}],
  FrameLabel →
   {StyleForm ["Position  x⁺", FontSize → 14],
    StyleForm ["Temperatures  θ", FontSize → 14]}]
```

Transient Temperature Plots

```
MatrixTimeHistoryPlot [m_] :=
 ListPlot [Table [{t_p, T_{m,p}}, {p, 0, pmax}],
  PlotLabel →
   FontForm [StringJoin ["x⁺=", ToString [x_m], "   CVs=",
     ToString [mm], "   Δt⁺=", ToString [t_1]], {"Times", 14}],
  FrameLabel →
   {FontForm ["Time  t⁺", {"Times ", 14}],
    FontForm ["Matrix  Temperature  θ", {"Times", 14}]}]


PartTimeHistoryPlot [m_] :=
 ListPlot [Table [{t_p, Tpt_{m,p}}, {p, 0, pmax}],
  PlotLabel →
   FontForm [StringJoin ["x⁺=", ToString [x_m], "   CVs=",
     ToString [mm], "   Δt⁺=", ToString [t_1]], {"Times", 14}],
    FrameLabel →
   {FontForm ["Time  t⁺", {"Times ", 14}],
    FontForm ["Particle  Temperature  θ", {"Times", 14}]}]
```

```
MatrixPartTimeHistoryPlot [m_] :=
 MultipleListPlot [Table [{tp, Tm,p}, {p, 0, pmax }],
  Table [{tp, Tpt m,p}, {p, 0, pmax }],
  PlotLabel →
   FontForm [StringJoin ["x+ =", ToString [xm], "   CVs =",
     ToString [mm], "   Δt+ =", ToString [t1]], {"Times ", 14}],
  FrameLabel →
   {FontForm ["Time  t+", {"Times  ", 14}],
    FontForm ["Temperatures  Θ", {"Times ", 14}]}]
```

Spatial Energy Distribution Plots

```
PartEnergyDistPlot [p_] :=
 ListPlot [Table [{xm, em,p}, {m, 1, mm}],
  PlotRange → All,
  PlotLabel →
   FontForm [StringJoin ["t+ =", ToString [tp], "   CVs =",
     ToString [mm], "   Δt+ =", ToString [t1]], {"Times ", 14}],
    FrameLabel →
   {FontForm ["Position   x+", {"Times  ", 14}],
    FontForm ["Particle  Energy   e+ ", {"Times ", 14}]}, Axes → False ]
```

Transient Energy Plots

```
PartEnergyTimeHistoryPlot [m_] :=
 ListPlot [Table [{tp, em,p}, {p, 0, pmax }],
  PlotLabel →
   FontForm [StringJoin ["x+ =", ToString [xm], "   CVs =",
     ToString [mm], "   Δt+ =", ToString [t1]], {"Times ", 14}],
    FrameLabel →
   {FontForm ["Time   t+", {"Times  ", 14}],
    FontForm ["Particle  Energy   e+ ", {"Times ", 14}]}, Axes → False ]
```

Spatial PhaseFraction Distribution Plots

```
PartPhaseFractionDistPlot [p_] :=
 ListPlot [Table [{xm, fpt m,p}, {m, 1, mm}],
  PlotRange → All,
  PlotLabel →
   FontForm [StringJoin ["t+ =", ToString [tp], "   CVs =",
     ToString [mm], "   Δt+ =", ToString [t1]], {"Times ", 14}],
    FrameLabel →
   {FontForm ["Position   x+", {"Times  ", 14}],
    FontForm ["Particle  Phase  Fraction  ", {"Times ", 14}]}]
```

Transient Phase Fraction Plots

```
PartPhaseFractionTimeHistoryPlot [m_] :=
 ListPlot [Table [{t_p, fpt_{m,p}}, {p, 0, pmax}],
  PlotLabel →
   FontForm [StringJoin ["x⁺=", ToString [x_m], "    CVs=",
     ToString [mm], "    Δt⁺=", ToString [t_1]], {"Times", 14}],
    FrameLabel →
   {FontForm ["Time   t⁺", {"Times  ", 14}],
    FontForm ["Particle  Phase  Fraction  ", {"Times", 14}]}]
```

3D Plots

```
Matrix3DimPlot  :=
 ListSurfacePlot3D  [Table [{x_m, t_p, T_{m,p}}, {m, 0, mm + 1}, {p, 0, pmax}],
    PlotRange → All,
    BoxRatios → {1, 1, 0.5},
    Axes → True,
    AxesLabel → {
            StyleForm ["x⁺", FontFamily → Times, FontSize → 14] ,
            StyleForm ["t⁺", FontFamily → Times, FontSize → 14],
            StyleForm ["θ(x⁺,t⁺)", FontFamily → Times, FontSize → 14] }]

Part3DimPlot  :=
 ListSurfacePlot3D  [Table [{x_m, t_p, Tpt_{m,p}}, {m, 1, mm}, {p, 0, pmax}],
    PlotRange → All,
    BoxRatios → {1, 1, 0.5},
    Axes → True,
    AxesLabel → {
            StyleForm ["x⁺", FontFamily → Times, FontSize → 14] ,
            StyleForm ["t⁺", FontFamily → Times, FontSize → 14],
            StyleForm ["θ(x⁺,t⁺)", FontFamily → Times, FontSize → 14] }]
```

Phase Plots

```
PhasePlot [m_] :=
 ListPlot [Table [{T_{m,p}, Tpt_{m,p}}, {p, 0, pmax}],
  AspectRatio → 1,
  PlotLabel →
   FontForm [StringJoin ["CVs=", ToString [mm], "    Δt⁺=", ToString [t_1]],
    {"Times", 14}],
     FrameLabel → {
            StyleForm ["Matrix  Temp", FontFamily → Times,
     FontSize → 14],
            StyleForm ["Particle  Temp", FontFamily → Times,
     FontSize → 14]}]
```

Results

Spatial Temperature Distribution Plots

```
MatrixTempDistPlot [pmax]
PartTempDistPlot [pmax]
MatrixPartTempDistPlot [pmax]
```

Transient Temperature Plots

```
MatrixTimeHistoryPlot [1]
PartTimeHistoryPlot [1]
MatrixPartTimeHistoryPlot [2]
```

3D Plots

```
Matrix3DimPlot
Part3DimPlot
```

Spatial Energy Distribution Plots

```
PartEnergyDistPlot [pmax]
```

Transient Energy Plots

```
PartEnergyTimeHistoryPlot [2]
```

Spatial Phase Fraction Distribution Plots

```
PartPhaseFractionDistPlot [pmax]
```

Transient Phase Fraction Plots

```
PartPhaseFractionTimeHistoryPlot [2]
```

Phase Plots

```
Show[PhasePlot [1], PhasePlot [2], DiagonalPlot ]
```

*** Modules ***

Input Functions:

Microstructure

```
Microstructure  :=
Module [{},
  Volume = AreaTotal * L;
  NumberDensity = NumberParticles / Volume;
  Vp = π ParticleDiameter^3 / 6;
  Ap = π ParticleDiameter^2;
  VolumeFractionMatrix = 1 - NumberDensity * Vp;
  VolumeFractionParticles = NumberDensity * Vp;
  H = h * NumberDensity * Ap]
```

Grid

```
GridUniform [L_, mm_] :=
Module [{m, i},
  mmZone [0] = 0;
  Table [mmZone [i] = mmZone [i - 1] + NCVZone [i], {i, 1, NZones }];
  (*mm=mmZone [NZones ];*)
  Table [△x_m = LZone [i] / NCVZone [i], {i, 1, NZones },
    {m, mmZone [i - 1] + 1, mmZone [i]}];
  △x_0 = 0;
  △x_(mm+1) = 0;
  x_0 = 0;
  Table [x_m = x_(m-1) + △x_(m-1) / 2. + △x_m / 2., {m, 1, mm + 1}]]
GridTable  := TableForm [Table [{m, x_m, x_m / In2M , △x_m}, {m, 0, mm + 1}],
    TableHeadings → {None , {"m", "x_m(m)", "x_m(inches )", "△x_m(m)"}}]
```

Material Properties

```
MaterialProperties  :=
Module [{m},
  Table [
    {k_m = (1 - NumberDensity * Vp) kMatrixZone [i],
     ρC_m = (1 - NumberDensity * Vp) ρCMatrixZone [i]}, {i, 1, NZones },
    {m, mmZone [i - 1], mmZone [i] + 1}];
```

```
If[TmParticlef1 == TmParticleb1 , TmParticlef2 = 1.02 * TmParticlef1 ,
   TmParticlef2 = TmParticlef1 ];
 Table [{
   ρParticleliq m = ρParticleliq1 ,
   ρParticlesol m = ρParticlesol1 ,
   CpParticleliq m = CpParticleliq1 ,
   CpParticlesol m = CpParticlesol1 ,
   ρCParticleliq m = ρCParticleliq1 ,
   ρCParticlesol m = ρCParticlesol1 ,
   TmParticleb m = TmParticleb1 ,
   TmParticlef m = TmParticlef2 ,
   λParticle m = λParticle1 },
  {m, 0, mm + 1}]]
```

Stability Condition

```
StabilityCondition :=
Module [{},
  Microstructure ;
  Minρ = Min [ρParticlesol1 , ρParticleliq1 ];
  MinCp = Min [If [TmParticleb1 == TmParticlef1 ,
     {CpParticlesol1 , CpParticleliq1 },
     {CpParticlesol1 , CpParticleliq1 ,
      λParticle1 / (TmParticlef1 - TmParticleb1 )}]];
  Max△t = (Minρ * MinCp ) * (NumberDensity * Vp) / (H);
  Print [" ***WARNING   WARNING *** For Stability Of This
     Program △tp Must Be Less Than ", Max△t,
   "  Please Choose a Proper △tp in Time Discretization  Section . "]]
```

Time Discretization

```
TimeDiscretization :=
Module [{p, per},

  (* p at end of each period *)
  pmaxPeriod [0] = 0;
  Table [pmaxPeriod [per] = pmaxPeriod [per - 1] + NTimeStepsPeriod [per],
   {per, NPeriods }];
  pmax = pmaxPeriod [NPeriods ];

  (* time steps *)
  Table [△tp = LPeriod [per] / NTimeStepsPeriod [per],
   {per, NPeriods },
   {p, pmaxPeriod [per - 1] + 1, pmaxPeriod [per]}];
```

Initial Temperatures

```
InitialConditions  :=
    Module [{},
    Table [T_{m,0} = Tpt_{m,0} = Tinitial , {m, 0, mm + 1}];

  Table [fpt_{m,0} = Which [
        Tpt_{m,0} < TmParticleb _m, 0,
        Tpt_{m,0} > TmParticlef _m, 1,
        TmParticleb _m <= Tpt_{m,0} <= TmParticlef _m, finitial ],
    {m, 0, mm + 1}] // TableForm ;

  Table [e_{m,0} = Which [
      Tpt_{m,0} < TmParticleb _m, e0 - CpParticlesol _m * (TmParticleb _m - Tinitial ),
      Tpt_{m,0} > TmParticlef _m,
      e0 + λParticle _m + CpParticleliq _m * (Tinitial - TmParticlef _m),
      TmParticleb _m <= Tpt_{m,0} <= TmParticlef _m, e0 + λParticle _m * finitial ],
    {m, 0, mm + 1}] // TableForm ;

  Table [eGuess _{m,1} = e_{m,0}, {m, 0, mm + 1}];

  Table [If [Tpt_{m,0} <= TmParticleb _m,
     ρCpt_m = NumberDensity  * Vp * ρCParticlesol _m; ρParticle _m = ρParticlesol _m;
     CpParticle _m = CpParticlesol _m,
     ρCpt_m = NumberDensity  * Vp * ρCParticleliq _m; ρParticle _m = ρParticleliq _m;
     CpParticle _m = CpParticleliq _m], {m, 0, mm + 1}] //
   TableForm ]
```

Boundary Conditions

BC at x=0

```
BoundaryConditionx0  :=
If [BCx0 == 1,
    Table [{Tx0_p = Tx0Period [per]},
     {per, NPeriods },
     {p, pmaxPeriod [per - 1], pmaxPeriod [per]}],
    Table [{qx0_p = qx0Period [per],
      hx0_p = hx0Period [per],
      T∞x0_p = T∞x0Period [per]},
     {per, NPeriods },
     {p, pmaxPeriod [per - 1], pmaxPeriod [per]}]];
```

BC at x=L

```
BoundaryConditionxL  :=
If[BCxL == 1,
  Table[{TxL_p = TxLPeriod[per]},
   {per, NPeriods},
   {p, pmaxPeriod[per - 1], pmaxPeriod[per]}],
  Table[{qxL_p = qxLPeriod[per],
    hxL_p = hxLPeriod[per],
    T∞xL_p = T∞xLPeriod[per]},
   {per, NPeriods},
   {p, pmaxPeriod[per - 1], pmaxPeriod[per]}]]
```

Heat Sources in the CV's

```
HeatSources  :=
  Module[{},
   Table[
    {Sc_{m,p} = ScZonePeriod[i, per],
     S_{m,p} = SZonePeriod[i, per]},
    {per, NPeriods},
    {i, NZones},
    {p, pmaxPeriod[per - 1], pmaxPeriod[per]},
    {m, mmZone[i - 1] + 1, mmZone[i]}];

   Table[Scpt_{m,p} = ScptPeriod[per], {per, NPeriods},
    {p, pmaxPeriod[per - 1], pmaxPeriod[per]}, {m, 1, mm}];
   Table[Spt_{m,p} = SptPeriod[per], {per, NPeriods},
    {p, pmaxPeriod[per - 1], pmaxPeriod[per]}, {m, 1, mm}];];
```

Computational Functions:

Compute Time Independent Coefficients

Interior CV's for the Matrix

```
ComputeConductances  :=
Module[{m},
  Table[aW_m = 2 k_{m-1} k_m / (Δx_{m-1} k_m + Δx_m k_{m-1}), {m, 1, mm + 1}];
  Table[aE_m = aW_{m+1}, {m, 0, mm}];
```

```
If[BCxL == 1, aW_{mm+1} = 0];
 If[BCx0 == 1, aE_0 = 0];

 (* upper and lower diagonals for Tridiagonal *)
 lower = Table[-aW_m, {m, 1, mm + 1}];
 upper = Table[-aE_m, {m, 0, mm}]]
```

Time Dependent Coefficients

Interior Coefficients for the Particles

$$\text{InteriorParticleCoefficients} :=$$

$$\text{Table}\left[\left\{ \text{aOpt}_m = \rho \text{Cpt}_m \frac{\Delta x_m}{\Delta t_p},\ \text{apt}_m = \text{aOpt}_m + H\,\Delta x_m + \text{Spt}_{m,p}\,\Delta x_m,\ \text{bpt}_m = \text{aOpt}_m\,\text{Tpt}_{m,p-1} + \text{Scpt}_{m,p}\,\Delta x_m \right\}, \{m, 1, mm\}\right];$$

Interior Coefficients for the Matrix

$$\text{InteriorMatrixCoefficients} :=$$

$$\text{Table}\left[\left\{ \text{aO}_m = \rho C_m \frac{\Delta x_m}{\Delta t_p},\ a_m = \text{aO}_m + \text{aE}_m + \text{aW}_m + S_{m,p}\,\Delta x_m + H\,\Delta x_m,\ b_m = \text{aO}_m\,T_{m,p-1} + \text{Sc}_{m,p}\,\Delta x_m \right\}, \{m, 1, mm\}\right];$$

Boundary at x=0

$$\text{CoefficientsAtx0} :=$$

$$\text{If}[\text{BCx0} == 1,\ a_0 = 1;\ b_0 = \text{Tx0}_p,\ a_0 = \text{aE}_0 + \text{hx0}_p;\ b_0 = \text{qx0}_p + \text{hx0}_p * \text{T}\infty\text{x0}_p];$$

Boundary at x=L

$$\text{CoefficientsAtxL} :=$$

$$\text{If}[\text{BCxL} == 1,\ a_{mm+1} = 1;\ b_{mm+1} = \text{TxL}_p,\ a_{mm+1} = \text{aW}_{mm+1} + \text{hxL}_p;\ b_{mm+1} = \text{qxL}_p + \text{hxL}_p * \text{T}\infty\text{xL}_p];$$

Unit Function

```
UnitFunction := Module[{},
  SU_{m,p} = UnitStep[e0 - eGuess_{m,p}];
  LU_{m,p} = UnitStep[eGuess_{m,p} - e0 - λParticle_m];
  MU_{m,p} = UnitStep[eGuess_{m,p} - e0] * UnitStep[e0 + λParticle_m - eGuess_{m,p}]]
```

Compute Temperatures and Energy

```
ComputeEnergyandTemperature :=
  Module[{},
 UnitFunction;
 {{e_{m,p}, Tpt_{m,p}}} =
  {Enew, Tnew} /.
   NSolve[{ρParticle_m * NumberDensity * Vp * (Enew - e_{m,p-1}) ==
       Δt_p * H * (T_{m,p} - Tpt_{m,p-1}) + (Scpt_{m,p} * Δt_p) - (Tnew * Spt_{m,p} * Δt_p),
     Tnew == (TmParticleb_m + ((TmParticlef_m - TmParticleb_m)/λParticle_m) * (Enew - e0)) *
       MU_{m,p} + (TmParticleb_m - 1/CpParticlesol_m (e0 - Enew)) * SU_{m,p} +
       (TmParticlef_m + 1/CpParticleliq_m (Enew - e0 - λParticle_m)) * LU_{m,p}}]]
```

Compute Phase Fractions

```
ComputePhaseFractions :=
 Module[{},
  fpt_{m,p} =
   (e_{m,p} - e0)/λParticle_m (UnitStep[e_{m,p} - e0] - UnitStep[e_{m,p} - e0 - λParticle_m]) +
    UnitStep[e_{m,p} - e0 - λParticle_m]]
```

Iterate Energy

```
IterateEnergy := Module[{},
  Test = 1;
  Niter = 0;
  While[Test == 1 && Niter < MaxNiter,
   ComputeEnergyandTemperature;
   Test = 0;
   TestConvergence;
   Niter = Niter + 1;]]
```

Test of Convergence

```
TestConvergence  := Module [{},
  If[Abs[(eGuess m,p - em,p)] ≥ ConvergenceRatio  , Test = 1];
  If[Test == 1,
   eGuess m,p = em,p,
   eGuess m,p+1 = em,p]]
```

Function: Compute Temperatures in the Matrix

```
ComputeMatrixTemperatures   :=
Module [{m},
  diagonal = Table[am, {m, 0, mm + 1}];
  rhs = Table[bm + H △xm * Tpt m,p-1, {m, 0, mm + 1}];
  temp = TridiagonalSolve [lower , diagonal , upper , rhs];
  Table[Tm,p = temp[[m + 1]], {m, 0, mm + 1}]]
```

Function: Compute Temperatures of the Particles

```
ComputeParticlesTemperatures   :=
Module [{},
  Do[IterateEnergy ;
   ComputePhaseFractions  , {m, 1, mm}];
  Tpt 0,p = Tpt 1,p;
  Tpt mm+1,p = Tpt mm,p;
  fpt 0,p = fpt 1,p;
  fpt mm+1,p = fpt mm,p;
  e0,p = e1,p;
  emm+1,p = emm,p]
```

Function: Phase Front

```
PhaseFront  :=
 Do[
  If[0 < fpt m,p < 1,
   PhF p = xm
  ],
  {m, 1, mm}]
```

Compute Temperatures Using the TDA

March Through Time

```
MarchTime :=
 Module [{},
  Do [
    PhF p = PhF p-1;
    (* Compute time dependent coefficients *)
    InteriorParticleCoefficients ;
     InteriorMatrixCoefficients ;
     CoefficientsAtx0 ;
     CoefficientsAtxL ;

    (* compute temps in the Matrix at time level p *)
    ComputeMatrixTemperatures ;

    (* compute temp of the particles at time level p *)
    ComputeParticlesTemperatures ;

    PhaseFront ,
    {p, 1, pmax}] // Timing ]
```

Compute Solution

```
ComputeSolution :=
 Module [{},
  Microstructure ;
  GridUniform [L, mm];
  MaterialProperties ;
  TimeDiscretization ;
  InitialConditions ;
  BoundaryConditionx0 ;
  BoundaryConditionxL ;
  HeatSources ;
  ComputeConductances ;
  MarchTime ]
```

C. ZONE SCHEMATIZE

C.1. Homogeneous Materials

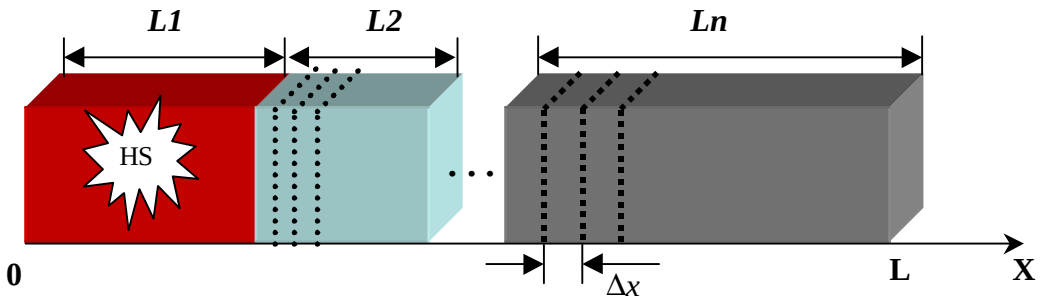

C.2. Heterogeneous Materials

(Zoned Matrix with Uniform Particles)

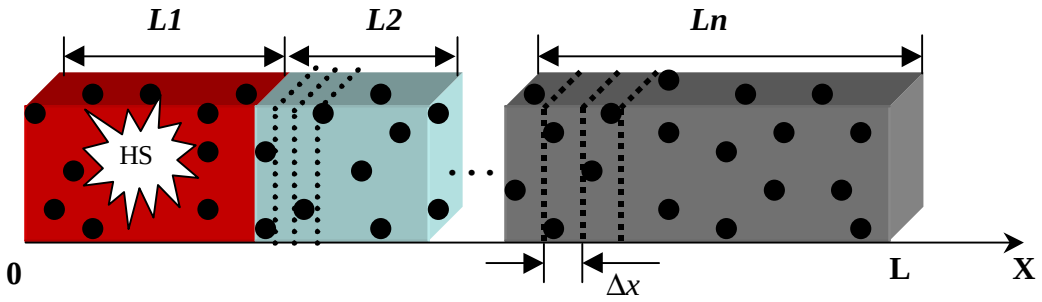

VITA

I was born in Tehran, Iran in a family with a background in engineering and science. From my childhood days, the material transformation from one phase to another has always intrigued me. This interest had inspired me to obtain my high school diploma with an emphasis in mathematics and physics in Iran. To continue my desire to obtain more knowledge in this area, I earned my Bachelor of Science degree in Mechanical Engineering at Tehran Polytechnic University, in Iran. I was very interested in continuing my academic goals by obtaining a masters degree. Therefore I moved to the United States of America in Virginia. I chose to continue my education at Virginia Polytechnic Institute and State University, in Blacksburg, Virginia, where I earned a Master of Science degree in Mechanical Engineering in December 2000. After graduation I will begin a career in San Francisco, California.

_____

Sepideh Sayar